REPRINTED FROM
PLASMA DIAGNOSTIC TECHNIQUES

ACADEMIC PRESS INC., NEW YORK

Chapter 4

Electric Probes

Francis F. Chen

1 Introduction

One of the fundamental techniques—the first one, in fact— for measuring the properties of plasmas is the use of electrostatic probes. This technique was developed by Langmuir as early as 1924 and con-

sequently is sometimes called the method of Langmuir probes. Basically, an electrostatic probe is merely a small metallic electrode, usually a wire, inserted into a plasma. The probe is attached to a power supply capable of biasing it at various voltages positive and negative relative to the plasma, and the current collected by the probe then provides information about the conditions in the plasma.

It is a fortunate property of plasmas that under a wide range of conditions the disturbance caused by the presence of the probe is localized, and the probe can act truly as a probe in the sense that its very presence has no effect on the quantities it is measuring. We shall find, however, that under certain circumstances, particularly in the presence of a strong magnetic field, the disturbance is *not* localized, and the probe current then depends not only on the plasma parameters (density and electron and ion temperatures), but also on the way in which the plasma is created and maintained. In such a case the method becomes obviously less useful.

In spite of the difficulties which arise when probes are used in present-day plasmas, the method is an important one because it has one advantage over all other diagnostic techniques: it can make local measurements. Almost all other techniques, such as spectroscopy or microwave propagation, give information averaged over a large volume of plasma.

Experimentally, electrostatic probes are extremely simple devices, consisting merely of an insulated wire, used with a dc power supply, and an ammeter or an oscilloscope. Nature, however, makes us pay a penalty for this simplicity: the theory of probes is extremely complicated. The difficulty stems from the fact that probes are boundaries to a plasma, and near the boundary the equations governing the motion of the plasma change their character. In particular, the condition of quasi-neutrality, which obtains in the body of the plasma, is not valid near a boundary; and a layer, called a "sheath," can form, in which ion and electron densities can differ and hence large electric fields can be sustained. A fundamental result of the original work of Langmuir and H. M. Mott-Smith, Jr. (see *1*, pp. 23–132) was that in many cases the sheath could be considered a thin layer near the probe surface and that the quasi-neutral equation could be used up to a "sheath edge," which in practice had a well-defined position. In recent years considerable progress has been made in the application of boundary-layer techniques to this problem, so that the artifice of a sheath edge has been removed and the continuous transition from boundary to plasma can be described, at least in the collisionless case. The sheath then appears as a natural consequence of the nature of the mathematical equations, and the accuracy of the approximations which Langmuir made with great

insight in the early days of plasma physics has been borne out in a large number of physically interesting cases.

It will be our purpose to summarize the available theoretical results, giving a sketch wherever possible of the way in which they were obtained, and to supplement this with practical information on experimental techniques. In Sec. 2 we begin with a short introduction to the physical notion of sheath. In Sec. 3 we shall present the well-documented theory of probes in a collisionless plasma. Although the theory of probes in the presence of collisions and magnetic fields is still in a primitive state, we shall treat this in some detail in Secs. 4 and 5 because of the current interest in magnetically confined plasmas. In the final sections we shall describe specialized techniques and practical considerations in the use of electrostatic probes. Quantities will be in cgs–es units.

The literature on probes is so extensive that we have not attempted to include here a complete survey of it. However, we have tried to include references to the most recent papers, from which references to earlier works can be obtained.

In order to get an over-all view of the situation, let use look at a physical plot of probe current versus probe voltage, as shown in Fig. 1. Here negative, or electron, current to the probe is plotted against V_p, the probe voltage with respect to an arbitrary reference point. This plot may be obtained continuously in a steady-state discharge, or point by point in a pulsed discharge, the probe bias being changed from pulse to

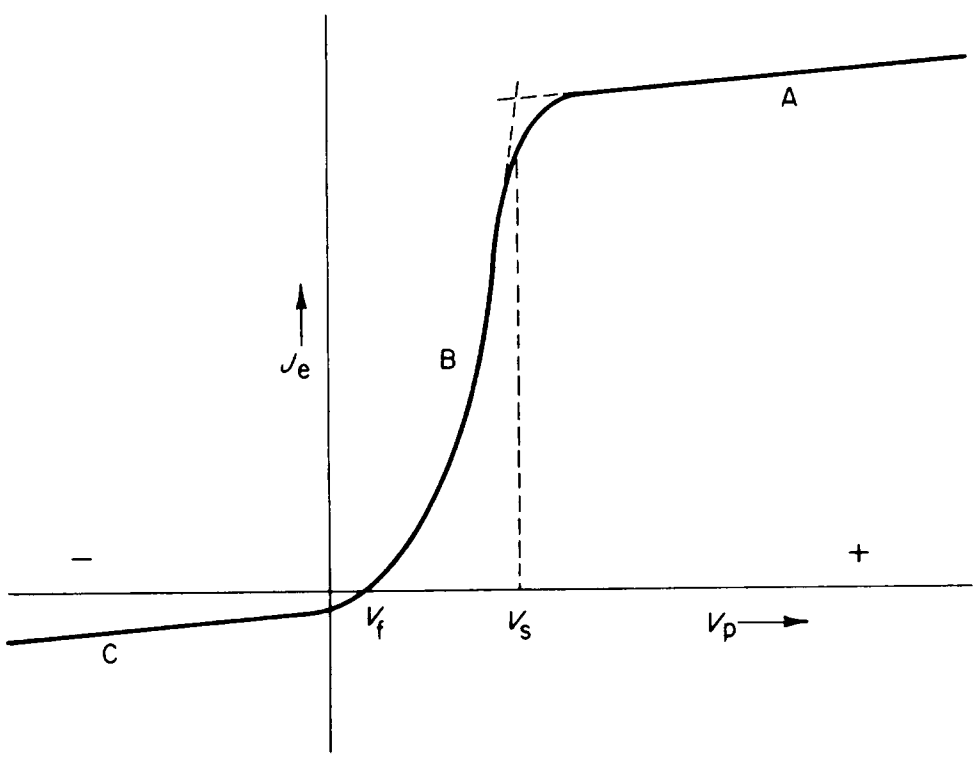

FIG. 1. Schematic of a typical probe current-voltage characteristic.

pulse; or the entire curve may be obtained in a few microseconds in a pulsed discharge by the use of a fast-sweeping voltage source.

The qualitative behavior of this curve can be explained as follows. At the point V_s, the probe is at the same potential as the plasma (this is commonly called the space potential). There are no electric fields at this point, and the charged particles migrate to the probe because of their thermal velocities. Since electrons move much faster than ions because of their small mass, what is collected by the probe is predominantly electron current. If the probe voltage is made positive relative to the plasma, electrons are accelerated toward the probe. Moreover, the ions are repelled, and what little ion current was present at V_s vanishes. Near the probe surface there is therefore an excess of negative charge, which builds up until the total charge is equal to the positive charge on the probe. This layer of charge, the sheath, is usually very thin, and outside of it there is very little electric field, so that the plasma is undisturbed. The electron current is that which enters the sheath through random thermal motions; and since the area of the sheath is relatively constant as the probe voltage is increased, we have the fairly flat portion A of the probe characteristic. This is called the region of saturation electron current.

If now the probe potential is made negative relative to V_s, we begin to repel electrons and accelerate ions. The electron current falls as V_p decreases in region B, which we shall call the transition region or retarding-field region of the characteristic. If the electron distribution were Maxwellian, the shape of the curve here, after the contribution of ions is subtracted, would be exponential. Finally, at the point V_f, called the floating potential, the probe is sufficiently negative to repel all electrons except a flux equal to the flux of ions, and therefore draws no net current. An insulated electrode inserted into a plasma would assume this potential.

At large negative values of V_p almost all the electrons are repelled, and we have an ion sheath and saturation ion current (region C). This is similar to region A; but there are two points of asymmetry between saturation ion and saturation electron collection aside from the obvious one of the mass difference, which causes the disparity in the absolute magnitude of the currents. The first point is that the ion and electron temperatures are usually unequal, and it turns out that sheath formation is considerably different when the colder species is collected than when the hotter species is collected. The second point is that when there is a magnetic field, the motion of the electrons is much more affected by the field than the motion of the ions. These two points, which were neglected in the original theory of Langmuir, are responsible for making impossible

the simple and straightforward application of probes as originally proposed by Langmuir.

If it is possible to place a probe in a plasma in such a way that the plasma is not greatly disturbed by the probe, then one can hope to obtain from the probe characteristic information regarding the local plasma density n, electron temperature kT_e, and space potential V_s. The shape of part B of the characteristic obviously is related to the distribution of electron energies and hence gives kT_e when the distribution is Maxwellian. The magnitude of the saturation electron current is a measure of $n(kT_e)^{1/2}$, from which n can be obtained. The magnitude of the ion saturation current depends on n and kT_e, but only slightly on kT_i, at least in the usual case where $kT_i \ll kT_e$; hence ion temperature is not easily measured with probes. Finally, the space potential can be measured by locating the junction between parts A and B of the curve or by measuring V_f and calculating V_s. In the presence of collisions or magnetic fields, the probe currents depend also on the transport coefficients of the plasma. In many instances, such as in a magnetic field, the absolute magnitude of n cannot be calculated with certainty; however, probes are still useful for finding the relative density in different parts of the plasma. In unstable plasmas probes are useful for measuring fluctuations in n or V_s, which are simply related to fluctuations in probe current or floating potential.

2 *Sheath Formation*

2.1 The Debye Shielding Length

Let us consider the effect of introducing a potential V_0 at some point $x = 0$ in a plasma of dimensions R and undisturbed density n_0. The potential is given by Poisson's equation, which, for simplicity, we write in one dimension:

$$\frac{d^2V}{dx^2} = -4\pi e(n_i - n_e). \tag{1}$$

If we normalize V, n_i, n_e, and x as follows:

$$\eta = -\frac{eV}{kT_e}, \qquad \nu_i = \frac{n_i}{n_0}, \qquad \nu_e = \frac{n_e}{n_0}, \qquad \xi = \frac{x}{R}, \tag{2}$$

the equation becomes

$$\frac{h^2}{R^2}\frac{d^2\eta}{d\xi^2} = \nu_i(\eta) - \nu_e(\eta), \tag{3}$$

where

$$h \equiv (kT_e/4\pi n_0 e^2)^{1/2}. \tag{4}$$

Since the quantity h/R is small in a plasma (by definition), Eq. (3) has the appearance of a boundary-layer equation; that is, the highest derivative in the equation is multiplied by a very small number. This means that the equation without the derivative, $\nu_e = \nu_i$, which is called the "quasi-neutral equation" or the "plasma equation," is valid over scale lengths of the order of R and that η changes considerably only within a small length of the order of h next to the boundary in order to satisfy the boundary condition at $\xi = 0$.

For example, let the ions be infinitely massive, so that n_i is constant, and let the electrons be in thermal equilibrium:

$$n_e = n_0 e^{-\eta}. \tag{5}$$

Poisson's equation then takes the form

$$\frac{d^2\eta}{d(x/h)^2} = 1 - e^{-\eta} \approx \eta. \tag{6}$$

Thus for small η the potential decays like

$$V = V_0 e^{-(x/h)}, \tag{7}$$

and the externally imposed potential is shielded within a distance of the order of h. The length h is called the Debye shielding length.

2.2 The Child-Langmuir Law

Let us now examine another idealized situation, that of two infinite plane-parallel plates, one which emits particles and is at zero potential, and the other which is perfectly absorbing and is at a potential V_B. This is shown in Fig. 2.

Consider first the case of emission at plane A of only one species of particle, with charge $-e$ and mass m, emitted at zero velocity. The particle velocity at a position where the potential is V is then

$$v = (2eV/m)^{1/2}. \tag{8}$$

If the emitted particle current density is j, the particle density at x will be

$$n(x) = j[2eV(x)/m]^{-1/2}. \tag{9}$$

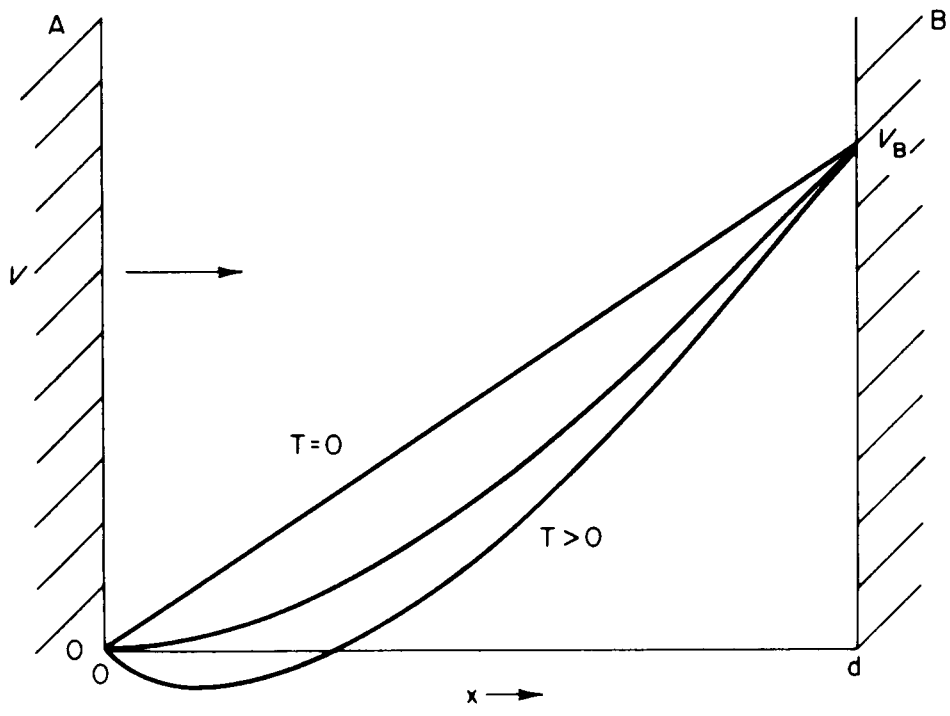

FIG. 2. Schematic of the potential distribution between two planes, one of which is emitting electrons.

Poisson's equation becomes

$$d^2V/dx^2 = 4\pi ej(2eV/m)^{-1/2}.$$

Multiplying by dV/dx and integrating from $x = 0$, we have

$$\begin{aligned}\frac{1}{2}\left(\frac{dV}{dx}\right)^2 &= 4\pi ej\int_0^V \left(\frac{2eV}{m}\right)^{-1/2} dV \\ &= 4\pi j(2me)^{1/2}V^{1/2} + \left(\frac{dV}{dx}\right)_0.\end{aligned} \tag{10}$$

By space-charge-limited flow, we mean that $(dV/dx)_0$ vanishes. We then have

$$V^{-1/4}\,dV = (8\pi j)^{1/2}(2me)^{1/4}\,dx. \tag{11}$$

Integrating from $x = 0$ to $x = d$, we have

$$\tfrac{4}{3}\,V_B^{3/4} = (8\pi j)^{1/2}(2me)^{1/4}\,d$$

or

$$j = \left(\frac{2}{me}\right)^{1/2}\frac{V_B^{3/2}}{9\pi d^2}, \tag{12}$$

which is the Child-Langmuir $\frac{3}{2}$-power law for space-charge-limited current flow between two planes separated by a distance d with a potential V_B between them.

The top curve of Fig. 2 represents the case of small j, when the space charge is small and the potential therefore a linear function of x. The middle curve shows the case when j is at the value given in Eq. (12); then the electric field is zero at A and a further increase in emission does not increase the current because no field acts on the particles at A.

If now the particles are allowed to have finite velocities when they are emitted, their inertia allows them to leave the surface A even when no electric field is present. This has the effect of depressing the potential below zero and building up a field which opposes the emission of electrons. The potential curve then looks like the bottom curve in Fig. 2, with a potential minimum V_m at $x = x_m$. In the case of a Maxwellian distribution of emitted electrons, the potential distribution can be found by integrating over the initial distribution of temperature kT. To first order in $\eta^{-1/2}$, where $\eta = eV/kT$, Langmuir (*1*, p. 379) finds for the space-charge-limited current

$$j = \left(\frac{2}{me}\right)^{1/2} \frac{1}{9\pi} \frac{(V - V_m)^{3/2}}{(d - x_m)^2} \left(1 + \frac{2.66}{\sqrt{\eta}}\right). \tag{13}$$

This shows clearly the increase of current due to finite temperature. The values of V_m and x_m in Eq. (13) must be found by a more complicated procedure, but for practical purposes they are small and may be neglected. Although we have for definiteness specified electrons, the Child-Langmuir law obviously holds also for ions if the appropriate mass and temperature are used.

2.3 The Sheath Criterion

Let us now introduce a second species of charged particle, so that we have a species 1 which is accelerated from A to B and a species 2 of equal and opposite charge which is repelled from B. We want eventually to identify surface A with the surface of the plasma and B with the surface of a wall or probe. Since a plasma is very nearly neutral (by definition), we require that $n_1 \approx n_2$ at A.

Our purpose in treating this problem is to gain some physical insight into the limitations of the approximation of a definite sheath edge which separates the plasma region, in which there are no electric fields, from the sheath region, in which large fields can exist. If the plane A in Fig. 2 is to represent the sheath edge, then to ensure a smooth transition to the plasma solution, the electric field of the sheath and its derivatives must nearly vanish there. We shall find that this condition imposes a requirement on the velocity distribution of the particles emitted at A and collected at B.

For simplicity, we shall treat first the somewhat degenerate case in which $T_1 = 0$, i.e., the accelerated particles have no random motion. In this case we must give them a nonvanishing drift velocity v_0 at A, since otherwise their velocity at A would be 0 and their density infinite if their current is to be finite.

Since there can be no particles of type 1 traveling from B to A, the distribution function of 1 is

$$\begin{aligned} f_1(0, v) &= n_0\delta(v - v_0), \qquad v_0 > 0 \\ f_1(x, v) &= n_0\delta\left[\left(v^2 + \frac{2q_1V}{m_1}\right)^{1/2} - v_0\right]. \end{aligned} \tag{14}$$

We now assume that the potential B is so large that almost all particles 2 are repelled; their distribution will then be Maxwellian:

$$f_2(x, v) = n_0\left(\frac{m_2}{2\pi kT_2}\right)^{1/2} \exp\left[-m_2\left(v^2 + \frac{2q_2V}{m_2}\right)/2kT_2\right]. \tag{15}$$

With the dimensionless variables

$$\eta = -\frac{q_1V}{kT_2}, \qquad u = v\left(\frac{m_1}{2kT^2}\right)^{1/2}, \qquad \xi = x\left(\frac{4\pi n_0q_1^2}{kT_2}\right)^{1/2}, \tag{16}$$

this becomes

$$f_2(\eta, u) = n_0\left(\frac{m_2}{\pi m_1}\right)^{1/2}\frac{1}{v_s}\exp\left(-\frac{m_2}{m_1}u^2 - \eta\right), \tag{17}$$

where we have set $q_1 = -q_2$, and where $v_s = (2kT_2/m_1)^{1/2}$. Note that since particles 1 are accelerated, q_1V is always negative, and therefore η always positive. Similarly, Eq. (14) becomes

$$f_1(\eta, u) = n_0v_s^{-1}\delta[(u^2 - \eta)^{1/2} - u_0]. \tag{18}$$

The densities are found by integrating with respect to $v_s\,du$:

$$\begin{aligned} n_2 &= n_0e^{-\eta} \\ n_1 &= n_0\int \delta(y - u_0)\frac{y\,dy}{(y^2 + \eta)^{1/2}} = n_0(1 + \eta u_0^{-2})^{-1/2}. \end{aligned} \tag{19}$$

Poisson's equation is then

$$\eta'' = n_0[(1 + \eta u_0^{-2})^{-1/2} - e^{-\eta}]. \tag{20}$$

With the usual integrating factor η', the integral from 0 to x is

$$\tfrac{1}{2}\eta'^2 = n_0\{2u_0^2[(1 + \eta u_0^{-2})^{1/2} - 1] + e^{-\eta} - 1\} + \tfrac{1}{2}\eta_0'^2. \tag{21}$$

For the moment, let us neglect η_0'. The left-hand side in Eq. (21) must be positive; hence

$$2u_0^2[(1 + \eta u_0^{-2})^{1/2} - 1] > 1 - e^{-\eta}. \tag{22}$$

Near the origin $\eta = 0$, this inequality becomes, upon expanding,

$$2u_0^2[\tfrac{1}{2}\eta u_0^{-2} - \tfrac{1}{8}\eta^2 u_0^{-4}] > \eta - \tfrac{1}{2}\eta^2$$

$$u_0 = \left(\frac{m_1 v_0^2}{2kT_2}\right)^{1/2} > \frac{1}{\sqrt{2}}. \tag{23}$$

This is the original sheath criterion derived by Langmuir (*2*, p. 140) and Bohm (*3*, Chapter 3). It states that in order for the sheath equation to have a solution for small η there is a restriction on the streaming velocity assumed for particles 1 at plane A: namely, that it be larger than $(kT_2/m_1)^{1/2}$.

The most common application of this criterion is in the case of ion collection, in which ions are particles 1 and electrons particles 2. In many discharges the ion temperature is much lower than the electron temperature, so that the assumption $T_1 = 0$ is applicable. Equation (23) then says that the ions must stream into the sheath boundary with an energy greater than $\frac{1}{2}kT_e$, which is much larger than their thermal energy.

The reason for this restriction on the cold species can be seen by plotting the density, as given by (19), logarithmically against potential η, as shown in Fig. 3. The trapped particles 2 have a density which appears as a straight line on the semilog plot. If η'' is rigorously zero, the curve for n_1 starts at the same point n_0 as does n_2, and its initial slope depends on u_0. If u_0 is small, n_1 is less than n_2 for small η. Referring to Poisson's equation,

$$n_0\eta'' = n_1 - n_2,$$

we see that if $\eta_0' = 0$ and η is to be positive, η'' must be positive near $\eta = 0$. If u_0 is too small, η'' is negative, and this will not permit a monotonic solution for $\eta(\xi)$. The solution will oscillate between two values of η, corresponding to an imaginary value of η'^2. If u_0 were large, we see from

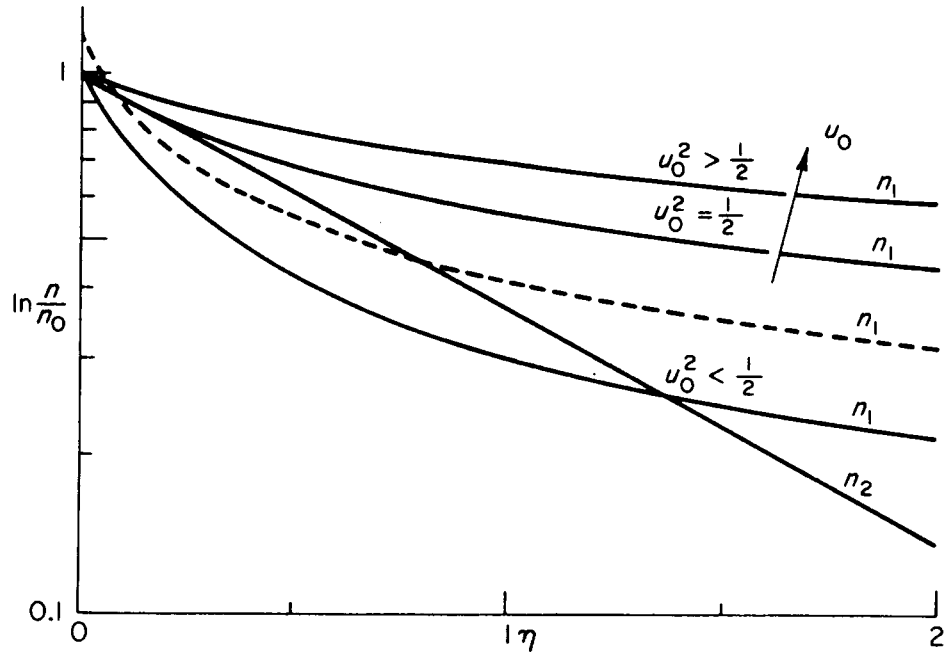

FIG. 3. Schematic of ion density (n_1) and electron density (n_2) distributions in a sheath as a function of potential η, for various values of incident velocity u_0 of the cold ions.

Fig. 3 that n_1 is always larger than n_2, and the problem does not arise. The critical condition is that

$$\left(\frac{dn_1}{d\eta}\right)_0 = \left(\frac{dn_2}{d\eta}\right)_0. \tag{24}$$

From Eq. (19), this is just

$$-\frac{n_0}{2} u_0^{-2} = -n_0, \qquad \text{or} \qquad u_0^2 = \tfrac{1}{2},$$

the same condition as Eq. (23). This equivalence was first pointed out by Allen and Thonemann (*4*).

The proof given above is subject to the criticism that η, η', and η'' cannot all vanish at $x = 0$, since then only the trivial solution is possible. In practice η_0' and η_0'' have small but finite values. If η'' is positive, for example, then by Eq. (20) n_1 must exceed n_2 at $x = 0$, as is illustrated by the dotted line in Fig. 3. The curve $n_1(\eta)$ may then dip below n_2, and the critical value of u_0 is reduced. This effect, however, is slight as long as the Debye length is small compared to the characteristic lengths in the plasma, such as the mean free path or an ionization length. The effect of finite η_0' and η_0'' has been computed by Ecker and McClure (*5*).

If now the accelerated particles are allowed to have a spread in energy at the sheath edge, the critical drift velocity u_0 given by Eq. (23) is considerably reduced; however, the value of u_0 then cannot be expressed simply, even for a Maxwellian distribution.

We may now point out the implications of the sheath criterion on the probe characteristic of Fig. 1. Consider the usual case in which $T_i \ll T_e$. Then in part A of the characteristic, where electrons are accelerated toward the probe, the sheath criterion (23) tells us that the electrons must enter the sheath with a drift velocity greater than $(kT_i/m)^{1/2}$. Since this is small compared to the random electron velocity, and the finite electron temperature makes the criterion even less severe, the current entering the sheath is closely approximated by the random electron current in the plasma. Use is made of this in Section 3.1. On the other hand, in part C of the characteristic, where ions are accelerated to the probe, the sheath criterion requires the ions to have a directed velocity greater than $(kT_e/M)^{1/2}$, which is much larger than the random velocity. The velocity distribution at the sheath edge is then unknown and the ion current must be computed laboriously, as is done in Sec. 3.3. However, for sheaths thin compared to the probe radius, so that the geometry is almost planar, it will turn out that the ion current density is given roughly by n_0 times this critical velocity. This is essentially the reason probes are insensitive to ion temperature. The situation is, of course, reversed if T_i is much larger than T_e.

We have, for purposes of illustration, considered the case of an infinite plane probe, but it is clear that such a probe cannot actually exist, since in the absence of ionization all the plasma would eventually be lost to the probe. The probe current in steady state is given by the rate of ionization in the plasma, and therefore the probe is in a sense actually an electrode. As we shall see in Section 3.3, the situation is different in the case of spherical or cylindrical probes, for which the probe current depends only on the properties of the plasma far from the probe and not on the mechanism which produces the plasma. However, except for geometrical factors, the basic prediction of the plane sheath criterion is still valid; that is, the shielding of the probe by the sheath is incomplete, and a total potential drop of order of magnitude kT_2 must exist in the plasma region to accelerate particles 1 to this energy by the time they reach the point near the boundary where the quasi-neutral assumption fails.

Further discussion of plane sheaths, which necessarily involves the ionization mechanism, may be found in the work of L. Tonks and Langmuir (*2*, p. 176). The particularly simple case of no collisions has been treated by Harrison and Thompson (*6*), Auer (*7*), and Self (*8*). A rigorous boundary-layer analysis of the plasma-sheath transition has been given by Caruso and Cavaliere (*9*). The stability of the ion stream in this case has been examined by Chen (*10*). The effect of a weak magnetic field on the sheath criterion has been studied by Allen and Magistrelli (*11*).

3 *Probe Theory in the Absence of Collisions and Magnetic Fields*

The exact way in which the plasma parameters are related to the probe characteristic will depend on the shape of the probe and the relative magnitudes of the collision length, the probe dimensions, the Debye length, the Larmor radius, and so forth. In this section we shall discuss the simplest case—that in which both collisions and magnetic fields are negligible. This case is essentially that covered by the original theory of Langmuir. There is, however, one exception; that is, in dealing with saturation ion current the effect of acceleration of ions in the plasma region (which we discussed in connection with the sheath criterion) was at first unknown to Langmuir. For the proper treatment of ion saturation current we shall have to turn to comparatively recent work. We shall confine ourselves to plasmas consisting of singly charged positive ions and electrons. Extensions of the theory to include negative ions or multiply charged ions is straightforward. The main difference from the discussion of Sec. 2.3 is that now we shall have to consider particle orbits in more than one dimension.

3.1 Probe Current in a Prescribed Electric Field

We now turn to the problem of sheath formation on actual probes, which are normally not planar but cylindrical or spherical, since such shapes do not disturb the plasma as much as a large flat surface. Particles can now move in orbits in a central force field, and the density is no longer a simple function of potential as it was in the one-dimensional case. Again we have Poisson's equation

$$\nabla^2 V = -4\pi(q_1 n_1 + q_2 n_2),$$

but now not only is the Laplacian more complicated but also n_1 is a complicated integral involving V. The solution for V must even in the simplest case be found numerically. However, in some physical situations the probe current can be found without knowing the exact behavior of $V(r)$. In these situations the original theory of Langmuir is applicable. In describing this theory we shall assume that the function $V(r)$ is already known.

3.1.1 *Thin Sheath: Space Charge Limited Current*

Suppose that the prescribed electric field is such that the potential drop around a charged spherical or cylindrical probe attracting particles of type 1 is concentrated in a thin layer of radius s surrounding the

probe of radius a. Suppose further that the velocity distribution is essentially Maxwellian at the edge of the sheath. This situation applies, for instance, to part A of the probe characteristic (saturation electron current), since in most plasmas $T_e \gg T_i$, and we have seen in Section 2.3 that the collection of the hotter species does not require a large drift velocity at the sheath edge. If $s - a$ is much smaller than a so that all particles entering the sheath hit the probe, and if the probe is perfectly absorbing, then the probe current is simply

$$I = j_r A_s , \tag{25}$$

where A_s is the area of the sheath, and j_r is the random current density crossing a unit area in one direction. For a Maxwellian distribution, this is given by

$$j_r = \tfrac{1}{4} n\bar{v} = \tfrac{1}{2} n \left(\frac{2kT_1}{\pi m_1}\right)^{1/2}. \tag{26}$$

We have omitted the charge q_1 and are therefore considering particle currents. The factor $\frac{1}{4}$ in j_r is composed of two factors of $\frac{1}{2}$. The first accounts for that fact that at the sheath edge the density is half the plasma density—the half consisting of particles heading *toward* the probe. The second factor of $\frac{1}{2}$ is merely the average of the direction cosine over a hemisphere. To the extent that $s - a \ll a$, A_s is equal to A_p, the probe area; and the current is independent of voltage in this limit.

The physical situation is clarified by Fig. 4. The collision mean free path λ is assumed to be much larger than s or a. The population at point P consists of particles which made their last collision approximately a distance λ from P. Since the probe subtends only a very small solid angle at P, the shadowing effect of the probe has negligible effect, and the distribution at P is closely Maxwellian. At point S, however, there can be no particles coming from the probe, and therefore the density must gradually change from n at P to $\frac{1}{2}n$ at S, if there is no ionization anywhere on the diagram. Since the particles of type 2, which are

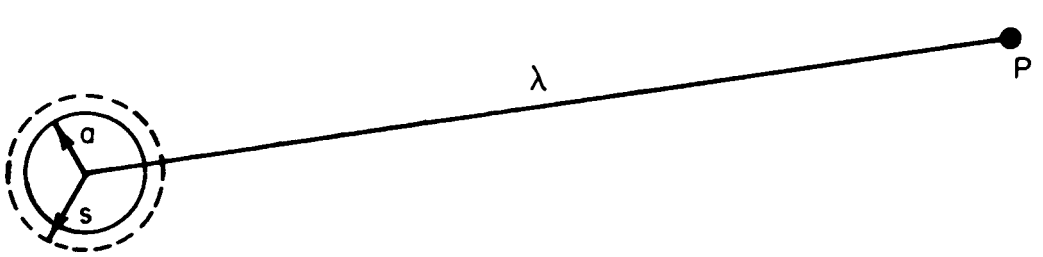

FIG. 4. Representation of a probe and its sheath when they are both much smaller than the mean free path.

repelled by the probe, are in thermal equilibrium, their density is given by

$$n_2 = ne^{-q_2V/kT_2}. \tag{27}$$

By assumption, all electric fields are concentrated within the sheath. However, in order to satisfy Eq. (27) and quasi-neutrality at S, we must have

$$\frac{q_2V_s}{kT_2} = \ln 2, \tag{28}$$

the potential at ∞ being 0. Our initial prescription for $V(r)$ can be approximately true in practice only if kT_2 is very small. This is the reason this theory can be used for the collection of hot electrons in a gas of cold ions but would not be nearly correct in the case of cold ion collection.

Although we have considered the potential distribution and hence the sheath thickness $s - a$ to be prescribed, this is sometimes not necessary. In mercury discharges of the type used by Langmuir, the sheath was visible, and its thickness could be measured, so that a measured value of A_s could be used in (25). Even if A_s cannot be measured, it can be calculated from the space charge equations. If we neglect the density of particles 2 in the sheath, the problem is the same as one we have already considered in Section 2.2: that of space charge limited emission from a plane A (the sheath edge) to a plane B (the probe surface). Thus the current density is given by Eq. (13):

$$j = \left(\frac{2}{em}\right)^{1/2} \frac{1}{9\pi} \frac{|V_p - V_s|^{3/2}}{(s-a)^2} \left(1 + \frac{2.66}{\sqrt{\eta}}\right), \tag{29}$$

where $\eta = |e(V_p - V_s)/kT_1|$. If $V_s = 0, j$ can be equated to j_r to give a value of the sheath thickness $s - a$; this can then be used to compute A_s.

If $s - a$ is not infinitely small, it is more accurate to replace the above equation for planar geometry by the corresponding space charge equations for cylinders and spheres. These are given by Langmuir and K. B. Blodgett (*12*, pp. 115 and 125):

$$\text{Cylinder:} \quad j = \frac{1}{9\pi}\left(\frac{2}{em}\right)^{1/2} \frac{|V_p - V_s|^{3/2}}{a^2\beta^2}\left(1 + \frac{2.66}{\sqrt{\eta}}\right) \tag{30}$$

$$\text{Sphere:} \quad = \frac{1}{9\pi}\left(\frac{2}{em}\right)^{1/2} \frac{|V_p - V_s|^{3/2}}{a^2\alpha^2}\left(1 + \frac{2.66}{\sqrt{\eta}}\right), \tag{31}$$

where

$$\beta = \gamma - 0.4\gamma^2 + \cdots$$

$$\alpha^2 = \gamma^2 - 0.6\gamma^3 + \cdots$$

and

$$\gamma = \ln \frac{a}{s} .$$

3.1.2 *Thick Sheath: Orbital Motions*

In the opposite limit of a thick sheath ($s \gg a$), not all particles entering the sheath will hit the probe because of the possibility of orbital motions. If the potential varies slowly enough (a condition we shall derive later), the probe current is still independent of the exact shape of $V(r)$. This is because the laws of conservation of energy and angular momentum concern only the initial and final values of the energy and angular momentum.

Consider the orbit of a particle in an attractive central force field. Let its initial velocity be v_0 and impact parameter, p. At its point of closest approach to the center (in either a spherically or a cylindrically symmetric system), let its velocity be v_a and its radius a. Then the conservation laws state:

$$\tfrac{1}{2} m v_0^2 = \tfrac{1}{2} m v_a^2 + q V_a \tag{32}$$

$$p v_0 = a v_a . \tag{33}$$

Solving for p, we have (for $qV < 0$)

$$p = a \left(1 + \frac{V_a}{V_0}\right)^{1/2} \tag{34}$$

where $-qV_0 = \frac{1}{2} m v_0^2$. If we identify a with the probe radius, we see that any particle with p smaller than that given by Eq. (34) will hit the probe and be collected. Hence the effective collecting radius of the probe is the larger value p, and this is independent of the shape of the potential distribution. It is clear, therefore, that for a monoenergetic beam of particles, or for an isotropic distribution of monoenergetic particles at infinity, the probe current is given by

$$\text{Cylinder:} \qquad I = 2\pi a l j_r \left(1 + \frac{V_a}{V_0}\right)^{1/2} \tag{35}$$

$$\text{Sphere:} \qquad I = 4\pi a^2 j_r \left(1 + \frac{V_a}{V_0}\right) . \tag{36}$$

Thus for a cylindrical probe the saturation electron current increases with the square root of the probe voltage. The current is limited by the impact parameter p and not by the sheath size, which can be infinitely large.

So far we have considered monoenergetic particles coming in from infinity. To do the more general problem we must take into account the finite size of the sheath and also the distribution of energies at the sheath edge. Again we shall presuppose that the potential distribution is known and that the entire potential drop occurs within a sphere or cylinder of radius s. Let qV be negative (attractive probe), and let u and v denote the radial and tangential components of velocity. Conservation of energy and angular momentum imposes the following relations between quantities at the sheath edge ($r = s$) and at the probe ($r = a$):

$$\begin{aligned} u_s^2 + v_s^2 &= u_a^2 + v_a^2 + \frac{2qV_a}{m} \\ sv_s &= av_a \,. \end{aligned} \tag{37}$$

Solving for u_a, we have

$$u_a^2 = u_s^2 + v_s^2\left(1 - \frac{s^2}{a^2}\right) - \frac{2qV_a}{m} \,. \tag{38}$$

A necessary condition for a particle to hit the probe is that $u_a^2 \geqslant 0$. This is not a sufficient condition, since u^2 must not vanish *anywhere* between s and a; sufficiency will be discussed in the next section. This condition then imposes limits on the value of v_s:

$$v_s^2 \leqslant \left(u_s^2 - \frac{2qV_a}{m}\right)\left(\frac{s^2}{a^2} - 1\right)^{-1} \equiv v_s^{*2}. \tag{39}$$

This argument clearly holds for both cylinders and spheres. If $G(u_s, v_s)$ is the distribution function at s, the current to a cylindrical probe is obviously the sheath area times the integral of $uG(u, v)$ taken over all u from 0 to ∞ and over v from $-v_s^*$ to $+v_s^*$:

$$I = A_s j \tag{40}$$

$$j = n\int_0^\infty u\,du\int_{-v^*}^{+v^*} G(u, v)\,dv, \tag{41}$$

where we have suppressed the subscript s.

Of particular interest is Maxwell's distribution in two dimensions:

$$G(u, v) = \left(\frac{m}{2\pi kT}\right)\exp\left(\frac{-m(u^2 + v^2)}{2kT}\right). \tag{42}$$

The integration of Eq. (41) using this distribution and Eq. (39) is straightforward and can be done explicitly. The answer is given by Langmuir and Mott-Smith (*1*, pp. 32 ff and 108 ff); the answer for the equation analogous to (41) for spheres is also given:

$$I = A_a j_r F \tag{43}$$

$$\text{Cylinder:} \quad F = \frac{s}{a} \operatorname{erf} \Phi^{1/2} + e^{\eta}[1 - \operatorname{erf}(\eta + \Phi)^{1/2}] \tag{44}$$

$$\text{Sphere:} \quad F = \frac{s^2}{a^2}[1 - e^{-\Phi}] + \mathrm{e}^{-\Phi}, \tag{45}$$

where

$$\eta = -\frac{eV_a}{kT}, \tag{46}$$

$$\Phi = \frac{a^2}{s^2 - a^2}\eta, \tag{47}$$

$$\eta + \Phi = \frac{s^2}{s^2 - a^2}\eta \tag{48}$$

$$\operatorname{erf} x = \frac{2}{\sqrt{\pi}} \int_0^x \exp(-t^2)\, dt \tag{49}$$

and j_r is given by Eq. (26).

We note two limiting cases: $s - a \ll a$ and $s \gg a$. In the thin sheath limit, the arguments of the error functions are large, and we can use the approximation

$$1 - \operatorname{erf} x \approx \frac{1}{\sqrt{\pi}} \frac{\exp(-x^2)}{x}. \tag{50}$$

When this is inserted into Eq. (44), the result is $F = s/a$, and we recover Eq. (25), as expected. Similarly, for large Φ we can neglect the exponentials in Eq. (45) and recover Eq. (25) for spheres.

In the thick sheath limit, Φ is small; and we can neglect it relative to η. The error function for small x is given by

$$\operatorname{erf} x \approx \frac{2}{\sqrt{\pi}} x, \tag{51}$$

and the exponential $e^{-\Phi}$ by $1 - \Phi$. Thus (44) and (45) become:

$$\text{Cylinder:} \quad F \cong \frac{2}{\sqrt{\pi}} \eta^{1/2} + e^{\eta}(1 - \operatorname{erf} \eta^{1/2}) \tag{52}$$

$$\text{Sphere:} \quad F \cong \eta + 1. \tag{53}$$

If, in addition, $\eta \gg 1$, Eqs. (52) and (50) yield

$$\text{Cylinder:} \qquad F \cong \frac{2}{\sqrt{\pi}}(\eta^{1/2} + \tfrac{1}{2}\eta^{-1/2}) \cong \frac{2}{\sqrt{\pi}}(\eta+1)^{1/2}. \tag{54}$$

Thus for large sheath radii I varies as V for spheres, in agreement with Eq. (36), while I varies as $V^{1/2}$ for cylinders, in agreement with Eq. (35). The latter is true only if $\eta \gg 1$ as well. Note that precise information on the sheath radius is not required in this limit, since Eqs. (52) and (53) do not depend on s.

Equation (54) suggests that the slope of the electron saturation current as well as its absolute magnitude may be a useful datum. From Eq. (43) we have

$$\begin{aligned} I &= A_a j_r \frac{2}{\sqrt{\pi}}(\eta + 1)^{1/2} \\ I^2 &= \frac{4}{\pi} A_a^2 j_r^2(\eta + 1). \end{aligned} \tag{55}$$

Thus if I^2 is plotted against V_a, there should be a linear region where the slope is

$$S = \frac{2}{\pi^2} A_a^2 \frac{e}{m} n^2, \tag{56}$$

giving a value for n. The intercept of this line at $I = 0$ gives the value of e/kT if V_s is known, or of V_s if kT is known. When such a linear plot of I^2 versus V can be obtained, therefore, the density and electron temperature can be obtained separately, rather than in combination, as in Eq. (43).

In the weakly ionized plasmas investigated by Langmuir, it was actually possible to get a good linear plot of I^2 versus V with cylindrical probes. This deviated from linearity at small V, where the approximation (54) becomes invalid, and at large V, where space charge limitation requires the use of (25). The use of Eq. (53) with spherical probes, however, turned out to be nearly impossible, since with actual probe sizes the condition $s \gg a$ could not be fulfilled; instead, spherical probes tended to draw space charge limited current.

Langmuir (*1*, p. 112) and Heatley (*13*) have also given approximate formulas for the very complicated case of a Maxwellian distribution with a superimposed drift and cylindrical geometry. The spherical case has been treated by Medicus (*14*) and Dote *et al.* (*15*).

3.1.3 *Range of Validity of Orbital Theory*

Aside from the requirements $\lambda \gg s$ and $\lambda \gg a$, the collisionless theory described above is subject to a requirement on the potential shape. This can be seen by imagining a potential which extends far from the probe ($s \gg a$) but which has most of the drop occurring in a thin layer around the probe. In such a case one would use the formula for the case $s \gg a$, but obviously the true answer cannot differ much from that given by the formula for $s - a \gg a$. Such a potential has an "absorption radius" r_0 larger than a which gives the effective collecting area inasmuch as all particles entering the surface at $r = r_0$ are destined to hit the probe. The condition that no such absorption radius exists will now be derived.

From Eq. (38) we have the following expression for the radial velocity of a particle at the probe in terms of its velocity components:

$$u_a^2 = u_s^2 + v_s^2\left(1 - \frac{s^2}{a^2}\right) + \phi_a\,, \tag{57}$$

where we have let

$$\phi = -\frac{2qV}{m} \geqslant 0. \tag{58}$$

If $u_a^2 \geqslant 0$, the particle will hit the probe, *provided* that it is not repelled at some larger radius r. The most stringent condition on ϕ is that even those particles barely able to reach the probe ($u_a = 0$) are not turned around at a larger radius r. If they were turned around, all those which get past r would strike the probe; and r would be an absorption radius.

To get the most stringent condition on ϕ, we consider those particles with $u_a = 0$, for which

$$u_s^2 = v_s^2\left(\frac{s^2}{a^2} - 1\right) - \phi_a\,. \tag{59}$$

At any radius $r > a$, their radial velocity is given by Eq. (57), with r replacing a:

$$u_r^2 = u_s^2 + v_s^2\left(1 - \frac{s^2}{r^2}\right) + \phi_r\,. \tag{60}$$

Eliminating v_s^2 between the last two equations, we have

$$\begin{aligned} u_r^2 &= u_s^2 + \phi_r + \left(1 - \frac{s^2}{r^2}\right)\frac{u_s^2 + \phi_a}{(s^2/a^2) - 1} \\ &= \phi_r + u_s^2\left(1 - \frac{a^2}{r^2}\,\frac{s^2 - r^2}{s^2 - a^2}\right) - \phi_a\left(\frac{a^2}{r^2}\,\frac{s^2 - r^2}{s^2 - a^2}\right). \end{aligned} \tag{61}$$

The condition that $u_r^2 > 0$ then gives this condition on ϕ_r :

$$\phi_r > g\phi_a - (1 - g)u_s^2 , \tag{62}$$

where

$$g(r) = \frac{a^2}{r^2}\frac{s^2 - r^2}{s^2 - a^2} . \tag{63}$$

If the initial distribution at s includes particles with $u_s^2 = 0, \phi_r$ must satisfy the condition

$$\phi_r > g\phi_a . \tag{64}$$

The meaning of this can be seen by letting s approach infinity. Then the potential falls less rapidly than $1/r^2$:

$$s \to \infty: \qquad \frac{\phi_r}{\phi_a} > \frac{a^2}{r^2} . \tag{65}$$

This is a rather gradual variation with r. This condition is not satisfied in a dense plasma, where the Debye length is small; then the potential must drop abruptly from ϕ_a and hence fall below the $1/r^2$ curve. The discussion above is clearly valid for both cylinders and spheres. Since for purely geometrical reasons one would expect the potential to fall more slowly away from a cylindrical probe than from a spherical probe, one would expect that the condition (65) is more easily satisfied for cylindrical probes, in agreement with Langmuir's observations.

Of course if an absorption radius exists, this can be called the sheath edge, and the theory would then apply. However, in this case the velocity distribution at the sheath edge is unknown and must be calculated. This is essentially the problem we shall consider in Section 3.3. The potential may also be such that there are closed orbits within $r = s$. The population in these orbits would then depend on collisions, and the problem would no longer be tractable. This possibility is also considered in Section 3.3 on ion currents.

3.1.4 *Summary of Langmuir's Theory*

This theory applies when (a) the hotter component of the plasma (usually electrons) is collected, so that the distribution at the sheath edge is approximately Maxwellian; (b) the pressure in the discharge is low enough that the mean free path is much larger than the probe or sheath dimensions; and (c) the plasma density or the probe potential is low enough that the potential distribution satisfies Eq. (64). The probe current is then independent of the exact shape of the potential.

When the sheath is thin compared to the probe radius, the current is limited by space charge and is given by Eq. (25). In this case the current varies with voltage only inasmuch as the sheath area changes; this change is given by Eqs. (29–31). The saturation electron current magnitude then gives a value for $n(kT_e)^{1/2}$. In this limit the condition (64) is never satisfied, but the result is insensitive to this requirement.

When the sheath is thick compared with the probe radius, the current is limited by orbital motions and is given approximately by Eqs. (35) and (36), or, more exactly, by Eqs. (43), (52), and (53). With intermediate sheath thicknesses, the current is always less than the smaller of (25) and (35), (36), and is given exactly by Eqs. (43)–(49). In the thick sheath limit, part A of the probe characteristic appears as follows for different probe shapes (Fig. 5):

The saturation electron current varies with V for spheres and as $V^{1/2}$ for cylinders; it does not change for planes since no orbits are possible and the sheath area is constant. The curve for a plane exists only by virtue of the assumption of a sheath edge; for reasons given in Section 2.3 there can be no complete theory of a plane probe in a collisionless, ionizationless plasma. What Eq. (25) gives for a large plane probe is the density at the sheath edge, and the way this is related to the density far from the probe depends critically on ionization and collisions. This

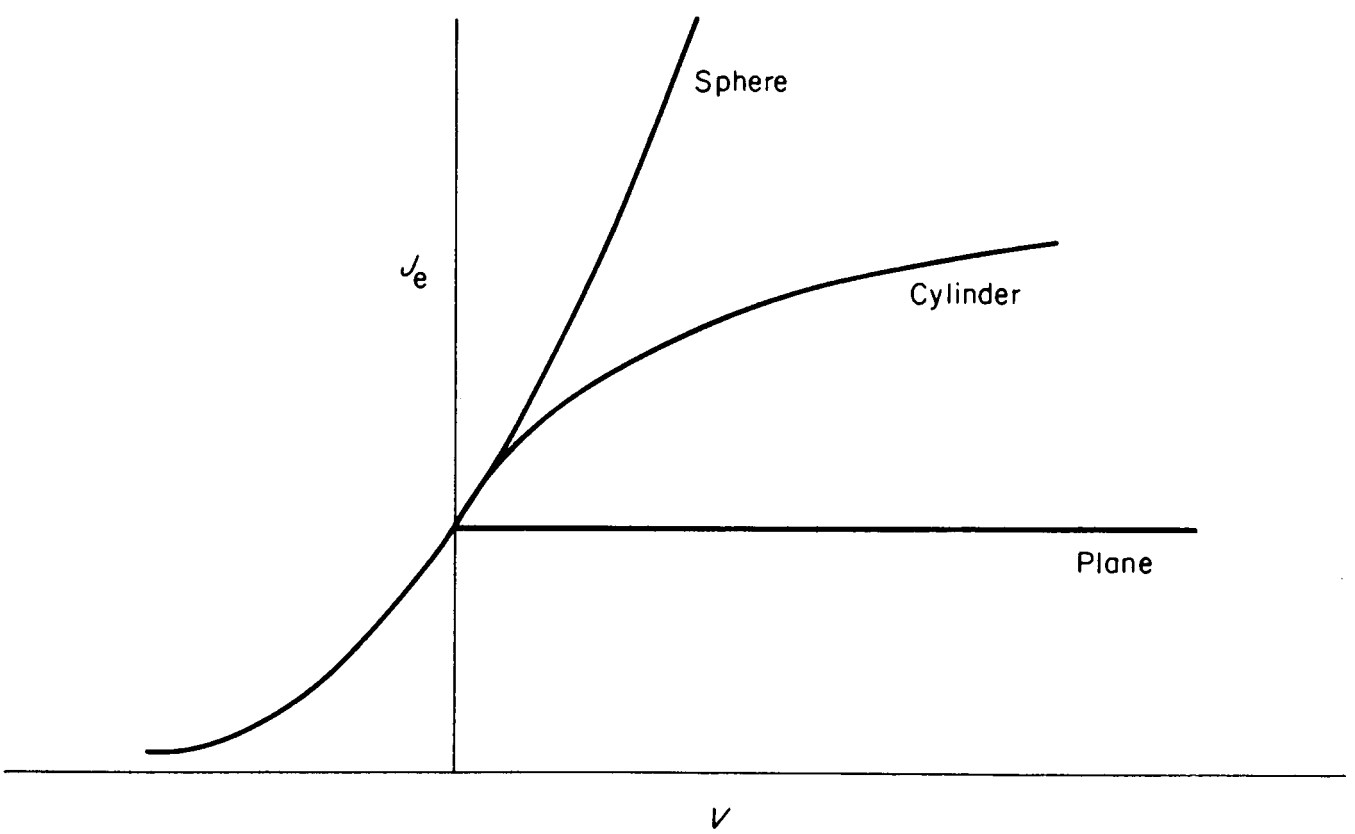

FIG. 5. Theoretical shape of the saturation current portion of the probe characteristic for various probe shapes when the probe current is limited by orbital motions.

is not true for a small plane probe which would collect from an ill-defined region because of edge effects and would exhibit a curvature in its electron saturation characteristic.

In most plasmas of today the Debye length is so small and the probe radius so large (so that the probe will not melt) that the Langmuir theory is useless, and the single formula (25) suffices to describe saturation electron current. Moreover, electron collection can seldom be used at all because the large currents involved seriously affect the plasma being measured.

3.2 The Transition Region

In region B of the probe characteristic the probe collects both ions and electrons. Fortunately, the ion current is much smaller than the electron current, because of the disparity in mass, and it can be subtracted out even if not accurately known. The probe, then, collects electrons moving against a repelling field. The current can be computed with the same formulas used in the section on orbital motions, but with $eV > 0$; however, for a Maxwellian distribution the answer is the same regardless of the sheath and probe sizes and even the shape of the probe.

3.2.1 *Maxwellian Distribution*

Suppose the probe is charged negatively to repel electrons and is perfectly reflecting. If the electron distribution is in thermal equilibrium, we know that the density follows the Boltzmann law

$$n = n_0 e^{-\eta}, \tag{66}$$

and that the distribution is still Maxwellian everywhere; only the density is changed by the potential. The random current hitting the probe is then merely

$$I = A_a j_r = A_a n \left(\frac{kT}{2\pi m}\right)^{1/2}. \tag{67}$$

where n is evaluated at the probe surface. Using Eq. (66), we find

$$I = A_a n_0 \left(\frac{kT}{2\pi m}\right)^{1/2} e^{-\eta}, \tag{68}$$

where $\eta = |eV/kT|$. Now if the probe is perfectly absorbing, the Maxwellian distribution near the probe is deprived of electrons coming back from the probe. However, the distribution of those going toward

the probe, which contribute to the current, is essentially unchanged, since it is determined by collisions far away from the probe, where the population is undisturbed by the presence of the probe. Therefore Eq. (68) is still approximately true for an absorbing probe, especially if η is large, so that the probe draws little current.

If $\ln I$ is plotted against η (or V), Eq. (68) predicts a straight line if the distribution is Maxwellian. The slope of the line is $| e/kT |$ and gives a good measure of the electron temperature. In Langmuir's plasmas the $\ln I$–V plot was linear over a ratio of 1000 : 1 in current. This was actually better adherence to the exponential law than one had a right to expect.

In the case of two groups of electrons at different temperatures, the $\ln I$–V plot would be a broken line, as shown in Fig. 6. The slopes of the two straight segments would give the temperatures of the two groups.

The space potential is often obtained by extrapolating parts A and B of the probe characteristic and finding the point of intersection; this is also shown in Fig. 6.

3.2.2 *Isotropic Distributions*

If the velocity distribution of electrons is not Maxwellian but is still isotropic, the shape of the transition region of the probe curve can give

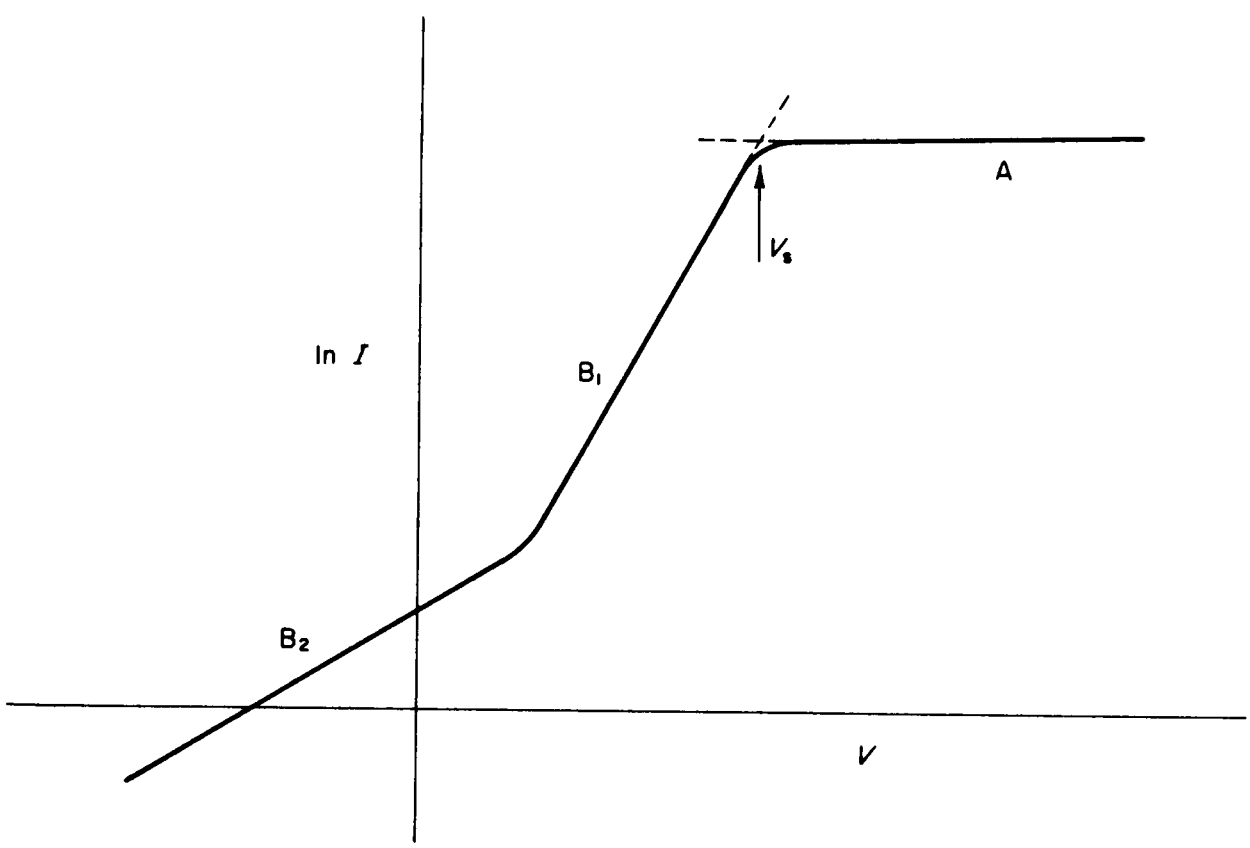

FIG. 6. Schematic of a $\ln I$-V curve with a bend in the transition region, indicating the presence of two groups of electrons with different temperatures.

information about the distribution function. This will be demonstrated for the case of a plane probe.

Let the isotropic distribution be $f(v)$, so that

$$n = \int_0^\infty f(v)\, d^3v = 4\pi \int_0^\infty v^2 f(v)\, dv \equiv \int_0^\infty g(v)\, dv. \tag{69}$$

Let a plane probe be at potential $-V$, so that electrons are repelled, and let

$$\phi = \frac{-2eV}{m} > 0. \tag{70}$$

The particle current density moving toward the probe at velocity v and at an angle θ relative to the normal is

$$dj = v \cos\theta\, f(v)\, d^3v. \tag{71}$$

For each v, only those electrons with $\theta < \theta^*$ will be energetic enough to strike the probe, where

$$v \cos\theta^* = \phi^{1/2}. \tag{72}$$

The minimum value of v is obviously $\phi^{1/2}$. The total current density striking the probe is thus the integral of (71) over these limits:

$$\begin{aligned} j &= \int_{\phi^{1/2}}^\infty v^3 f(v)\, dv \int_0^{\theta^*} 2\pi \sin\theta \cos\theta\, d\theta \\ &= \int_{\phi^{1/2}}^\infty \tfrac{1}{2} v g(v)\, dv \int_0^{\cos\theta^*} -\cos\theta\, d(\cos\theta) = \int_{\phi^{1/2}}^\infty \tfrac{1}{4} v g(v)\, dv [\cos^2\theta]_{\cos\theta^*}^0 \end{aligned} \tag{73}$$

$$j = \tfrac{1}{4} \int_{\phi^{1/2}}^\infty v g(v) \left(1 - \frac{\phi}{v^2}\right) dv. \tag{74}$$

If we differentiate with respect to ϕ, the integrated part drops out, leaving

$$\frac{dj}{d\phi} = \frac{1}{4} \int_{\phi^{1/2}}^\infty \frac{-g(v)}{v}\, dv.$$

A second differentiation yields

$$\frac{d^2j}{d\phi^2} = \tfrac{1}{4}\phi^{-1/2} g(\phi^{1/2})\, \tfrac{1}{2}\phi^{-1/2} = \frac{1}{8}\frac{g(\phi^{1/2})}{\phi}. \tag{75}$$

Thus the distribution function $g(v)$ is given by

$$g(\phi^{1/2}) = 8\phi j''. \tag{76}$$

Similar results have been obtained by Langmuir (*1*) for spherical and cylindrical probes.

Since a double differentiation of the probe curve is involved, the curve must be obtained extremely accurately before the distribution function can be found. This requires the plasma to be quiescent. A number of circuits have been given in the literature for performing the double differentiation electrically, by use of an oscillating probe voltage. In any case the accuracy required is such that this technique is not generally useful except in extremely quiescent plasmas.

3.3 Saturation Ion Currents: Unknown Electric Field

In the Langmuir theory it was assumed that the velocity distribution of the collected particles is known at the sheath edge. We have seen, however, in Section 2.3 that when the colder species is collected, as is usually the case in dealing with ion currents, the ions must have a drift velocity upon entering the sheath. Therefore, if the sheath edge is taken close to the probe, the ion velocity distribution is unknown. Alternatively, if one takes the sheath edge to be far away, to include the electric fields which impart this drift velocity to the ions, then an absorption radius exists, the condition (64) is not satisfied, and the Langmuir theory does not apply. This means that the ion current is not independent of the potential shape, and one must actually solve for the potential by using Poisson's equation. Since the ion density term in this equation is a complicated integral involving ion orbits, the solution cannot be given explicitly even in the simplest case.

In the case of a plane surface the ion drift velocity is acquired in the plasma region, where ion production exists. For spheres and cylinders this is not necessary, and a well-posed problem exists even if one neglects collisions and ionization everywhere. Before tackling the complexities of orbits, we shall examine the simple case of ions starting at rest, so that all motions are radial.

3.3.1 *Zero Temperature Limit*

This special case is the theory of Allen *et al.* (*16*) for a spherical probe. Let I be the total ion current; in the absence of collisions and ionization, I is conserved. If ions start from rest at ∞, where $V = 0$, their velocity at r, where the potential is V, is

$$v_i = \left(-\frac{2eV}{M}\right)^{1/2} = v_s \eta^{1/2}, \tag{77}$$

where

$$\eta = -eV/kT_e \qquad \text{and} \qquad v_s = (2kT_e/M)^{1/2}. \tag{78}$$

The ion density at r is given by this velocity, the area, and the current I:

$$n_1 = I/4\pi r^2 v_s \eta^{1/2}. \tag{79}$$

With n_e given by Maxwell's distribution, Poisson's equation in spherical coordinates is

$$\frac{1}{r^2}\frac{d}{dr}\left(r^2\frac{dV}{dr}\right) = -4\pi e\left(\frac{I}{4\pi r^2 v_s \eta^{1/2}} - n_0 e^{-\eta}\right). \tag{80}$$

Introducing the usual dimensionless length

$$\xi = r/h = r(4\pi n_0 e^2/kT_e)^{1/2}, \tag{81}$$

we can put this in the form

$$\frac{1}{\xi^2}\frac{d}{d\xi}\left(\xi^2\frac{d\eta}{d\xi}\right) = I(4\pi h^2 n_0 v_s \eta^{1/2}\xi^2)^{-1} - e^{-\eta}. \tag{82}$$

We define a current I_λ such that

$$I_\lambda = 4\pi h^2 n_0 v_s = (kT_e)^{3/2}(2/Me^4)^{1/2}. \tag{83}$$

From its form it is easy to see that I_λ is the random ion current crossing a Debye sphere, if the ions had the temperature of the electrons. Poisson's equation is, finally,

$$\left(\frac{d^2\eta}{d\xi^2} + \frac{2}{\xi}\frac{d\eta}{d\xi} + e^{-\eta}\right)\eta^{1/2}\xi^2 = \frac{I}{I_\lambda}. \tag{84}$$

An approximate solution of this can be obtained by defining a sheath edge. The quasi-neutral equation, which obtains in the plasma region, is

$$\eta^{1/2}e^{-\eta} = \frac{I}{I_\lambda}\xi^{-2}. \tag{85}$$

Differentiating this, we have

$$e^{-\eta}(\tfrac{1}{2}\eta^{-1/2} - \eta^{1/2})\frac{d\eta}{d\xi} = \frac{-2I}{I_\lambda}\xi^{-3}. \tag{86}$$

From this, we see that the coefficient of $d\eta/d\xi$ vanishes at $\eta = \frac{1}{2}$, so that $d\eta/d\xi$ must be infinite there. This point marks the breakdown of the quasi-neutral solution and may be defined as the sheath edge. If $\eta = \frac{1}{2}$ at the sheath edge, and $\xi \approx a/h$ there (a being the probe radius), then we have from Eq. (85)

$$I = I_\lambda a^2 h^{-2} 2^{-1/2} e^{-1/2} = A_a 2^{-1/2} e^{-1/2} n_0 v_s = 0.61 A_a (kT_e/M)^{1/2} n_0. \tag{87}$$

We give this approximate solution because Bohm (*3*) used the same method to evaluate I for the case of monoenergetic ions with non-

vanishing velocity. That calculation was very complicated because azimuthal motions had to be taken into account, but the method of approximation using a sheath edge was the same as given here. Bohm obtained coefficients of 0.57 and 0.54 instead of 0.61 in (87), for ion energies 0.01 and 0.5 times kT_e, respectively. Thus the saturation ion current is quite independent of kT_i and gives instead the product $n(kT_e)^{1/2}$. This is because ions are pulled into the sheath by a potential drop of order kT_e. The reverse would be true of saturation electron current if the electrons were colder than the ions.

The exact solution of Eq. (84) was obtained numerically by Allen *et al.* (*16*). Consider the asymptotic behavior of Eq. (84). The term corresponding to the ion density is $I/(I_\lambda \eta^{1/2}\xi^2)$. As $\xi \to \infty$ we see that if η varies asymptotically as ξ^{-4}, the ion density is finite at infinity. This is in contrast to the plane case, where as $v_i \to 0$, $n_i \to \infty$. If $\eta \to \xi^{-4}$, we see that η'' and $2\eta'/\xi$ approach zero, and (84) reduces asymptotically to the quasi-neutral equation, as expected. If we let $\zeta = \xi(I_\lambda/I)^{1/2}$, we have

$$\left(\frac{I_\lambda}{I}\right)^2 \left(\frac{d^2\eta}{d\zeta^2} + \frac{2}{\zeta}\frac{d\eta}{d\zeta} + e^{-\eta}\right)\eta^{1/2}\zeta^2 = 1. \tag{88}$$

The solutions of this for each value of I/I_λ agree at large ζ and are shown in Fig. 7a. The corresponding η–ξ curves are shown in Fig. 7b. The probe potential for each value of I is found by the intersection of the appropriate potential curve with a vertical line at $\xi = a/h$. The shape of part C of the probe characteristic is found from these intersections; this is shown in Fig. 7c for various values of a/h. This variation of I with V was not computed by Bohm (*3*).

3.3.2 *Finite Temperature: Orbital Motions*

When the ions have a finite angular momentum and can make orbits, the calculation of the ion density is so complicated that it will not be worthwhile to follow this in detail. Instead, we shall sketch the general procedure, following the method of Bernstein (*17*).

Suppose that we have a spherical probe at negative potential, that the electrons are Maxwellian, and that the ion distribution is known at some large radius λ where the collisionless region ends. If there is spherical symmetry, Boltzmann's equation has the general steady-state solution

$$f = f(E, J), \tag{89}$$

where E and J are the two constants of the motion, energy and angular

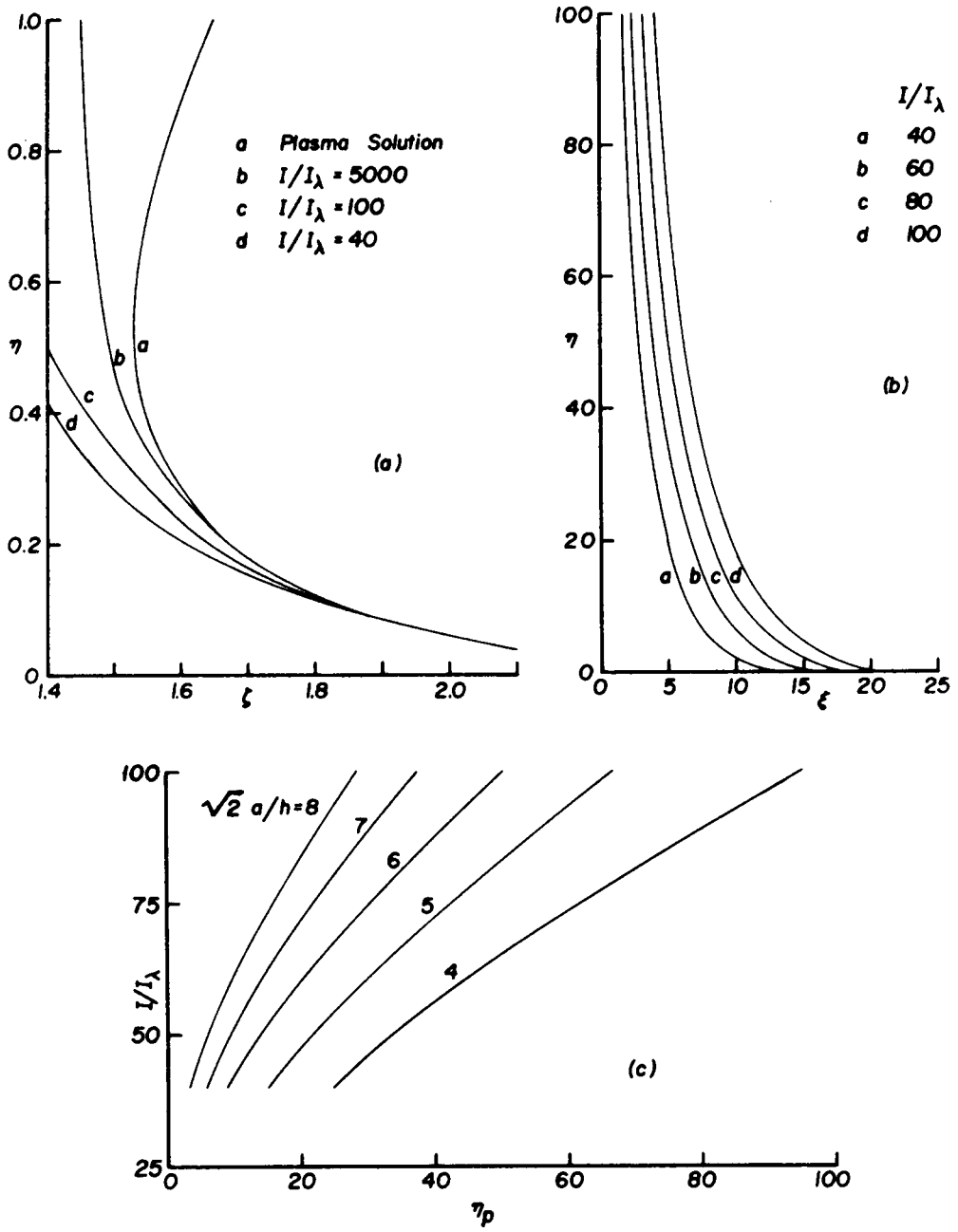

FIG. 7. Potential distribution (a) and (b), about a spherical probe in a cold-ion plasma, and the saturation ion probe characteristic (c). In (a) and (b), ζ and ξ are different normalizations of the radius. [J. E. Allen, R. L. F. Boyd, and P. Reynolds, *Proc. Phys. Soc.* (*London*) **B70**, 297 (1957).]

momentum. If u and v are the radial and tangential components of velocity, V the potential, and e the ion charge, we have

$$\begin{aligned} E &= \tfrac{1}{2} M(u^2 + v^2) + eV(r) \\ J &= Mrv. \end{aligned} \tag{90}$$

Solving for u, we have

$$\tfrac{1}{2} Mu^2 = E - eV - J^2/2Mr^2. \tag{91}$$

Thus it is convenient to define an effective potential energy U, such that

$$U(r, J) = eV(r) + J^2/2Mr^2. \tag{92}$$

The distribution $f(E, J)$ can be divided into f^+ and f^-, corresponding respectively to ions moving away from and toward the probe. The function f^- is assumed to be known at some large radius and is therefore known everywhere. The complexity of the problem comes from finding f^+. Obviously, f^+ will be zero for those orbits which intersect an absorbing probe and will be equal to f^- for those that do not. Thus in integrating over f to find the ion density to put into Poisson's equation, a procedure with which we are by now familiar, the domain of integration must be divided up, depending on whether $f^+ = 0$ or $f^+ = f^-$.

If $\lambda \gg a$ (λ and a being the mean free path and probe radius, respectively), one would expect that f^- would be almost Maxwellian at λ, since this distribution comes from ions which had a collision about λ cm away, and the probe subtends a very small angle at this distance. The distribution f^+ at λ will be depleted of those ions of low angular momentum which have hit the probe, but this small number does not greatly affect the total density there and does not affect the probe current, since these are particles traveling away from the probe. Thus the specification of f^- at λ should determine the problem if $\lambda \to \infty$, which is the regime of validity of the theory. Of course λ must not be equal to ∞, since all angular momenta are infinite there, and the specification of f^- at ∞ would not tell anything about the distribution of angular momenta at finite radii.

The classification of orbits is best described by Bernstein's diagram of the effective potential energy U (Fig. 8). For $J = 0$, the potential is everywhere negative, and the ion merely falls into the probe. For small J, we assume that the centrifugal force term in Eq. (92) dominates at sufficiently small radii, and there is a centrifugal barrier there. As J is increased, a maximum as well as a minimum will appear. At some critical J_c, the minimum will disappear, and there is only an inflection point. Finally, for very large J's the effective potential is always positive.

We note that for small J's there is a potential well. Ions trapped in this well will make closed orbits around the probe and never reach $r = \lambda$. Therefore, the population in these orbits will not be determined by the specification of $f^-(E, J)$ at $r = \lambda$ but will depend sensitively on collisions near the probe. The existence of such trapped ions would alter the potential distribution in a manner which is difficult to predict and would invalidate the theory. Hence one of the results of this theory is that the probe radius must be larger than the radius of the inflection point in J_c^2; then no potential minimum can exist outside the probe and no particles can be trapped.

Consider now a probe of radius R and the curve J_R^2 which has its maximum at R. All ions with energy higher than E_R, the energy of this

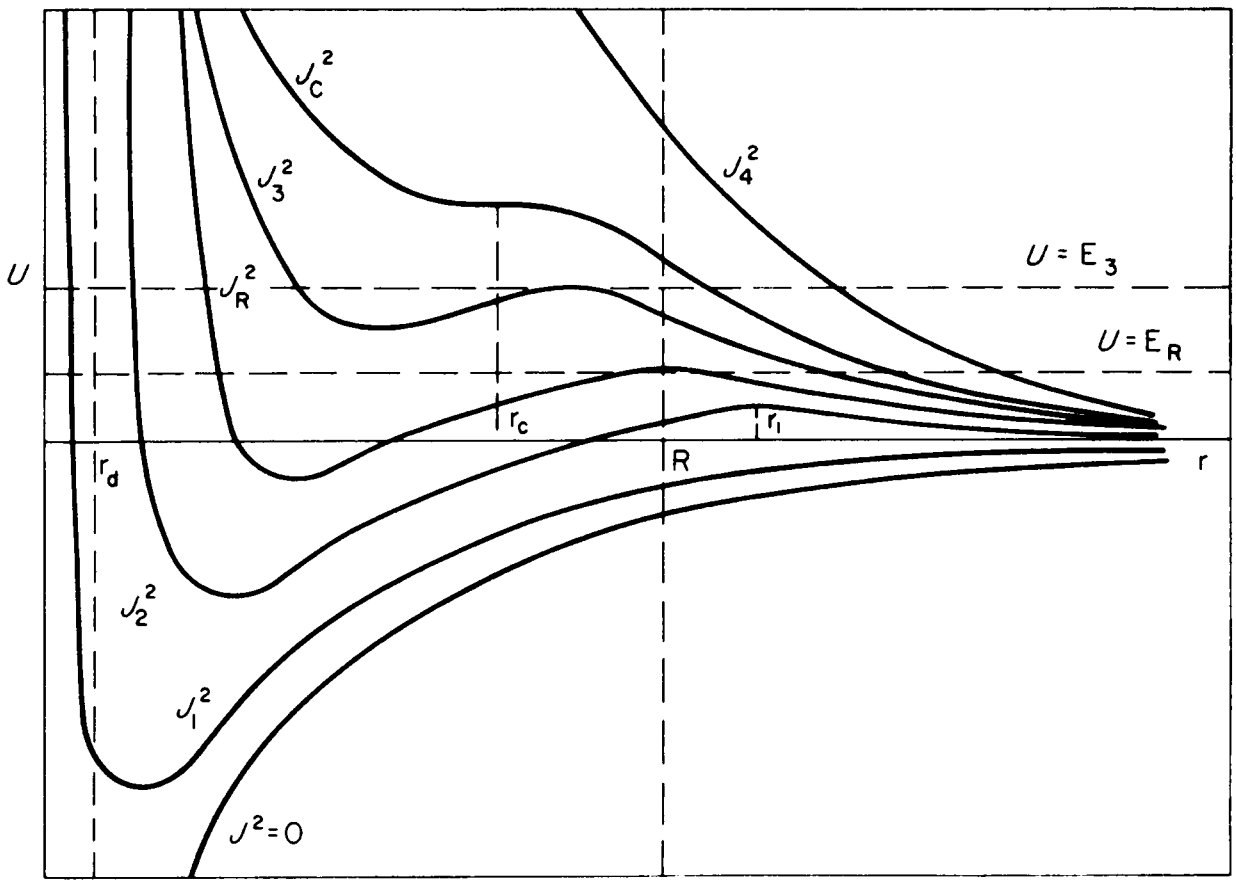

FIG. 8. Effective potential energy U as a function of radius, for various values of the angular momentum $\mathcal{J}$ of an ion incident upon a spherical probe. [I. B. Bernstein and I. Rabinowitz, *Phys. Fluids* **2**, 112 (1959).]

maximum, will be collected; and $f^+ = 0$ for such ions. Ions with $E < E_R$ will be either collected or reflected, depending on the relative magnitude of E and J^2. At any radius $r_1 > R$, the ions with E smaller than the magnitude of the maximum in U ar r_1 will not reach r_1, and therefore $f^+ = f^-$. Ions with very large energy or very small angular momentum will be collected, and for these $f^+ = 0$, $f^- = f^-$. Thus when the density is computed, the distribution f must be integrated over the E, J phase space; and this space must be divided up into regions, depending on the probe radius R, in which f^+ and f^- are related in different ways to the known function f^-.

The ion density appears, then, as a complicated integral. This must be set equal, in Poisson's equation, to the Laplacian of V in spherical coordinates, minus the Maxwellian electron density term. For the case of a continuous distribution of ion velocities at large radii, this integro-differential equation can be solved only by tedious numerical computation.

3.3.3 *Case of a Monoenergetic Isotropic Ion Distribution*

The integral in n_i can be evaluated if $f^-(E) \cong \delta(E - E_0)$. The solution of Poisson's equation still involves a difficult machine com-

putation, but this has been done by Bernstein and Rabinowitz (*17*). It has also been done by Bohm with E. H. S. Burhop and H.S.W. Massey (see *3*) for the numerically much easier case in which the conditions at a "sheath edge" are assumed (cf. Section 3.3.1). We shall examine the final equation in order to gain some insight into the nature of the solution.

The following dimensionless parameters are used:

$$\begin{aligned} \xi &= r(4\pi n_0 e^2/kT_e)^{1/2} \\ \iota &= 4I(e^2/kT_e v_s), \qquad v_s = (2kT_e/M)^{1/2} \\ \beta &= E_0/kT_e \\ \eta &= -eV/kT_e\,, \end{aligned} \tag{93}$$

where the notation is consistent with that used so far. In terms of these variables, Poisson's equation for the spherical case is

$$\begin{aligned} \frac{1}{\xi^2}\frac{d}{d\xi}\left(\xi^2\frac{d\eta}{d\xi}\right) &= \frac{1}{2}\left(1+\frac{\eta}{\beta}\right)^{1/2} + \frac{1}{2}\left(1+\frac{\eta}{\beta}-\frac{\iota}{\beta^{1/2}\xi^2}\right)^{1/2} - e^{-\eta}, \qquad \xi \geqslant \xi_0 \\ &= \frac{1}{2}\left(1+\frac{\eta}{\beta}\right)^{1/2} - \frac{1}{2}\left(1+\frac{\eta}{\beta}-\frac{\iota}{\beta^{1/2}\xi^2}\right)^{1/2} - e^{-\eta}, \qquad \xi \leqslant \xi_0 \end{aligned} \tag{94}$$

where ξ_0 is determined by the condition that the second bracket on the right-hand side and its derivative vanish at ξ_0. It is the radius at which the maximum in the curve of $U(r)$ has a height equal to the initial ion energy E_0. For $\xi < \xi_0$ the ion density is smaller than for $\xi > \xi_0$, because a number of ions are reflected by the potential hill to the right.

If we keep β finite and let ξ go to ∞ in (94) and expand in small η/β, the first of Eqs. (93) becomes

$$\frac{1}{\xi^2}\frac{d}{d\xi}\left(\xi^2\frac{d\eta}{d\xi}\right) \cong 1 + \frac{1}{2}\frac{\eta}{\beta} - \frac{1}{4}\frac{\iota}{\beta^{1/2}\xi^2} - (1-\eta) = \eta\left(1+\frac{1}{2\beta}\right) - \frac{1}{4}\frac{\iota}{\beta^{1/2}}\frac{1}{\xi^2}\,. \tag{95}$$

Thus if η goes asymptotically as ξ^{-2}, the right-hand side can be made to vanish for large ξ; this is the behavior expected in the plasma region.

On the other hand, if we let β (essentially the ion temperature) go to 0 *first*, ξ_0 must go to ∞ to make the second bracket on the right-hand side of (94) vanish. Thus we must expand the second of Eqs. (94) for *large* η/β. This gives

$$\begin{aligned} \frac{1}{\xi^2}\frac{d}{d\xi}\left(\xi^2\frac{d\eta}{d\xi}\right) &= \frac{1}{2}\left(\frac{\eta}{\beta}\right)^{1/2}\left(1+\frac{1}{2}\frac{\beta}{\eta}\right) - \frac{1}{2}\left(\frac{\eta}{\beta}\right)^{1/2}\left(1+\frac{1}{2}\frac{\beta}{\eta}-\frac{\iota\beta^{1/2}}{2\eta\xi^2}\right) - e^{-\eta} \\ &= \frac{1}{4}\frac{\iota}{\eta^{1/2}\xi^2} - e^{-\eta}. \end{aligned} \tag{96}$$

This is the same as (84) derived before for $T_i = 0$. Here η must behave asymptotically as ξ^{-4} to achieve quasi-neutrality at large ξ.

The solution thus has the nature of a boundary-layer problem in which η satisfies different equations for large and small ξ, and the solutions are matched at some radius, in this case ξ_0. When the ions are strictly cold, the region of large ξ is never reached. This explains why the solution of Allen *et al.* goes as ξ^{-4} instead of ξ^{-2}, as in the case of finite β. In practice ξ can never be allowed to go to infinity but only to some large distance λ. Whether η goes as ξ^{-2} or ξ^{-4} near λ will depend on whether λ is larger or smaller than ξ_0, which, in turn, depends on the smallness of β.

For any given ι, (94) gives a curve of η versus ξ. These curves may then be cross-plotted to give the probe characteristic for a given value of ξ. An example of such normalized I_i–V curves is given in Fig. 9.

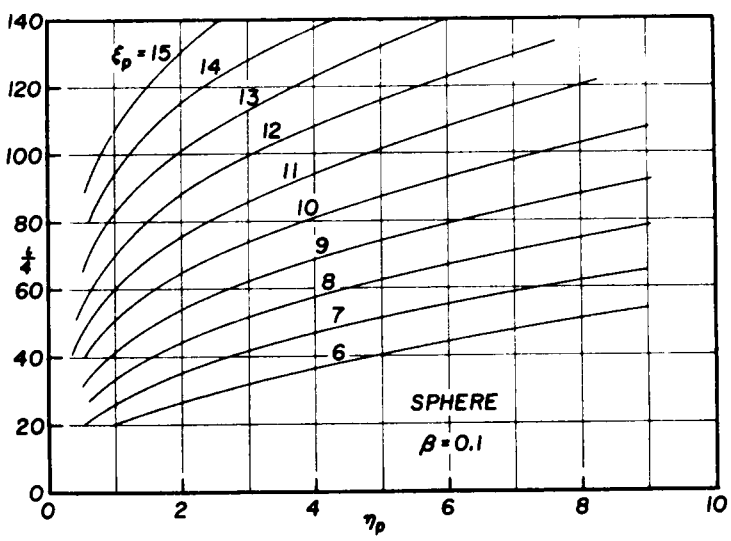

FIG. 9. Saturation ion current characteristics for spherical probes of various sizes in a plasma with a monoenergetic isotropic distribution of ions of energy $E_0 = \beta k T_e$. [I. B. Bernstein and I. Rabinowitz, *Phys. Fluids* 2, 112 (1959).]

Further computational results are given by Chen (*18*). The dependence on ion energy is exemplified by the curves of Fig. 10 for $\xi_p = 10$. Such a cross-plot must be made for each probe. One notes that the variation of probe current with ion temperature is slight ($\sim$20%), in agreement with Bohm (*3*). This result also justifies the use of a delta function distribution for the ions.

The case of a cylindrical probe has also been worked out analogously by Bernstein (*17*). In this case the appropriate dimensionless variables are the same as in Eq. (93) with the exception

$$\iota = \frac{\pi e^2}{k T_e} \frac{m}{2E_0} \frac{I^2}{n_0}. \tag{97}$$

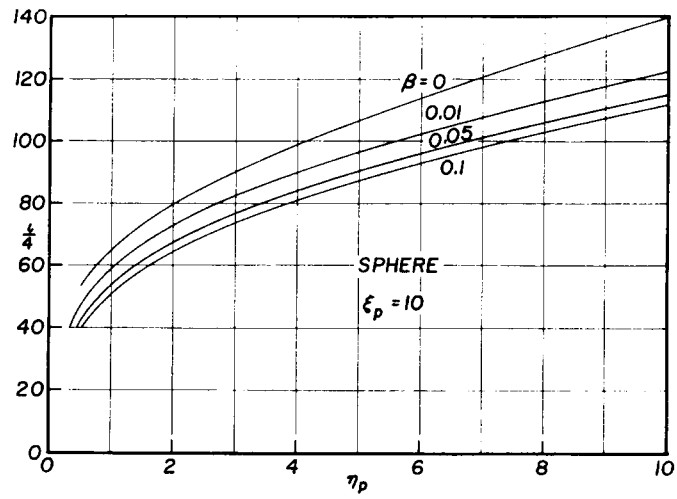

FIG. 10. Dependence of the saturation ion current characteristic on ion energy $E_0 = \beta k T_e$, for a probe radius of $10h$. [I. B. Bernstein and I. Rabinowitz, *Phys. Fluids* **2**, 112 (1959).]

The equation for a cylindrical probe is then

$$\frac{1}{\xi}\frac{d}{d\xi}\left(\xi\frac{d\eta}{d\xi}\right) = 1 - \frac{1}{\pi}\sin^{-1}\left(\frac{\iota/\xi^2}{1+\eta/\beta}\right)^{1/2}, \qquad \xi \geqslant \xi_0$$

$$= \frac{1}{\pi}\sin^{-1}\left(\frac{\iota/\xi^2}{1+\eta/\beta}\right)^{1/2}, \qquad \xi \leqslant \xi_0 . \tag{98}$$

The absorption radius ξ_0 is the point at which the argument of $\sin^{-1}$ is unity. This formula is valid for an ion distribution at ∞ which is independent of J_z and which is an arbitrary function of the velocity component parallel to the probe axis. Note that this is *not* an isotropic distribution. Typical probe characteristics for a cylinder are shown in Fig. 11. Further data are given by Chen (*18*). In Fig. 11 we have plotted the function $Y = \pi^{-1}(\beta\iota)^{1/2}\xi_p$, which is more convenient to use because it is independent of n_0. To obtain n_0, one computes the ordinate from the experimental data and the known value of kT_e and places the experimental points on the diagram. The value of ξ_p resulting from the best fit then gives the value of h, and hence of n_0.

The method of Bernstein and Rabinowitz is not easy to use experimently because of the dimensionless variables and the difficult computations necessary. Fortunately, this theory is necessary only for small probes; that is, for small values of $\xi_p = a/h$. For large ξ_p and η_p (the probe voltage), a recent boundary-layer analysis by Lam (*19*) gives the solution of Eq. (94) or (98) in terms of a single universal curve. In Lam's theory it is shown that a continuous solution of these equations can be constructed from the solutions in four distinct regions: a quasi-

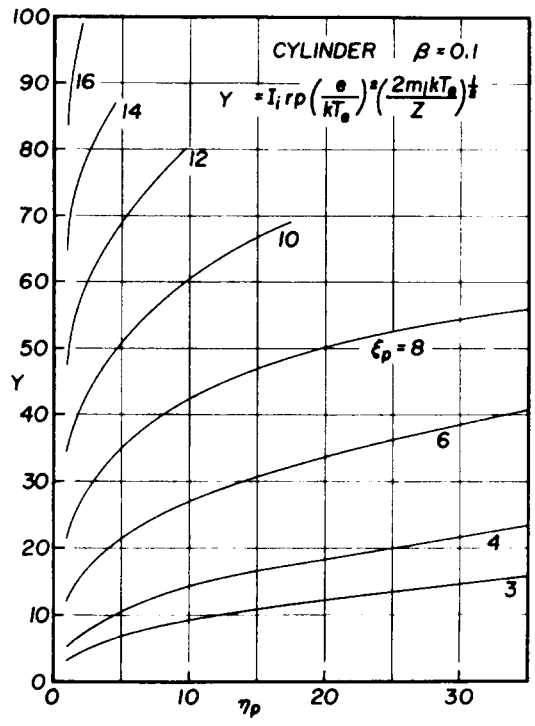

FIG. 11. Saturation ion current characteristics for cylindrical probes of various sizes in a plasma with an isotropic distribution of projected ion velocities [F. F. Chen, *J. Nucl. Energy*: *Pt. C* **7**, 47 (1965).] Only one value of β is shown because of the insensitivity to β.

neutral region in which the Laplacian of η can be neglected, two transitional layers, and the sheath region in which n_e is negligible. Furthermore, it is shown rigorously that the thickness of the transitional layers is of order $\xi_p^{-4/5}$, so that for large probes Langmuir's assumption of a well-defined sheath edge is accurate to this order. To compute the potential distribution, one has only to locate the sheath edge by finding where the quasi-neutral solution $\eta(\xi)$ has infinite slope and therefore breaks down, and then to use this sheath edge to solve the Langmuir-Blodgett sheath problem [cf. Eqs. (30) and (31)].

The theory of Lam (*19*) provides a convenient procedure for finding the ion probe charaeteristic or the plasma density. To find the I_i–V curve for highly negative probes for given values of n_0, kT_e, and kT_i, one uses the diagram of Fig. 12. The parameter A depends on the position of the sheath edge and is a function of $\beta = E_0/kT_e$. In fact, the ion temperature appears only in A. For $\beta \lesssim 0.2$, A is insensitive to β and may be approximated by a constant. To use Fig. 12, one needs the following definitions:

$$\eta_p = -eV_p/kT_e, \qquad \xi_p = r_p/h, \qquad v_s = (2kT_e/m_i)^{1/2} \tag{99}$$

$$\text{Sphere:} \qquad A \cong 1.9, \qquad I_B \cong 1.5\pi r_p^2 n_0 v_s \tag{100}$$

$$\text{Cylinder:} \qquad A \cong 2.2, \qquad I_B \cong 1.9 r_p n_0 v_s \tag{101}$$

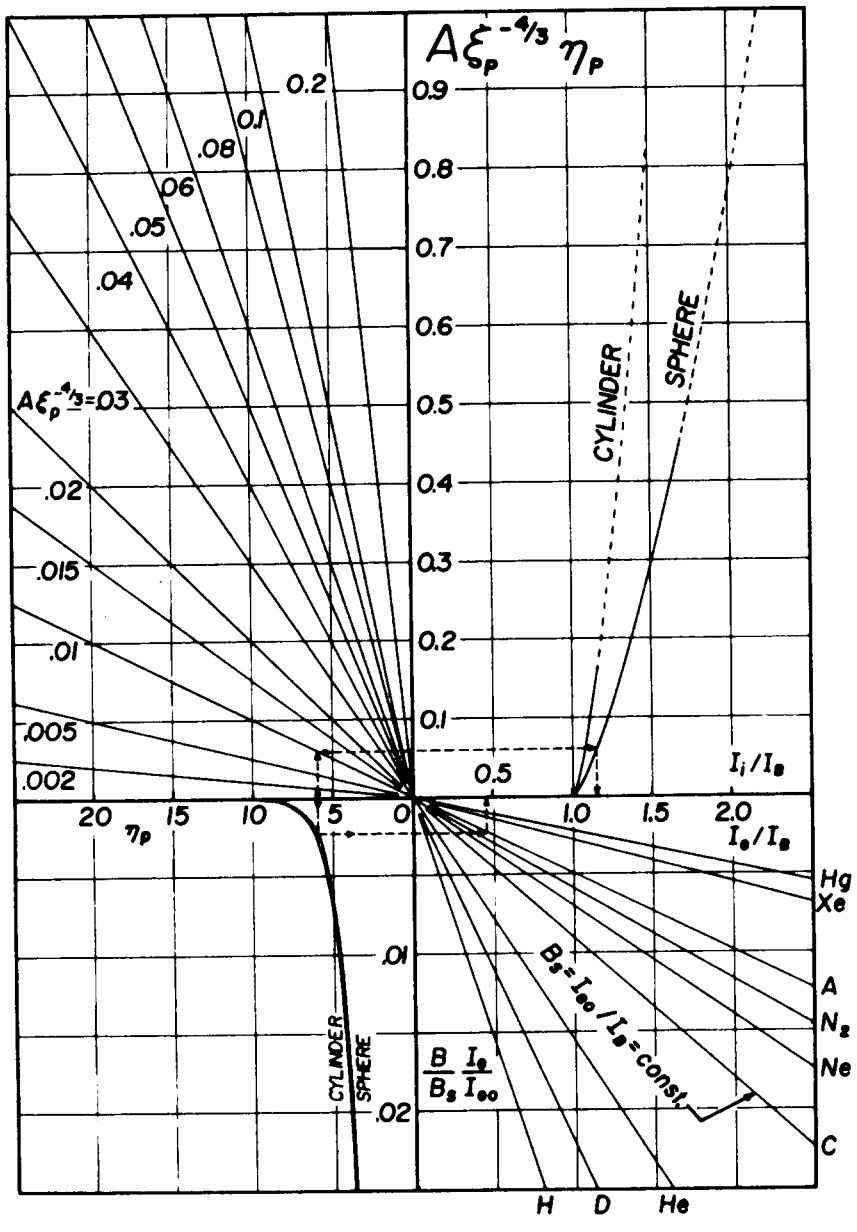

FIG. 12. Lam diagram for computation of probe characteristics for given probe and plasma parameters. The dashed portions indicate ranges where trapped ions are possible. The curves for a cylinder and a sphere are not directly comparable, because slightly different velocity distributions were used.

The curve $I(\eta_p)$ is then found by following a path like the dotted one shown in the upper half plane. The current I_B is essentially the current predicted by Bohm (*3*). It is also a weak function of β for small β, but we have approximated the coefficient in I_B by a constant. It is clear from Fig. 12 that I_B is the ion current in the limit of large ξ_p or small η_p, when the sheath is infinitely thin compared with the probe radius. The increase of I over I_B as η_p is increased is a consequence of the increase in sheath thickness; this effect was neglected in the work of Bohm *et al.* (*3*). This variation of sheath thickness is given also by the Langmuir–Blodgett formulas (30) and (31), but in Langmuir's theory the acceleration of ions in the quasi-neutral region, resulting in the $(kT_e)^{1/2}$ dependence of I_B, was neglected.

The total probe current also contains an electron component which may not be negligible at the smaller values of η_p . The value of I_e for a Maxwellian electron distribution may be found from the lower half of Fig. 12. The relative importance of I_e obviously depends on m_i/m_e ; hence there is one curve for each element. The dashed portions of the ion curves indicate the region in which trapped ions are possible. However, there has been no experimental evidence that trapped ions affect the probe current appreciably even if η_p is very large.

To find the plasma density n_0 from a single measurement of I_i , it is easier to use Figs. 13 and 14 and the following formulas:

$$\text{Sphere:} \qquad -\frac{V_p}{(eI_i)^{2/3}} = \left(\frac{m_i}{2e}\right)^{1/3} A_s(\tau), \tag{102}$$

$$\text{Cylinder:} \qquad -\frac{V_p}{(eI_i r_p)^{2/3}} = \left(\frac{2m_i}{e}\right)^{1/3} A_c(\tau) \tag{103}$$

$$\tau = I_i/I_B \, . \tag{104}$$

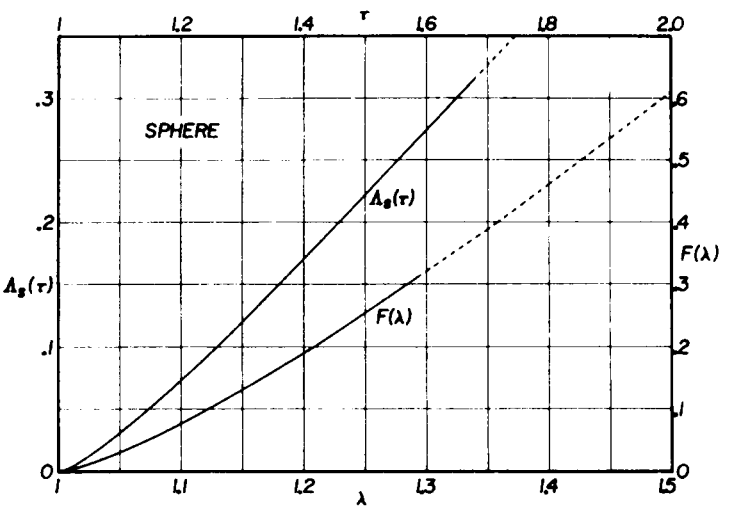

FIG. 13. The functions $A_s(\tau)$ and $F(\lambda)$ used in the theory of Lam for computing the plasma density from the saturation ion current to a spherical probe. The dotted portions indicate the possibility of ion trapping.

The left-hand side of Eq. (102) or (103) can be computed from the measured current, and the value of A_s or A_c can be found from Fig. 13 or 14. The resulting value of τ gives I_i/I_B , and hence I_B and n_0 , from Eq. (100) or (101).

3.3.4 *Summary of Theories of Ion Collection*

All of the theories presented so far are valid only for strictly collisionless, quiescent plasmas without magnetic fields. The geometry of the probe is assumed to be an ideal sphere with no supporting wires, or an

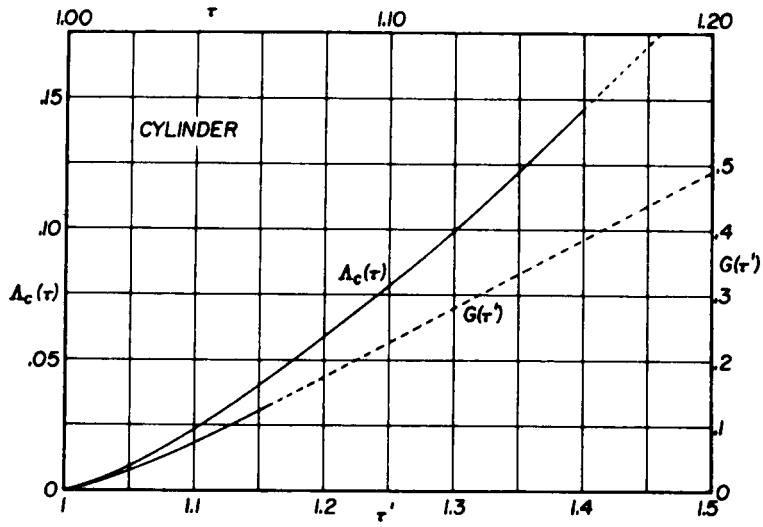

FIG. 14. The functions $A_c(\tau)$ and $G(\tau')$ used in the theory of Lam for computing the plasma density from the saturation ion current to a cylindrical probe. The dotted portions indicate the possibility of ion trapping.

infinite cylinder with no end effects. In all cases the electron distribution is assumed to be Maxwellian; the collection of electrons at low voltages, which changes the electron concentration and hence the potential near the probe, is neglected.

The original Langmuir theory (Section 3.1.2) is valid for very low densities and small probes, where an absorption radius larger than the probe radius does not exist. This condition is generally not satisfied in ion collection if the ions are colder than the electrons. However, this theory may be applicable in the tenuous plasmas of outer space or in the case that the probe is an extremely thin wire.

The theory of Bohm, Burhop, and Massey (see *3*) concerns the case of a spherical probe and monoenergetic ions of energy 0.01 and 0.5 times kT_e. The dependence on ion energy was found to be slight, and the approximate result for saturation ion flux was found to be

$$I = \tfrac{1}{2} n_0 A \left(\frac{kT_e}{M}\right)^{1/2}, \tag{105}$$

where A is the probe area, n_0 the plasma density, and M the ion mass. In deriving this result the approximation of a "sheath edge" was made; consequently, no dependence on probe voltage is given. The formula (105) is thus quite inexact but nonetheless quite useful. It shows immediately the dependence on the plasma parameters, and it gives an absolute number which can be compared quickly with experiment. To this order of accuracy Eq. (105) can be used even for nonspherical probes and probes in a magnetic field, provided the appropriate area is substituted for A. This gives an immediate order-of-magnitude check on the plasma density. The density profile is given more accurately than the absolute

density provided the electron temperature can be assumed to be constant or if its profile is known.

To take into account the variation of I with V, one must use the theory of Lam, which is valid for large values of ξ_p and η_p and for cylindrical as well as spherical probes. The results are summarized by Figs. 12, 13, and 14 and Eqs. (99–104). The dependence on ion temperature is slight and has been neglected here, but it is given by Lam (*19*) and by Chen (*18*).

For probes so small that the condition $\xi_p \gg 1$ is not fulfilled, numerical computations are necessary. The theory of Allen *et al.* (Section 3.3.1) is for a spherical probe and is limited to completely cold ions. The solution is exact to large radii, and the variation of ion current with probe voltage (i.e., the shape of part C of the characteristic) is given graphically. Since the dependence on ion temperature is small, the assumption of zero temperature is not restrictive. Comparison with experiment must be done graphically, and a separate cross-plot of the given curves must be made for each value of the probe radius measured in Debye lengths. This theory has the advantage that the equation is fairly easy to solve numerically, so that curves for additional values of the parameters can readily be obtained.

The theory of Bernstein and Rabinowitz (Section 3.3.3) is the most accurate and the most difficult to use. Again the solution is carried to large radii, and the variation with voltage given. Moreover, finite ion energies are considered; and the important cylindrical case is given as well as the spherical case. Comparison with experiment, however, involves a tedious process of cross-plotting and reduction of dimensionless parameters to real variables, for each assumed value of the plasma parameters. The numerical solution is so complicated that curves other than the ones given are difficult and expensive to obtain.

The case of a continuous distribution of ion energies necessitates an even more tedious computation, unless $T_i \gg T_e$ so that Langmuir's theory of Section 3.1.1 can be used. However, because of the insensitivity to ion energy, this problem is not expected to give an answer much different from those already obtained. All these theories suffer from the fact that the electric field from the probe accelerates ions from large distances; hence collisions and external electric fields, such as those required to maintain the discharge, are apt to influence the probe current.

4 Probe Theory in the Presence of Collisions

In weakly ionized plasmas at high pressures the results of the previous section will be modified by collisions between the collected particles

and neutral atoms. The species repelled by the probe will not be greatly affected by collisions, since it is ordinarily assumed to be in thermal equilibrium anyway. We now consider the effects of collisions, not because the case of high pressures is important in modern plasmas but because this is a necessary prelude to the case of strong magnetic fields, in which particles can move transversely *only* by collisions.

The effects of collisions on the foregoing theory are twofold. First, if the mean free path λ is less than the characteristic length of the potential (roughly h), the equation of motion of particles in the sheath will differ from the free-fall equation, and one would expect that the potential profile and hence the probe current would be altered. Second, if λ is not considerably larger than the probe radius a, the distribution of velocities at the edge of the collisionless region will differ from the undisturbed distribution, since the probe is large enough to block a nonnegligible portion of the particles arriving at this edge. This depletion of the plasma at the boundary of the collisionless region can be calculated only by considering the collision-dominated region. Thus the effects of collisions must be considered if either the condition $\lambda \gg h$ or the condition $\lambda \gg a$ is not satisfied.

4.1 Probe at Space Potential

The second effect, that of depletion of the plasma when $\lambda \gg a$ is not satisfied, can be readily illustrated in the case of a probe at space potential, when there are no electric fields to be taken into account. The treatment of Bohm *et al.* (*3*) is valid for almost any shape of probe.

Consider a probe of area A_p and any convex shape immersed in a plasma. One mean free path λ from its surface we draw an imaginary surface of area A_λ. Outside this surface we shall assume that particle motion is collision dominated, while inside the motion is collisionless. If n_λ is the density at the surface A_λ, and if the velocity distribution were isotropic there, as would be the case if $A_p \ll A_\lambda$, the random flux crossing A_λ inwards would be

$$j_r = \tfrac{1}{4} n_\lambda \bar{v}, \tag{106}$$

where $\bar{v}$ is the average magnitude of the thermal velocity. The current striking the probe would then be this times the probe area:

$$I = \tfrac{1}{4} n_\lambda \bar{v} A_p . \tag{107}$$

On the other hand, if $A_p \to A_\lambda$, that is, if the mean free path is so short that the surface A_λ is very close to the surface A_p, then the distribution at A_λ cannot be isotropic, since there cannot be any particles there

coming from the probe. In this case the density n_λ is only half as large, and the probe current is instead

$$I = \tfrac{1}{2} n_\lambda \bar{v} A_p \,. \tag{108}$$

In general, for arbitrary λ,

$$I = \frac{n_\lambda \bar{v} A_p}{4K}, \tag{109}$$

where K is a constant varying between 1 and $\frac{1}{2}$, depending on the relative magnitude of A_λ and A_p .

The current I can be computed another way. In the region outside A_λ, the particle current density is controlled by diffusion and mobility and is given by

$$\mathbf{j} = -D\nabla n - \mu n \nabla V, \tag{110}$$

D and μ being the coefficients of diffusion and mobility, respectively. Since the probe is at space potential, we shall assume that there are no electric fields, and ∇V vanishes. We shall examine this assumption later. In the exterior region j is conserved, so that $\nabla \cdot \mathbf{j} = 0$. From Eq. (110) we see that if D is constant,

$$\nabla \cdot \mathbf{j} = -D\nabla^2 n = 0. \tag{111}$$

The probe current is the integral of the normal component of $\mathbf{j}$ over any surface enclosing the probe. Choosing this surface to be A_λ, we have

$$I = \int_{A_\lambda} -\mathbf{j} \cdot d\mathbf{s} = D \int_{A_\lambda} \nabla n \cdot d\mathbf{s}, \tag{112}$$

$\mathbf{j}$ and $d\mathbf{s}$ being oppositely directed. This integral depends only on the geometry of the surface A_λ, since n is a harmonic function outside A_λ. This can be seen by making an analogy with the problem of electrostatics.

Consider a conductor with a surface A_λ immersed in a vacuum. Outside A_λ, the potential V satisfies Laplace's equation $\nabla^2 V = 0$. Integrating Poisson's equation

$$\nabla^2 V = -4\pi\rho$$

over the volume inside A_λ, we have for the total charge on the conductor

$$-4\pi q = \int \nabla^2 V \, d^3r = \int_{A_\lambda} \nabla V \cdot d\mathbf{s}. \tag{113}$$

We know that q depends only on the geometry and is given by the capacitance of the surface A_λ:

$$q = C(V_\lambda - V_\infty). \tag{114}$$

Since n and V satisfy the same equations, we can make an analogy between I and q. From Eqs. (112)–(114), we have

$$I = -4\pi qD = -4\pi CD(V_\lambda - V_\infty) = 4\pi CD(n_0 - n_\lambda), \tag{115}$$

n_0 being the density at ∞.

Now we can equate this to the value of I computed for the collisionless region (109):

$$I = 4\pi CD(n_0 - n_\lambda) = n_\lambda \bar{v} A_p/4K. \tag{116}$$

Solving for n_λ and I, we have

$$n_\lambda = n_0 \frac{4\pi CD}{4\pi CD + \bar{v}A_p/4K}, \tag{117}$$

and

$$I = \frac{\bar{v}A_p}{4K} n_0 \frac{4\pi CD}{4\pi CD + \bar{v}A_p/4K} = \frac{n_0 \bar{v} A_p}{4} \left(K + \frac{\bar{v}A_p}{16\pi CD}\right)^{-1}. \tag{118}$$

Specializing now to the case of a sphere, we have that $A_p = 4\pi a^2$ and $C = a + \lambda$, this being the capacity of a sphere of radius $a + \lambda$. Since the classical diffusion coefficient is

$$D = \frac{\lambda \bar{v}}{3}, \tag{119}$$

the probe current becomes

$$I = \tfrac{1}{4} n_0 \bar{v} A_p \left(\frac{3}{4}\frac{a}{\lambda}\frac{a}{a+\lambda} + K\right)^{-1}. \tag{120}$$

In the limit of large λ/a, K becomes unity and Eq. (120) reduces to the collisionless random current, $I = n_0 \bar{v} A_p/4$. In the limit $\lambda \ll a$ Eq. (120) becomes

$$I = \frac{n_0 \bar{v} A_p}{4} \cdot \frac{3}{4}\frac{\lambda}{a}. \tag{121}$$

Thus in the limit of small λ, collisions reduce the probe current by approximately a factor λ/a.

We now return to the assumption of zero electric field. The expression for n_λ [Eq. (117)] is of course valid for either species of particle, as are all the formulas in this section. Since $D \sim \lambda\bar{v}$, $\bar{v}$ will cancel out of the equation. All the remaining parameters depend only on geometry, except λ. Thus if λ is different for ions and electrons, n_λ will differ, and an electric field must be set up to re-establish quasi-neutrality. Consequently, for small λ/a it is not really possible to bias a probe at space potential, since its very presence changes the space potential. Our derivation of (121) must therefore be regarded as approximate.

4.2 Saturation Current in the Limit $\lambda \ll h$

We now consider the opposite extreme when a large voltage is put on the probe and electric fields are important. The problem is simplified if we assume that the mean free path is much shorter than any other length in the problem, including the Debye length, so that particle motion is collision-dominated everywhere, even in the sheath. We shall then see how this "diffusion sheath" differs from the collisionless sheaths we have considered up to now. We shall pay particular attention to the case of a cylindrical probe for two reasons: the integrals are tractable, and the result may be directly applicable to the case of a strong magnetic field.

4.2.1 *Cylindrical Probe*

Let an infinite cylindrical probe of radius a be immersed in a plasma of density n_0. Let particles 1 be collected so that e_1V is negative, and let the potential be so high that particles 2 are essentially Maxwellian. Further, let the motion of particles 1 be completely collision-dominated, so that the flux is describable in terms of a diffusion coefficient D and a mobility μ (pertinent to species 1):

$$\mathbf{j}_1 = D\nabla n_1 - \mu n_1 \nabla V. \tag{122}$$

Poisson's equation is

$$\nabla^2 V = -4\pi e_1(n_1 - n_0 e^{-e_2 V/kT_2}). \tag{123}$$

For any probe current I, j_1 is known since I is conserved, and these two equations may be solved simultaneously for n_1 and V. To make further progress, we must now make the first of two important simplifications: that the probe potential is so large compared to kT_1 that the D term in Eq. (122) can be neglected relative to the μ term. This can be seen as follows. If Λ_n and Λ_v are the characteristic lengths of the

gradients of n and V, then in view of Einstein's relation for classical diffusion,

$$\mu = \frac{eD}{kT}, \tag{124}$$

we have

$$\frac{D\nabla n_1}{\mu n_1 \nabla V} \approx \frac{kT_1}{eV}\frac{\Lambda_V}{\Lambda_n}. \tag{125}$$

Providing that the Λ's are of the same order of magnitude, the D term is smaller than the μ term by the ratio kT_1/eV.

With this simplification, (122) gives the ion density:

$$n_1 = \frac{-j_1}{\mu \nabla V}. \tag{126}$$

In cylindrical symmetry, the total current I per unit length to the probe is

$$I = -2\pi r j_1. \tag{127}$$

With $e_2 = -e_1$, Poisson's equation now becomes, in cylindrical coordinates,

$$\frac{1}{r}\frac{d}{dr}\left(r\frac{dV}{dr}\right) = -4\pi e_1\left[\frac{I}{2\pi r\mu\, dV/dr} - n_0 e^{e_1 V/kT_2}\right]. \tag{128}$$

In dimensionless form this becomes

$$\frac{1}{\rho}\frac{d}{d\rho}\left(\rho\frac{d\eta}{d\rho}\right) = \frac{-\iota}{\rho\, d\eta/d\rho} - e^{-\eta}, \tag{129}$$

where

$$\begin{aligned} \eta &= -e_1 V/kT_2 \\ \rho &= r/h, \qquad h^2 = kT_2/4\pi n_0 e_1^2 \\ \iota &= I/I_0 \\ I_0 &= 2\pi n_0 \mu_1 kT_2/e_1. \end{aligned} \tag{130}$$

From Eq. (129) it is clear that a quasi-neutral solution at large radii can be obtained only if $d\eta/d\rho$ approaches $-\iota/\rho$ as ρ approaches ∞ and η approaches 0. Then the right-hand side vanishes at ∞, corresponding to equal charge densities. Thus the asymptotic behavior of η is

$$\eta \underset{\rho\to\infty}{\to} \int_\infty^\rho \frac{d\eta}{d\rho}\, d\rho \to \int_\infty^\rho \frac{-\iota}{\rho}\, d\rho. \tag{131}$$

This integral diverges, so that strictly speaking the cylindrical problem in not a well-formulated one. Consideration of the D term, which we neglected, does not help the asymptotic behavior; the potential simply falls so slowly that one would expect an infinite current per centimeter to a cylindrical probe. In actuality this, of course, does not happen because there are (a) ionization and (b) end effects, so that I is not strictly constant with radius. From (131) it is apparent that any decrease, however slight, of I and hence of ι will make the integral converge. The cylindrical probe at high pressures is therefore not a true probe in that its influence necessarily extends into the region where ion production is important.

The solution of (129) can be found if we impose a "sheath edge" at $r = s$ or $\rho = \sigma$ and assume that $d\eta/d\rho = 0$ at $\rho = \sigma$. To solve this analytically we must also make our second approximation: that the potential is so high that the density of particles 2 can be neglected. Then Poisson's equation becomes

$$\frac{1}{\rho}\frac{d}{d\rho}\left(\rho\frac{d\eta}{d\rho}\right) = \frac{-\iota}{\rho\, d\eta/d\rho},$$

or

$$\frac{1}{\rho}\frac{df}{d\rho} = \frac{-\iota}{f}, \qquad f\frac{df}{d\rho} = -\iota\rho \tag{132}$$

where

$$f(\rho) = \rho\frac{d\eta}{d\rho}.$$

Integrating from σ to ρ, we have

$$\tfrac{1}{2}f^2 = \tfrac{1}{2}\rho^2\left(\frac{d\eta}{d\rho}\right)^2 = \frac{\iota}{2}(\sigma^2 - \rho^2), \tag{133}$$

$$\frac{d\eta}{d\rho} = \iota^{1/2}\left(\frac{\sigma^2}{\rho^2} - 1\right)^{1/2}, \tag{134}$$

$$\eta - \eta_s = \iota^{1/2}\int_\sigma^\rho \left(\frac{\sigma^2}{\rho^2} - 1\right)^{1/2} d\rho. \tag{135}$$

carrying out the integration, we find finally that

$$\eta - \eta_s = \iota^{1/2}\left\{(\sigma^2 - \rho^2)^{1/2} - \sigma\log\left[\frac{\sigma}{\rho} + \left(\frac{\sigma^2}{\rho^2} - 1\right)^{1/2}\right]\right\}, \tag{136}$$

where $\sigma/\rho = s/a$. This is, then, the high-pressure equivalent of the Langmuir–Blodgett space-charge equation (30). If we convert (136)

back to esu by (130), we will find that the dependences on kT_e and n_0 cancel out; and, aside from the geometrical factor, the current I is proportional to $(V - V_s)^2$, as contrasted with $(V - V_s)^{3/2}$ in the collisionless case.

The condition $\lambda \ll h$ is usually not fulfilled in highly ionized plasmas, and this theory is then inapplicable. However, if there is a strong magnetic field, the mean free path is effectively reduced to r_L, the Larmor radius, in directions perpendicular to the field; and this may, for electrons, become smaller than s. Since in the case of the infinite cylinder all motions are transverse to the axis, this theory is directly applicable in strong magnetic fields if μ is replaced by $\mu_\perp$, or $\mu/\omega^2\tau^2$. However, an independent determination of the sheath thickness s is required.

4.2.2 *Spherical Probe*

The case of a sphere is entirely similar, except that one must replace Eq. (127) by

$$I = -4\pi r^2 j_1 \tag{137}$$

and Eq. (130) by

$$I_0 = 4\pi h n_0 \mu k T_2/e_1 \,. \tag{138}$$

Poisson's equation in spherical coordinates is then

$$\frac{1}{\rho^2}\frac{d}{d\rho}\left(\rho^2 \frac{d\eta}{d\rho}\right) = \frac{-\iota}{\rho^2\, d\eta/d\rho} - e^{-\eta}. \tag{139}$$

In order to achieve a quasi-neutral solution, we must have for large ρ,

$$\frac{d\eta}{d\rho} \to \frac{-\iota}{\rho^2} \tag{140}$$

or

$$\eta \to \frac{\iota}{\rho} \,. \tag{141}$$

In this case the potential *does* fall fast enough to allow a solution which does not depend on conditions far from the probe.

If we neglect the exponential term and make the transformation $x = 1/\rho$, Eq. (139) becomes

$$x^4 \frac{d^2\eta}{dx^2} = \iota \frac{dx}{d\eta}$$

$$\frac{d^2\eta}{dx^2}\frac{d\eta}{dx} = \frac{\iota}{x^4} \,. \tag{142}$$

In neglecting $e^{-\eta}$ we have, however, destroyed the asymptotic behavior and must assume a sheath edge at x_s. The last equation can be integrated once from x_s to x to give

$$\frac{d\eta}{dx} = \left(\frac{2}{3}\iota\right)^{1/2}\left(\frac{1}{x_s^3} - \frac{1}{x^3}\right)^{1/2}. \tag{143}$$

The final integration must be done numerically.

4.2.3 *Plane Probe*

In this case we have

$$-j_1 = I, \tag{144}$$

$$I_0 = n_0\mu kT_2/e_1h, \tag{145}$$

and

$$\frac{d^2\eta}{d\xi^2} = \frac{-\iota}{d\eta/d\xi} - e^{-\eta}. \tag{146}$$

For a quasi-neutral solution at $\xi = \infty$, $d\eta/d\xi$ must approach a constant, equal to $-\iota$. It is clear why this is so. Since j_1 is constant by Eq. (144), there must be a finite electric field to drive this current no matter how far from the probe one goes, as long as ionization is neglected. Hence the plane case is even worse than the cylindrical case asymptotically, and the probe current depends strongly on the ionization mechanism.

We can, nonetheless, solve the space charge problem of two parallel plates at $\xi = 0$ and $\xi = \xi_s$, with $d\eta/d\xi = -\iota$ and $\eta = 0$ at ξ_s. Multiplying (146) by $d\eta/d\xi$ and integrating from $\xi = \xi$ to $\xi = \xi_s$, we have

$$\frac{\iota^2}{2} - \frac{1}{2}\left(\frac{d\eta}{d\xi}\right)^2 = -\iota(\xi_s - \xi) - e^{-\eta} + 1$$

$$-\frac{d\eta}{d\xi} = [\iota^2 + 2\iota(\xi_s - \xi) + 2e^{-\eta} - 2]^{1/2}. \tag{147}$$

The final integration can be carried out if we neglect $e^{-\eta}$:

$$\eta = \int_{\xi_s}^{0} \frac{d\eta}{d\xi}\,d\xi = \int_{\xi_s}^{0} -[\iota^2 - 2 + 2\iota(\xi_s - \xi)^{1/2}]\,d\xi$$

$$\eta_p = (3\iota)^{-1}[(\iota^2 - 2 + 2\iota\xi_s)^{3/2} - (\iota^2 - 2)^{3/2}]. \tag{148}$$

This gives the potential profile for space charge limited flow, to be compared with the collisionless formula (12).

4.3 Asymptotic Analysis of Large Spherical Probes

The formula (143) for a spherical probe requires that the sheath thickness be known. Since the problem of a sphere has a well-behaved solution at ∞, the constant of integration x_s can be obtained from the solution in the quasi-neutral region. This is done in the boundary-layer analysis of Su and Lam (*20*), which shows that the solution, as in the collisionless case, can be divided into partial solutions for the quasi-neutral region, a transition region, and a sheath region, and that the thickness of the transition layer can be neglected in the limit of large probes and high potentials. This theory is applicable in the limit of small λ, when the macroscopic transport equations are valid. In this limit there is a fourth boundary layer immediately next to the probe called the ion-diffusion layer in which the D term of Eq. (122) is dominant and the ion density falls rapidly to 0 to satisfy the boundary condition $n_i = 0$ at the probe. This layer has a negligible effect on the probe characteristic. Typical I–V curves for large negative probes, computed by Su and Lam, are shown in Fig. 15. These curves show good saturation at high probe potentials; that is, the probe current is more constant than

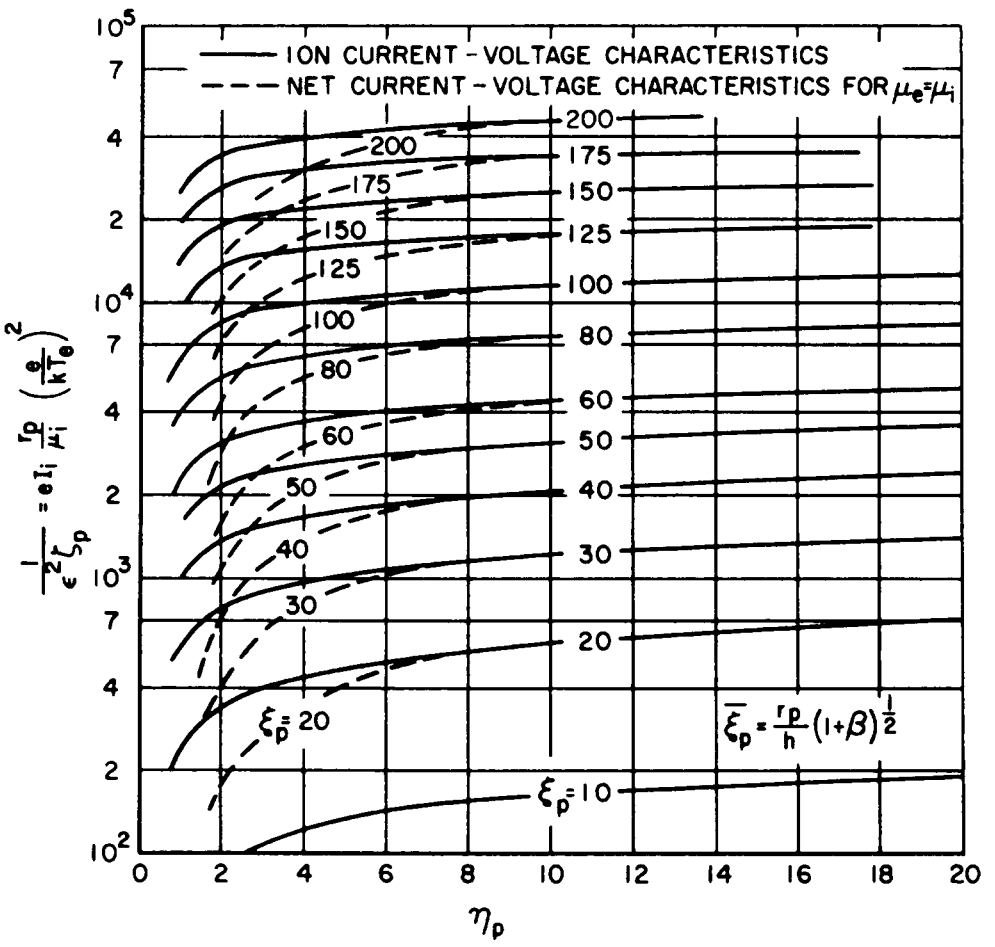

FIG. 15. Saturation ion current characteristics for various sizes of spherical probes in a collision-dominated plasma. [C. H. Su and S. H. Lam, *Phys. Fluids* **6**, 1479 (1963).]

the collisionless theory would predict. This often occurs in experiment; and when it does occur, one should suspect that the current is diffusion limited.

When the probe is near space potential the current of electrons collected is no longer negligibly small, and the theory becomes more complicated. Computations for arbitrary η_p and large ρ_p are given by Cohen (*21*). If η_p is much less than 1, however, a simplication can be made by linearizing the governing equations. For $\eta_p \ll 1$ and $[(1 + \beta^{-1})(\lambda/r_p)(\lambda/h)^2]^{1/3} \ll 1$, Su and Lam (*20*) obtain

$$I = 4\pi r_p n_0 D_i \left\{1 + \frac{3\eta_p}{\beta \ln[(1 + \beta^{-1})\rho_p^2]}\right\}, \tag{149}$$

where $\beta = T_i/T_e$.

4.4 Summary of Probe Theories with Collisions

When the mean free path is neither large nor small, the theory becomes extremely complicated, since there is no simple equation of motion. The first analysis of a probe at high pressures was made by Davydov and Zmanovskaja (*22*), who assumed that $\lambda \approx h$, so that quasi-neutrality obtained in the diffusion region, and free-fall occurred in the sheath. Ionization was taken into account, but the sheath criterion (23) seemed to be unknown to them. In 1951, R. L. F. Boyd (*23*) considered the case of intermediate mean free path by dividing space into four regions and matching boundary conditions at each interface: a sheath region in which $n_i \neq n_e$, an abnormal mobility region in which $n_i \approx n_e$ and $v_i \sim (\nabla V)^{1/2}$, a normal mobility region where Eq. (122) is satisfied, and an undisturbed plasma region. A result of this very complicated analysis was that the probe current cannot be computed without prior knowledge of the sheath thickness.

The transition from collisionless to collision-dominated collection by a cylindrical probe was studied by Schulz and Brown (*24*). For no collisions, the Langmuir theory was used. With one collision in the sheath, the probe current was found to be increased, since the orbital motion was disrupted. With several (2 to 10) collisions in the sheath, the ions can be scattered out, and a plural scattering calculation by Cobine was used. For many collisions in the sheath, Eq. (136) was used. Semiempirical formulas were given for each case, and the theory was checked against microwave measurements of density, with extremely good agreement.

Waymouth (*25*) has attempted to match the solution in the collision-dominated region directly to that in the free-fall region; however, the

validity of such a procedure is open to question. Ecker *et al.* (*26*) have done the same for a cylindrical probe; it was of course necessary to consider ionization in this case. The primary effect of collisions seems to be a decrease in the plasma density at $r = \lambda$ due to the blocking effect of the probe. The magnitude of this effect is given by Eq. (117).

Only in the continuum limit, when the macroscopic fluid equations can be used everywhere, and only for spherical probes, has the theory been worked out in detail. The elegant boundary-layer analyses of Su and Lam (*20*) and of Cohen (*21*) are summarized by the saturation ion curves of Fig. 15. For other geometries Eqs. (136), (143), and (148) may be used if the sheath thickness can be estimated.

In all this work the classical diffusion and mobility constants were assumed. In fully ionized plasmas the diffusion coefficient varies with density, and these theories would not hold. However, the mean free path for Coulomb collisions is usually so long that the collisionless theory usually would apply, except in dense, cold, fully ionized plasmas.

5 *Probe Theory in the Presence of a Magnetic Field*

As we have already seen, probe theory in the absence of magnetic fields is sufficiently complicated that in most cases of interest numerical solutions of the equations are necessary. When a magnetic field is added, the problem becomes so difficult that it has received only very spotty treatment up to the present time. This is unfortunate, since most plasmas of interest today employ a magnetic field to aid in confinement; this applies both to plasmas of thermonuclear interest and to the Van Allen belts.

The main difficulties introduced by a magnetic field are twofold. First, particles are constrained to gyrate about the lines of force, so that particles move at different rates along and across the field. This introduces an anisotropy which makes the problem at least two-dimensional. Second, the effective mean free path across the field is of the order of the Larmor radius, since particles can travel only this far without making a collision; and since the Larmor radius is quite small for electrons even for moderate fields, there is essentially no collisionless theory in such a case. In fact, for very strong fields any probe will resemble a plane probe, since particles can come to it from only one direction; and we have seen that the current to plane probes depends on the mechanism of plasma production in the entire volume and is not a local property of the plasma itself. We shall first consider the problem in general and then discuss the few specific cases which have been treated.

5.1 Over-all View of the Problem

When a magnetic field is applied, the most noticeable effect is that the saturation electron current is decreased below its value in the absence of a field. The ratio of I_e to I_i is normally of the order of the ratio of electron to ion thermal velocities, i.e., $(kT_e/m)^{1/2}/(kT_i/M)^{1/2}$, and this is of the order of 10^2. In a magnetic field weak enough that the ion Larmor radius r_{Li} is large compared to the probe radius a and the Debye length h and hence that I_i is not affected, but strong enough that r_{Le} is comparable to or smaller than the relevant dimensions, this ratio falls to 10 or 20. This is presumably because the available electron current, which normally is that diffusing to a sphere of radius of order λ, is decreased by the magnetic field B to that diffusing *at a reduced rate* across B into a cylindrical tube defined by the lines of force intercepted by the probe.

The normal diffusion coefficient D, as given by kinetic theory, is $\lambda\bar{v}/3$. The diffusion coefficient across a magnetic field, in the case of classical collisions with neutrals, is

$$D_\perp = D/(1 + \omega^2\tau^2), \tag{150}$$

where ω is the cyclotron angular frequency, and τ the mean collision time. Equation (150) also holds for fully ionized gases. Since $\omega\tau$ for electrons is typically above 10^2 (at 100 G and 10 μ neutral pressure), $D_\perp$ is severely reduced even at small fields. For ions, ω is decreased by m/M while $\tau = (n_0\bar{\sigma}\bar{v})^{-1}$ is increased by approximately $(M/m)^{1/2}$, so that $\omega^2\tau^2$ is at least 2000 times smaller than for electrons. Thus $D_{\perp i}$ is decreased severely only for large B, and the conditions assumed in the previous paragraph can actually occur. At large magnetic fields anomalous diffusion almost always occurs, in which $D_\perp$ is much larger than the value in Eq. (150). An important function of probes is to measure the unknown anomalous value of $D_\perp$.

Another effect of the magnetic field is to destroy electron saturation; that is, part A of the probe characteristic continues to increase with voltage. This may be because the effective length of the flux tube into which electrons can diffuse to reach the probe increases continuously with voltage; however, this part of the characteristic has not been analyzed in detail, and it is not possible to give an exact physical picture.

As for the transition region, part B of the characteristic, it seems reasonable that at high negative voltages, when the drain of electrons is small, the plot of $\ln I_e/V_p$ should still be linear when the distribution is Maxwellian, and the slope should still give the electron temperature. The sheath around a spherical probe may now be asymmetrical, but the

addition of a magnetic field cannot change the state of thermodynamic equilibrium, and this state is such that the velocity distribution in any direction is exponential. However for strong fields it is possible that a complete equilibrium is not reached, but instead the plasma is describable by different temperatures $T_\perp$ for motions perpendicular to B and $T_\parallel$ for parallel motions. In such a case one would expect that the slope of part B would give $T_\parallel$, since most electrons reach the probe by traveling along B. The exact analysis of this part of the characteristic has not been done.

Near the space potential, the absolute magnitude of the electron current has been estimated by Bohm *et al.* (Section 5.2), and the variation with potential by Bertotti (Section 5.3). However, the behavior is sufficiently obscure that at the present time it is not known which point on the characteristic corresponds to the space potential. Indeed, it may not even be possible to define a space potential. The point of intersection found by extrapolating parts B and A of the characteristic therefore does not have its usual significance.

Part C of the characteristic, the ion saturation current, has so far defied all attempts at analysis in the case of a strong field, when r_{Li} is comparable to or smaller than other relevant lengths in the problem. In weak fields, as mentioned before, the ion current should not be greatly affected. Since the electron motion is affected, one would expect that the ion sheath around a negatively charged symmetrical probe would not necessarily be symmetric. The effect of this on the ion current has not been treated.

5.2 Electron Current near the Space Potential

The electron current at small positive probe voltages can be estimated in a manner similar to that in Section 4.1. This approach was originally suggested by Bohm, Burhop, and Massey (*3*). Consider a probe of arbitrary shape immersed in a plasma in a magnetic field. Let the positive probe potential be so large that very few ions are collected, but small enough that the electric field has little effect on the motions of electrons. Obviously these conditions are compatible only if $T_i \ll T_e$. Let the mean free path along B be λ, the Larmor radius be r_L, and the diffusion and mobility coefficients along and across the field be D, $D_\perp$, μ, and $\mu_\perp$, where $D_\perp$ is defined by Eq. (150) and $\mu_\perp$ is defined similarly.

As in Sec. 4.1, we assume that the motion across the last mean free path is unhindered, so that in terms of the density n_λ one mean free path away from the probe the current is given by Eq. (109):

$$I = A_p \frac{n_\lambda \bar{v}}{4K}, \tag{151}$$

where K is a constant varying from $\frac{1}{2}$ (if the surface A_λ is far from the probe) to 1 (if A_λ is close to the probe). With the magnetic field, the surface A_λ will be skewed, somewhat as shown in Fig. 16, since the

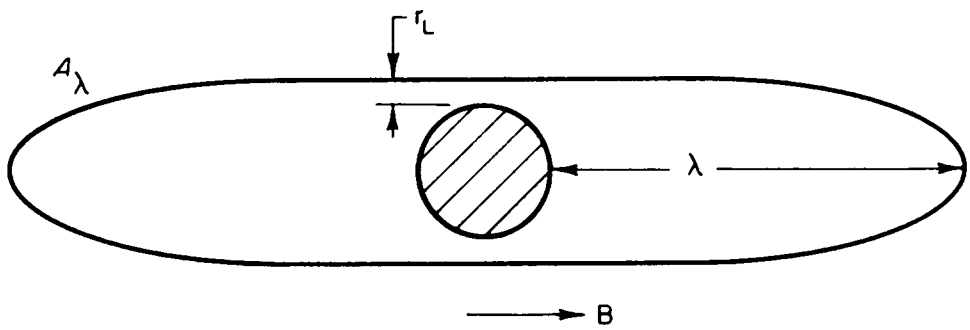

FIG. 16. Schematic of the shape of the surface A_λ bounding the collisionless region around a probe in a magnetic field.

length of a free path along B is λ, while across B it is only r_L. The exact shape is not important. In the region exterior to A_λ, we shall assume that the collision-dominated equations obtain and that current is conserved. The electron flux is given by

$$\mathbf{j} = -\mathsf{D} \cdot \nabla n + n\boldsymbol{\mu} \cdot \nabla V, \tag{152}$$

where D and $\boldsymbol{\mu}$ are diagonal matrices:

$$\mathsf{D} = \begin{pmatrix} D_\perp & 0 & 0 \\ 0 & D_\perp & 0 \\ 0 & 0 & D \end{pmatrix}, \qquad \boldsymbol{\mu} = \begin{pmatrix} \mu_\perp & 0 & 0 \\ 0 & \mu_\perp & 0 \\ 0 & 0 & \mu \end{pmatrix}. \tag{153}$$

The mobility term can be evaluated if we assume quasi-neutrality in the exterior region. Then n_e is equal to n_i, which in turn is given by the Boltzmann relation:

$$n_e = n_i = n_0 e^{-eV/kT_i}. \tag{154}$$

Thus,

$$\nabla n = n\left(\frac{-e}{kT_i}\right)\nabla V. \tag{155}$$

Using this and the Einstein relation (124) (assuming the latter to hold even in a magnetic field), we obtain for the current

$$j = -\mathsf{D} \cdot \nabla n\left(1 + \frac{T_i}{T_e}\right). \tag{156}$$

We shall ignore the correction factor $(1 + T_i/T_e)$ since this must be

close to unity from our original model. Since current is conserved and D is assumed constant,

$$-\nabla \cdot \mathbf{j} = D_\perp \nabla_\perp^2 n + D \frac{\partial^2 n}{\partial z^2} = 0. \tag{157}$$

If we let

$$\alpha = D_\perp / D \tag{158}$$

and

$$\zeta = \sqrt{\alpha}\, z, \tag{159}$$

Eq. (157) becomes

$$0 = D_\perp \left(\nabla_\perp^2 n + \frac{\partial^2 n}{\partial \zeta^2} \right) = D_\perp \nabla_\zeta^2 n, \tag{160}$$

where ∇_ζ^2 is the Laplacian in ζ-space, in which lengths in the direction of B have been contracted by a factor $\sqrt{\alpha}$. Thus n is a solution of Laplace's equation in ζ-space.

The probe current is found in terms of n_λ by integrating j over A_λ:

$$I = \int_{A\lambda} -\mathbf{j} \cdot d\mathbf{S} = \int_{A\lambda} d\mathbf{S} \cdot \mathsf{D} \cdot \nabla n = D_\perp \int_{A\lambda} d\mathbf{S}_\perp \cdot \nabla_\perp n + D \int_{A\lambda} dS_\parallel \cdot \frac{dn}{dz}. \tag{161}$$

To transform the integrals to ζ-space, we note that $\partial/\partial z = \sqrt{\alpha}\, \partial/\partial \zeta$ and $dS_\perp = dS'_\perp/\sqrt{\alpha}$, while $dS_\parallel$ and $\nabla_\perp n$ are unchanged by the transformation (the primes indicate quantities in ζ-space), so that

$$I = D\sqrt{\alpha} \int_{A'_\lambda} \nabla' n \cdot d\mathbf{S}'. \tag{162}$$

This integral can be evaluated for any simple surface A'_λ (the transformed surface A_λ), but there is no need to do this, since we saw in Eq. (115) that this is given in terms of the capacity of the surface A'_λ relative to infinity. Thus

$$I = 4\pi\sqrt{\alpha} CD(n_0 - n_\lambda). \tag{163}$$

From this and Eq. (151), we have

$$I = A_p \frac{n_\lambda \bar{v}}{4K} = 4\pi\sqrt{\alpha} CD(n_0 - n_\lambda), \tag{164}$$

$$n_\lambda = \frac{n_0}{1 + \dfrac{A_p \bar{v}}{16\pi K \sqrt{\alpha} CD}},$$

and

$$I = \frac{n_0 \bar{v} A_p}{4} \left(K + \frac{A_p \bar{v}}{16\pi \sqrt{\alpha C D}} \right)^{-1}. \tag{165}$$

For strong fields we can neglect the first term in the brackets; the area of the probe then no longer enters. It is the area of the surface A'_λ, contained in C, which matters. Putting $D = \lambda \bar{v}/3$, we have

$$I = \frac{4\pi n_0 \bar{v}}{3} \sqrt{\alpha} C \lambda. \tag{166}$$

If, in calculating C, we assumed A_λ and hence A'_λ to be an infinite cylinder with its axis in the z-direction, or if we assumed the probe to be an infinitely long wire, we would find that $C \sim L/\ln(b/a)$, where a is the radius of the surface A_λ, b is the outer radius, and L the length of the region in question. Since we are interested in the limit $b \to \infty$, $L \to \infty$, the value of C depends on how these limits are approached. Thus we recover the result of Sec. 4.2.1 that an infinite cylindrical probe in the collision-dominated case is not a well-posed problem. The finite length of the surface A'_λ must be taken into account.

Returning to the case of a spherical probe, we note that the surface A_λ in this case can be approximated by a prolate spheroid of minor radius $a + r_L$ and semimajor axis $a + \lambda$. In ζ-space, the transformed surface A'_λ then has a radius b perpendicular to B and a semiaxis d along B, where

$$\begin{aligned} b &= a + r_L \approx a \\ d &= \sqrt{\alpha}(a + \lambda) \approx \sqrt{\alpha}\,\lambda. \end{aligned} \tag{167}$$

This spheroid is prolate or oblate depending on whether a is less than or greater than $\sqrt{\alpha}\lambda$. The capacitance of such a spheroid can be found from standard texts to be

$$C = \frac{d(1 - p^2)^{1/2}}{\tanh^{-1}(1 - p^2)^{1/2}}, \qquad p = b/d \leqslant 1 \tag{168}$$

$$C = \frac{d(p^2 - 1)^{1/2}}{\tan^{-1}(p^2 - 1)^{1/2}}, \qquad p = b/d \geqslant 1. \tag{169}$$

These formulas, together with (167) and (165) or (166), then give the saturation electron current at a small positive potential under the assumptions that $T_i \ll T_e$, that orbital motions can be neglected in the free-fall region, and that quasi-neutrality obtains elsewhere. The

neglect of K in (165) is justified whenever the field is strong enough to make I much less than its zero-field value.

The expression for C diverges as $d \to \infty$ as one would expect; the potential in the infinite cylindrical case falls so slowly that if one could maintain a density n_0 at infinity, the current would be infinite. When $p \to 1$, the inverse tangent and hyperbolic tangent can be replaced by their arguments, and both expressions reduce to the spherical case, $C = b$. When $d = 0$, (169) reduces to the capacity of a disk:

$$C = 2b/\pi. \tag{170}$$

This differs only slightly from $C = b$. Thus in the range $p \gtrsim 1$ the probe current depends insensitively on the assumed length and shape of the surface A'_λ; the opposite is true if $p \ll 1$. Fortunately, the interesting range of p centers around 1. This may be seen as follows if one assumes classical diffusion:

$$p = \frac{b}{d} \cong \frac{a}{\sqrt{\alpha}\,\lambda} \cong \frac{a\omega}{\bar{v}}. \tag{171}$$

For average laboratory conditions, $a = 10^{-2}$ cm, $\omega = 2 \times 10^{10}$ sec^{-1} (1000 G), and $\bar{v} = 2 \times 10^8$ cm/sec ($kT_e \sim 10$ eV), p is just 1. At higher fields and larger probe radii, in principle p can be as large as 100; however, what normally happens at high fields is that transverse diffusion becomes much larger than the classical value, and this increase in α reduces p back to the order of unity.

The dependence of I on $D_\perp$ can be seen if we approximate C by b ($\approx a$); then from (166),

$$I = \frac{n_0 \bar{v} A_p}{4} \cdot \frac{4}{3}\frac{\lambda}{a}\sqrt{\alpha}, \tag{172}$$

where a is the probe radius, and $\alpha = D_\perp/D$. Thus I varies only as the square root of $D_\perp$; this is because part of the probe current comes from diffusion along B, and this is unaffected by a change in $D_\perp$.

Equations (172) and (105) are crude but useful approximations to the saturation electron and ion currents to an arbitrarily shaped probe in moderate magnetic fields ($r_{Le} \ll a \ll r_{Li}$). If kT_e and λ are known, Eq. (172) gives the value of $D_\perp$ whether it is classical or not. Unfortunately, it is not clear at which point of the characteristic I should be measured.

5.3 "Collisionless" Theory of a Probe in Strong Magnetic Fields

In the previous section we considered the particle currents in the collision-dominated region but neglected the detailed behavior of the electric field and particle motions in the collisionless region near the probe. Now we shall describe the theory of Bertotti (*27*), which treats this region but neglects the asymptotic behavior in the transverse direction. In order to obtain a tractable problem it was necessary to reduce the problem to one dimension and to make a number of mathematical simplifications.

Consider a probe of cross-sectional area A_p in a strong magnetic field B. Let the probe voltage be so high that particles 2 are essentially all repelled and therefore are Maxwellian. This is of course true in the long run in spite of the magnetic field, since the latter cannot affect the thermodynamic equilibrium of particles 2. Because of the weak communication across lines of force, however, it takes longer to achieve this equilibrium in a field than without one, and we must assume that the time concerned is short relative to the confinement time of particles 2. The size of the Larmor radius of particles 2 then makes no difference; the density is given by the Boltzmann law whether the gyroradius is large or small. The gyroradius of the collected particles 1 will be assumed small compared to the probe radius.

The probe is assumed to collect only particles traveling along B in a tube of radius $a + r_L$, where a is the probe radius and r_L the gyroradius of particles 1, and $a \gg r_L$. The population of particles in this tube will be controlled by transverse diffusion into the tube from the undisturbed plasma. The diffusion coefficient $D_\perp$ can be classical or anomalous (caused, say, by fluctuating electric fields), but the theory is most useful in the case of anomalous diffusion. Ordinary collisions suffered by a particle in the course of its travel along B in the tube defined by the probe are completely neglected. The theory is "collisionless" to the extent that a $D_\perp$ which does not depend on collisions with particles can be used.

The basic assumption of this theory is that the radial fall-off of potential (and hence density) as one leaves the probe and the tube of force it intersects has a characteristic length of the order of the larger of r_L and h, both of which are small compared with a. Hence the undisturbed density n_0 is reached in a relatively short distance radially. This assumption will be discussed later. All quantities will then be averaged over the cross section of the tube, and this will become a one-dimensional theory in the dimension z, along B. As one goes away from the probe in the z-direction, the undisturbed density will be approached

asymptotically, since there will be a larger and larger distance in which particles can diffuse into the tube and replenish the particles lost to the probe. The behavior of n and V in the z-direction will be given by the theory. This problem is very similar to the problem of a collisionless discharge between infinite parallel plates. Instead of ionization we have here transverse diffusion which feeds particles into our one-dimensional space. There is here however a "recombination" mechanism due to the loss of particles from the tube due to the same transport mechanism which brought them in.

The transverse "diffusion" is imagined to be given by a frequency s, which is constant in space and time and gives the rate at which particles are exchanged between lines of force. Thus into a volume $\pi a^2\,dz$ of the tube of force defined by a probe of circular cross section, there are $\pi a^2 n_0 s\,dz$ particles per second transported from outside the tube (where the density is n_0), and there are $\pi a^2 n_1(z) s\,dz$ particles per second transported similarly out of this volume. The net flux is then found by dividing the difference by the area:

$$j = \frac{\pi a^2 s\,dz(n_0 - n_1)}{2\pi a\,dz} = \tfrac{1}{2} sa(n_0 - n_1). \tag{173}$$

The parameter s can be related approximately to $D_\perp$ by assuming that the radial gradient of n has a scale length r_L, the gyroradius of particles 1; then the flux is also

$$j = D_\perp(n_0 - n_1)/r_L\,, \tag{174}$$

and so

$$D_\perp \sim \tfrac{1}{2} s a r_L\,. \tag{175}$$

The perpendicular transport mechanism, however, need not be a diffusion mechanism at all.

If n_1 and V are understood to be average density and potential over a cross section of our tube, they are related by the following one-dimensional Poisson equation for $e_1 = -e_2$:

$$\frac{d^2V}{dz^2} = -4\pi e_1(n_1 - n_0 e^{-e_2 V/kT_2}). \tag{176}$$

We shall employ the usual dimensionless variables:

$$\begin{aligned} \eta &= -e_1 V/kT_2 > 0 \\ \xi &= z/h \\ h &= (kT_2/4\pi n_0 e_1^2)^{1/2} \\ u &= v/v_s\,, \qquad v_s = (2kT_2/m_1)^{1/2} \\ \nu &= n_1/n_0\,. \end{aligned} \tag{177}$$

Equation (176) then becomes

$$\eta'' = \nu - e^{-\eta}, \tag{178}$$

and conservation of energy for particles 1 gives

$$u^2(\xi) - \eta(\xi) = u^2(\zeta) - \eta(\zeta). \tag{179}$$

We can also define a dimensionless diffusion coefficient Δ and a corresponding dimensionless σ:

$$\begin{aligned} \Delta &= D_\perp / v_s h \\ \sigma &= sh/v_s\,, \end{aligned} \tag{180}$$

so that Eq. (175) becomes

$$\Delta \approx \tfrac{1}{2}\sigma a^* r_L^*\,, \tag{175a}$$

where a^* and r_L^* are measured in units of h.

The next task is to calculate ν in terms of σ and the initial velocities of particles 1. For simplicity Bertotti assumes that these have a uniform velocity $\pm u_0$ in the ξ-direction, half the particles going in each direction. The extension to a continuous velocity distribution complicates the equations but does not introduce any new effects. Let $\iota(\xi, \zeta)$ be the dimensionless particle current (normalized to $n_0 v_s$) which enters the tube in a unit length at ζ and reaches ξ. The current that enters at ζ, $\iota(\zeta, \zeta)$, is given by the diffusion parameter σ:

$$\iota(\zeta, \zeta) = \pm\tfrac{1}{2}\sigma, \tag{181}$$

the $\pm\frac{1}{2}$ indicating that half goes one way and half the other. As this component of current travels toward ξ, it is being diminished by diffusion out of the tube at a rate proportional to σ and to the density ι/u:

$$\frac{\partial \iota(\xi, \zeta)}{d\xi} = \frac{-\sigma \iota(\xi, \zeta)}{u(\xi, \zeta)}\,, \tag{182}$$

where u is given by Eq. (179):

$$u^2(\xi\,, \zeta) = u_0^2 + \eta(\xi) - \eta(\zeta). \tag{183}$$

It is clear then that ι varies exponentially:

$$\iota(\xi, \zeta) = \pm\tfrac{1}{2}\sigma e^{-\sigma\tau(\xi, \zeta)}, \tag{184}$$

where $\tau(\xi, \zeta)$ is the time, normalized to h/v_s, taken to go from ζ to ξ:

$$\tau(\xi, \zeta) = \int_{\zeta}^{\xi} \frac{d\xi'}{u(\xi', \zeta)} > 0. \tag{185}$$

Of course, if u_0^2 were too small compared to η, some particles entering the tube heading away from the probe would be turned around by the potential. These would contribute twice to the density and would greatly complicate the equations. Hence we must assume for all η:

$$u_0^2 \geqslant \eta. \tag{186}$$

This means that the theory is limited to small probe potentials, and usually to electron collection, since if $T_i \ll T_e$, a probe potential smaller than kT_i/e would not be sufficient to repel most of the electrons and cause saturation. With this assumption, the density at ξ is given by the integral over all partial currents from $\xi = 0$ (at the probe) to $\xi = \infty$:

$$\nu(\xi) = \int_0^{\infty} \frac{\iota(\xi, \zeta)}{u(\xi, \zeta)}\, d\zeta = \tfrac{1}{2}\sigma \int_0^{\infty} \frac{e^{-\sigma\tau(\xi,\zeta)}}{|\, u(\xi, \zeta)\,|}\, d\zeta. \tag{187}$$

Because of the absolute value sign this is conveniently broken up into two integrals. Let $\rho = \zeta - \xi$. Then using (187) for ν and (183) for u, we have for Poisson's equation (178)

$$\begin{aligned} \eta'' + e^{-\eta} = {} & \frac{\sigma}{2} \int_0^{\infty} \frac{e^{-\sigma\tau}\, d\rho}{[u_0^2 + \eta(\xi) - \eta(\xi + \rho)]^{1/2}} \\ & + \frac{\sigma}{2} \int_0^{\xi} \frac{e^{-\sigma\tau}\, d\rho}{[u_0^2 + \eta(\xi) - \eta(\xi + \rho)]^{1/2}}, \end{aligned} \tag{188}$$

where $\tau = \tau(\xi, \xi + \rho)$ is given by (185) and (183) in terms of η. This is an integro-differential equation for $\eta(\xi)$, with $\eta(0) = \eta_p$, $\eta(\infty) = 0$.

The probe current density j is the integral over the partial currents $\iota\, d\zeta$:

$$j = n_0 v_s \int_0^{\infty} d\zeta\, \iota(0, \zeta) = \frac{n_0 v_s \sigma}{2} \int_0^{\infty} e^{-\sigma\tau(0,\zeta)}\, d\zeta \tag{189}$$

by (184). Here τ is given by (185) and (183) once η is known.

The complexity of this equation is apparent. The nature of the solution can be seen, however, in a much simplified case, in which

$$\alpha = \frac{kT_2}{m_1 v_0^2} = \frac{1}{2}\left(\frac{v_s}{v_0}\right)^2 = \frac{1}{2u_0^2} \to 0. \tag{190}$$

In this case u_0 is so large that in (183) u can be replaced by $\pm u_0$; in other words, the particle motion is unaffected by the potential. This corresponds to collection of one species which is much hotter than the other; usually this implies electron collection in the presence of cold ions. Also, the time τ in (185) is approximated by $\tau(\xi, \zeta) = u_0^{-1}|\xi - \zeta|$. Equation (188) then simplifies to

$$\begin{aligned} \eta'' + e^{-\eta} &= \frac{\sigma}{2u_0}\int_0^\infty e^{-\sigma\rho/u_0}\,d\rho + \frac{\sigma}{2u_0}\int_0^\xi e^{-\sigma\rho/u_0}\,d\rho \\ \eta'' + e^{-\eta} &= 1 - \tfrac{1}{2}e^{-\sigma\xi/u_0}. \end{aligned} \tag{191}$$

This equation has a rather peculiar behavior if we set $\sigma = 0$, corresponding to no transverse diffusion. Then

$$\eta_0'' + e^{-\eta_0} - \tfrac{1}{2} = 0. \tag{192}$$

This means that quasi-neutrality can never be attained: the equation for η_0 cannot be satisfied for $\eta_0 = 0$ and $\eta_0'' = 0$. The physical meaning of this is clear. If there are no collisions and no transverse diffusion, the very presence of an absorbing probe removes all particles 1 traveling toward the probe, and hence the density at ∞ can be only $\frac{1}{2}n_0$. On the other hand, if we first change the unit of distance so that

$$\xi^* = \sigma\xi/u_0 \tag{193}$$

and Eq. (191) reads

$$\sigma^2 u_0^2 \frac{d^2\eta_\infty}{d\xi^{*2}} + e^{-\eta_\infty} = 1 - \tfrac{1}{2}e^{-\xi^*}, \tag{194}$$

and *then* let $\sigma \to 0$, we get

$$e^{-\eta_\infty} + \tfrac{1}{2}e^{-\xi^*} - 1 = 0 \tag{195}$$

or

$$\eta_\infty = -\ln(1 - \tfrac{1}{2}e^{-\sigma\xi/u_0}). \tag{196}$$

This solution and its derivatives do approach 0 for $\xi \to \infty$. In fact the quasi-neutral solution is guaranteed in this case because as $\sigma \to 0$ in (194) the differential operator is neglected.

This is therefore a boundary-layer type of problem in which two different equations obtain for different regions, and the solutions must be matched at the common boundary. The position of this boundary will depend on the size of σ. The solution η_∞ of Eq. (196), then, applies to the quasi-neutral region far from the probe. There is a very gradual

falloff of potential corresponding to the gradual replenishment by diffusion of particles lost to the probe. At $\xi = 0$, $\eta_\infty = \ln 2$.

The solution η_0 of Eq. (192) is valid for the sheath region and must be matched to η_∞ by letting $\eta_0(\infty) = \ln 2$. With $\eta_0(0) = \eta_p$, η_0 can easily be found numerically. The first integration can be done analytically the usual way. Note that the scale length for η_0 is of order 1 (h in real units), while for η_∞ it is u_0/σ (v_0/hs in real units), which is generally very much larger. Thus the last term in (191) can be set equal to $\frac{1}{2}$ in the sheath, and η_0 is the proper solution there.

The probe current follows from Eq. (189). In the limit of large u_0, τ is approximately ζ/u_0, so that the current density is approximately $j = \frac{1}{2}n_0 v_s u_0 = \frac{1}{2}n_0 v_0$, which is just the thermal random current. With the first-order correction found from the numerical solution of (192), the probe current density is

$$j = \tfrac{1}{2}n_0 v_0(1 + 0.1642\alpha) + \tfrac{1}{2}n_0 s\alpha \int_0^\infty dz[\eta_0(z) - \ln 2], \tag{197}$$

where α is defined in (190). The integrand is always positive.

This result is clearly in contradiction to experiment, since it predicts an electron current in excess of the current (approximately $\frac{1}{2}n_0 v_0$) which would be collected in the absence of a magnetic field. The reason is also clear and bears out our previous statement that there is really no collisionless probe theory for a magnetic field. We have seen that an infinite cylindrical probe collects infinite current in the collision-dominated case. Since any shape of probe acts like a long cylindrical probe in a magnetic field because it collects particles along a long tube of force, one would expect that the surrounding plasma would be severely drained of electrons. Hence the original assumption that the plasma density has its undisturbed value n_0 a small distance r_L radially away from the probe is invalid; the radial falloff distance is actually very large. In this "collisionless" theory the density just outside the tube of force is assumed to be replenished to n_0 by free motion along lines of force. However, because of the length of the scale distance for η_∞, these particles must travel a very long distance along z, and their motion is eventually limited by collisions. Thus the decrease in j when $B \neq 0$ depends eventually on λ, the mean free path along B, as was found by Bohm (Section 5.2); and the largeness of (197) is due to the neglect of λ.

This theory can perhaps be salvaged, however, since for n_0 one merely has to substitute n_λ, as calculated by Bohm for the collision-dominated region [cf. Eq. (164)]. This will give the correct magnitude of j, while the last term in (197) will give its dependence on η_p, i.e., the shape of part A of the characteristic. This shape is somewhat

unexpected, since the computation of the integral in (197) shows that the slope of j *increases* with η_p. Thus according to this theory the floating potential occurs to the *left* of the inflection point in the probe characteristic (Fig. 1), contrary to the case when $B = 0$. The reason for j to increase with η_p is merely that the sheath thickness δ increases with η_p; hence there is a larger region where ∇n is large. The reason for the slope of j to increase is more obscure. This is probably because electrons are accelerated more by higher η_p, so that they have less chance to be scattered out of the tube. This acceleration was neglected in calculating η_0, as was diffusion; but it was included in the first order term in the expression for j. This effect would probably be completely masked in practice by the $I - V$ dependence of the solution in the collision-dominated region.

In a second paper by Bertotti the restriction to $\alpha \to 0$ was removed, but it was necessary to treat the case of slow diffusion, $\sigma \to 0$, in which the second integral in (188) could be neglected because the interval was finite. The restriction (186) on probe potential was also removed by considering particles which are turned around by the electrostatic field. After a tedious calculation Bertotti arrives at an expression for j valid for arbitrary α. In the limit of large η_p he finds that $j \sim \eta_p^{3/4}$. There is thus no saturation. However, this result is suspect for several reasons. First, the collisional effects mentioned above would certainly become important. Second, the asymptotic analysis in which η is divided into η_0 and η_∞ is valid only if $\sigma\tau$ is small, i.e., the time of travel is small compared to σ^{-1}. For large sheaths this may not be true. Third, in the presence of gradients of η in both z and r directions, there is a second-order drift which moves particles radially even when $\sigma = 0$. The neglect of this drift would not be valid if the value of σ is too small. The theory of Bertotti makes its primary contribution in demonstrating the mathematical nature of this boundary-layer problem.

5.4 Summary of Probe Theories with a Magnetic Field

As early as 1936 Spivak and Reichrudel (28) made a study of electron collection in a weak magnetic field, primarily by cylindrical probes. Their point of view was that the Langmuir orbital theory (Section 3.1.2), which has the advantage that the probe current is independent of the potential distribution, had a limited range of applicability (the sheath had to be large), and that this range could be extended by applying a weak magnetic field. Electron collection is then controlled by orbital motions in the magnetic field over a larger range of possible potential distributions. The current is again independent of potential shape, and

Poisson's equation and ion density are not considered. In order to solve the orbital problem, however, Spivak and Reichrudel had to assume a boundary at which the magnetic field's effects abruptly stopped; and the velocity distribution at this boundary was assumed to be known. This rather unrealistic assumption limits the credibility of the theory, even though the resulting curves for parts A and B of the probe characteristic vary with B in a manner similar to that observed in experiments. Detailed comparison with experiment was attempted; but since the entire discharge changed with B, this was not definitive. In any case the theory is valid only for very weak fields (below 100 G) and very low densities.

In 1954, Bickerton (*29*) considered electron collection by a plane placed parallel to a magnetic field. Three cases were considered: $h \ll r_L$, $h \gg r_L$, and $h \sim r_L$. The procedure was to assume that electron motion is prescribed by perpendicular diffusion and mobility (152) and that the electric field is given by Child's law (12) for space-charge-limited *ion* flow from the plasma to the collector. The latter assumption may be valid for the lower portion of the transition region of the probe characteristic, but Bickerton also used this assumption even near space potential. With a known V and $j(n)$, the density in the sheath can be found in terms of that at the sheath edge. The latter was found from the quasi-neutral solution for the plasma region; convergence was achieved by including ionization.

For $h \ll r_L$, the electron motion inside the sheath is unaffected by the magnetic field, while that outside the sheath is unaffected by the electric field. If the velocity distribution is known at a distance $\sim r_L$ from the sheath edge, and all electrons entering the sheath are collected, consideration of orbits in the outer region gives for the probe current density (for classical diffusion)

$$j = \frac{n_0 \bar{v}}{4} \frac{\pi}{\omega\tau} e^{-\eta}, \tag{198}$$

where ω is the electron gyrofrequency. If collisions during the last Larmor orbit are taken into account, the result quoted by Bickerton and von Engel (*30*) is

$$j = \frac{n_0 \bar{v}}{4} \left[\frac{8 + \omega^2\tau^2(1 - e^{-2\pi/\omega\tau})}{2(4 + \omega^2\tau^2)} \right]. \tag{199}$$

This expression reduces to $n_0\bar{v}/4$ for $\omega = 0$ and to (198) for $\omega \to \infty$. The density n_0 is that near the plane probe; its relation to the density at ∞ is not known, since no asymptotic analysis was given. Moreover an abrupt sheath edge was assumed. Therefore some caution must be exercised in using (199). Although (198) resembles the result of Bohm

(166) in that the current goes as $1/B$, the two theories do not agree in detail because of the difference in the original model.

The magnitude of the electron current near space potential is given by Bohm [Eq. (165)] for a probe of arbitrary shape. This theory neglects electric fields and orbital motions and is valid only for $kT_e \gg kT_i$.

The variation of electron current with potential is given by Bertotti [Eq. (197)] for the case of a probe of arbitrary shape in a strong magnetic field, when the probe potential and the ion temperature are both small, and the transverse diffusion coefficient is constant. The result is not expressible in simple terms. Collisions are neglected.

The variation of saturation probe current with potential is also given by Bertotti (*27*) for the case of slow diffusion and large potentials. The temperature ratio is arbitrary, so presumably this theory can be used for ion collection as well. However, the assumptions of the theory are so restrictive that extreme caution should be exercised in its use.

No satisfactory theory, particularly of the important regions B and C of the probe characteristic in a magnetic field, is available. However, as long as the electrons are in thermal equilibrium and the ion Larmor radius is much larger than the probe dimensions, the usual theories of ion collection may be used. The electron temperature is probably correctly given by the $\ln I_e$–V curve in the range in which it is linear. Even in a strong magnetic field the range of electron velocities thus sampled is usually greater than in the method of double probes.

Much of the uncertainty in measurements in a magnetic field can be removed by using auxiliary floating probe to measure the change in the potential of the plasma caused by the current-collecting probe. The auxiliary probe should be small, so that it does not block the current to the main probe, and should be on the same line of force as the main probe, so that it is in a region with the same space potential.

6 *Floating Probes*

6.1 Floating Potential

Although space potential is usually the quantity of interest, what is easily measured is instead the floating potential, the voltage at which the probe draws no current. Therefore the exact relation between V_s and V_f is of interest. V_f is of course negative relative to V_s.

In the absence of a magnetic field an approximate relation can be obtained by using Eq. (105) for the ion current:

$$j_i = \tfrac{1}{2}n(kT_e/M)^{1/2}. \tag{200}$$

Since most electrons are repelled, their distribution, if originally Maxwellian, remains so in the presence of the probe, and the electron current is merely the random current times the Boltzmann factor:

$$j_e = \tfrac{1}{4} n \bar{v}_e e^{eV_f/kT_e} = \frac{1}{2} n \left(\frac{2kT_e}{\pi m}\right)^{1/2} e^{eV_f/kT_e}, \tag{201}$$

V_f being negative. Setting j_i equal to j_e, we have

$$\frac{eV_f}{kT_e} = \frac{1}{2} \ln \left(\frac{\pi}{2} \frac{m}{M}\right). \tag{202}$$

Thus for hydrogen V_f is about 3.6 times kT_e negative relative to space, and the factor is somewhat larger for heavier elements. For a more exact answer, the numerical results for j_i (Section 3.3) must be used.

In the presence of a magnetic field the magnitude of V_f is uncertain because no theory exists for j_i at small negative probe potentials. If the field is so weak (less than a few hundred gauss, say) that r_{Li} is much larger than the Debye length and the probe radius, then it may be permissible to use Eq. (200) still. The electron current, however, will be constrained to flow along the field, even at quite low fields, so that the effective collecting area is reduced to something like the projection of the probe area on a plane perpendicular to B. Thus for a cylindrical floating probe perpendicular to B the electron current is, very approximately,

$$I_e = 4alj_e, \tag{203}$$

where a and l are the radius and length, while the ion current is

$$I_i = 2\pi alj_i. \tag{204}$$

If we use Eqs. (200) and (201) for j_i and j_e, the resulting value of eV_f/kT_e differs by only a constant equal to $\ln(\frac{1}{2}\pi) = 0.45$, and this is probably insignificant in view of the approximations made.

6.2 Double Probes

In most gas discharges there is an electrode in good contact with the plasma which can be used as a reference point for potential when applying a bias voltage to a probe. Such an electrode can be the anode or cathode of a discharge, or the metallic wall or limiter of an electrodeless discharge, such as that in a stellarator or a toroidal pinch. In some instances such a reference point is not available. Examples of this are a toroidal rf discharge in a glass tube or the plasma in the ionosphere.

In such a case a double probe must be used. The double-probe method was originally proposed by Johnson and Malter (*31*), and we shall give a simplified version of their thorough analysis. This method was invented for use in decaying plasma, in which the plasma potential changed with time, so that it was difficult to maintain a constant probe-plasma potential difference. With two probes biased with respect to each other but insulated from ground, the entire system "floats" with the plasma and therefore follows the change of plasma potential.

Figure 17 shows the geometry. Probes 1 and 2 have areas A_1 and A_2,

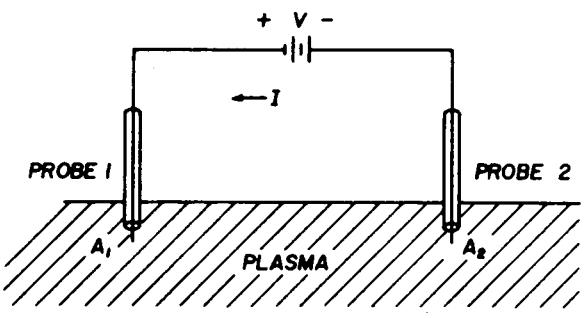

FIG. 17. Schematic of a floating double-probe system showing the convention used for the sign of I.

respectively, and are located in a plasma which has constant properties within the spacing of the probes. A voltage V is applied between 1 and 2, but the entire system is not connected to any electrode. For definiteness we shall assume V_1 is positive relative to V_2, and therefore

$$V = V_1 - V_2 > 0. \tag{205}$$

A current $I(V)$ flows between 2 and 1 and is positive if V is positive, by definition.

The potential distribution is shown schematically on Fig. 18. Since the electron velocities are much higher than the ion velocities, the probes in general must both be negative with respect to space to prevent a net electron current from flowing to the whole system. This condition can be violated only if one probe is so much larger than the other that the ion current to the larger probe can cancel the saturation electron current to the smaller probe; we shall not consider such a case.

Figure 19 shows what the probe characteristic will look like. This is drawn for the case $A_1 > A_2$; the curve will of course be symmetrical for $A_1 = A_2$. At $V = 0$, both probes are at floating potential and no net current goes to either one; hence $I = 0$. If V is now made slightly positive, V_1 will become less negative and V_2, more negative; thus more electrons will flow to 1 and fewer to 2. This results in a positive

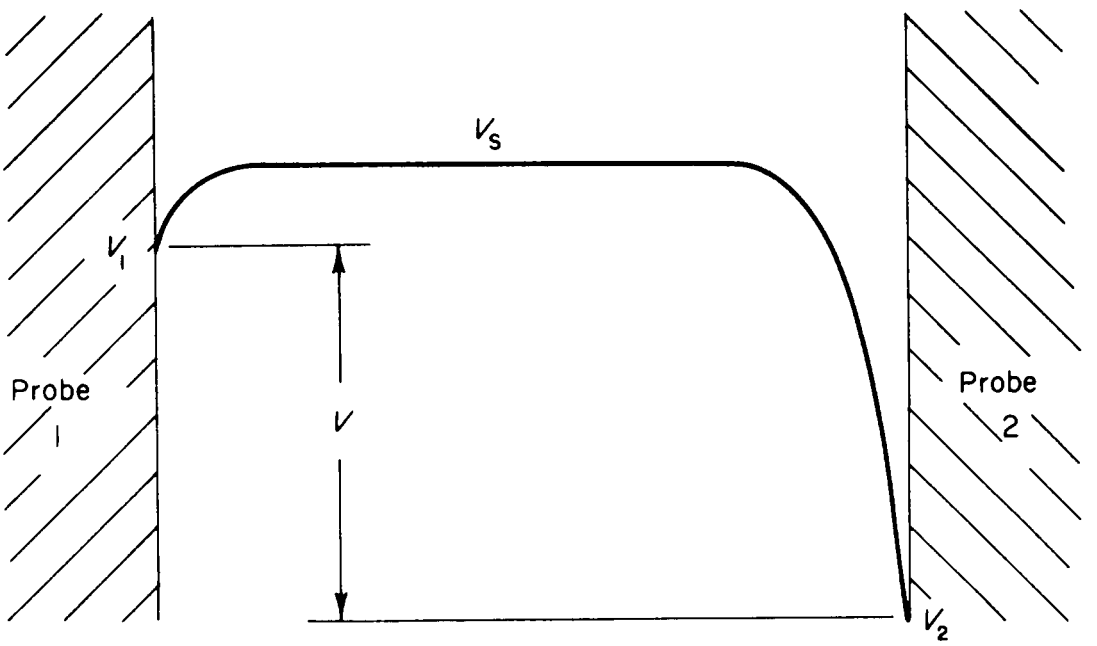

FIG. 18. Schematic of the potential distribution between the probes of a floating double-probe system.

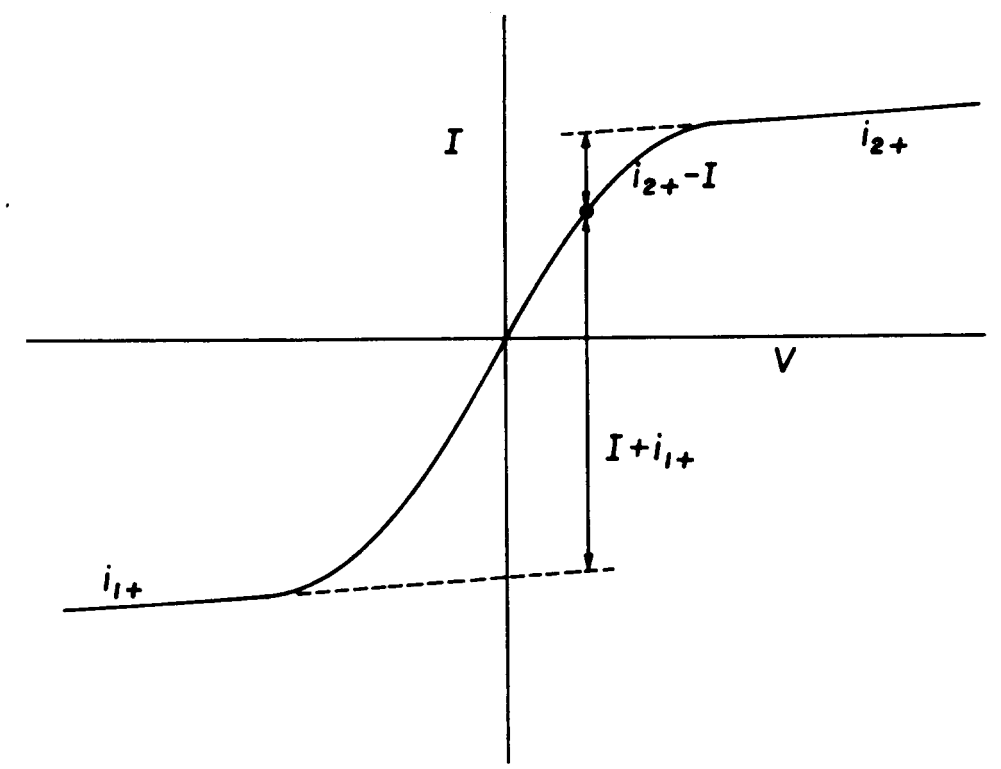

FIG. 19. Schematic of a double-probe characteristic in the general case when the probe areas are unequal.

current flow from 2 to 1, that is, a positive I; this is shown by the dot on Fig. 19. For large positive V's, probe 2 will be very negative, drawing saturation ion current. Probe 1 will still be negative, but close enough to V_s to collect a sufficient electron current to cancel the ion current to probe 2. Thus the probe characteristic assumes the shape of the saturation

ion characteristic of probe 2. With negative V the current is reversed, and the same general behavior occurs; the magnitude of the saturation current will be different if the probe areas are different.

This qualitative description reveals an important advantage of the double probe method: the total current to the system can never be greater than the saturation ion current, since any electron current to the total system must always be balanced by an equal ion current. Thus the disturbance on the discharge is minimized. This has the disadvantage, however, that only the fast electrons in the tail of the distribution can ever be collected; the bulk of the electron distribution is not sampled.

To find the current $I(V)$ quantitatively, we define i_{1+}, i_{1-}, i_{2+}, and i_{2-} to be the ion and electron currents *to* probes 1 and 2 at any given V. The condition that the system be floating is

$$i_{1+} + i_{2+} - i_{1-} - i_{2-} = 0. \tag{206}$$

The current I in the loop is given by

$$i_{2+} - i_{2-} - (i_{1+} - i_{1-}) = 2I. \tag{207}$$

If we add and subtract (206) and (207), we obtain

$$I = i_{1-} - i_{1+} = i_{2+} - i_{2-}\,. \tag{208}$$

The currents i_- are given by Eq. (201) for the electron current density to a probe in the transition region:

$$i_{1-} = A_1 j_r e^{eV_1/kT_e}; \qquad \text{similarly for } i_{2-}\,. \tag{209}$$

Here j_r is the random electron current density. Substituting this into the first of (208) and using (205), we have

$$I + i_{1+} = A_1 j_r e^{eV_1/kT_e} = A_1 j_r e^{e(V+V_2)/kT_e}$$

$$= \frac{A_1}{A_2}\, i_{2-} e^{eV/kT_e}. \tag{210}$$

From the second of Eq. (208),

$$\frac{I + i_{1+}}{i_{2+} - I} = \frac{A_1}{A_2}\, e^{eV/kT_e}. \tag{211}$$

The basic assumption of this theory is that the probes are always negative enough to be collecting essentially saturation ion current;

therefore, i_+ can be accurately estimated at any V by smoothly extrapolating the saturation portions of the double-probe characteristic. The quantities in the numerator and denominator of Eq. (211) are then easily obtained; they are shown in Fig. 19. The slope of a logarithmic plot of this ratio against V then yields the electron temperature.

We note two special cases. If $A_1 = A_2$, then $i_{1+} \cong i_{2+} \cong i_+$, and Eq. (211) can be solved for I:

$$I = i_+ \tanh(eV/2kT_e). \tag{212}$$

This formula has been found to fit the experimental curve quite well. On the other hand, if $A_1 \gg A_2$, we can assume that probe 1 is essentially unaffected by probe 2 and is almost at floating potential, with $i_{1+} \cong i_{1-}$. Thus

$$I \ll i_{1+} = A_1 j_+ . \tag{213}$$

Since $i_{2+} - I = i_{2-}$, Eq. (211) can be written

$$A_1 j_+ \cong \frac{A_1}{A_2} i_{2-} e^{eV/kT_e}; \tag{214}$$

and

$$i_{2-} = A_2 j_+ e^{-eV/kT_e} = A_2 j_+ e^{-e(V_1 - V_2)/kT_e}. \tag{215}$$

Since $i_{1+} \cong i_{1-}$, we have $j_+ \cong j_r \exp(eV_1/kT_e)$. With this, Eq. (215) becomes

$$i_{2-} = A_2 j_r e^{eV_2/kT_e}. \tag{216}$$

This is just the transition current to a single probe, as one would expect, since probe 1 has become a large reference electrode. This case of $A_1 \gg A_2$ has application in space physics, where a nose cone casing often serves as a large reference probe.

The logarithmic plotting of (211) to determine kT_e is quite laborious. Since only a few electrons are sampled anyway, sufficient accuracy on kT_e can be obtained by merely measuring the slope of the characteristic at the origin. If we assume that i_+ is independent of V, we obtain from (208)

$$\frac{dI}{dV} = \frac{di_{1-}}{dV} = -\frac{di_{2-}}{dV} . \tag{217}$$

Using (209), we have

$$A_1 j_r e^{eV_1/kT_e} \frac{e}{kT_e} \frac{dV_1}{dV} + A_2 j_r e^{eV_2/kT_e} \frac{e}{kT_e} \frac{dV_2}{dV} = 0. \tag{218}$$

From (205) we have

$$1 = \frac{dV_1}{dV} - \frac{dV_2}{dV}, \tag{219}$$

so that (218) becomes

$$A_1 e^{eV_1/kT_e} \frac{dV_1}{dV} + A_2 e^{eV_2/kT_e} \left(\frac{dV_1}{dV} - 1\right) = 0. \tag{220}$$

At $V = 0$, we have $V_1 = V_2$; and so

$$\left.\frac{dV_1}{dV}\right]_0 = \frac{A_2}{A_1 + A_2}. \tag{221}$$

The first of Eq. (217) therefore becomes, at $V = 0$,

$$\left.\frac{dI}{dV}\right]_0 = \frac{A_1 A_2}{A_1 + A_2} j_r \frac{e}{kT_e} e^{eV_f/kT_e}. \tag{222}$$

Since

$$j_+ = j_r e^{eV_f/kT_e}, \tag{223}$$

we have

$$\left.\frac{dI}{dV}\right]_0 = \frac{e}{kT_e} j_+ \frac{A_1 A_2}{A_1 + A_2}. \tag{224}$$

Finally, since $i_{1+} = A_1 j_+$ and $i_{2+} = A_2 j_+$, we have

$$\left.\frac{dI}{dV}\right]_0 = \frac{e}{kT_e} \frac{i_{1+} \cdot i_{2+}}{i_{1+} + i_{2+}}. \tag{225}$$

From this, kT_e can be computed from the slope at the origin and the measured magnitudes of i_{1+} and i_{2+} .

Once kT_e is known, the plasma density can be calculated from either saturation current, with the help of one of the theories of ion collection summarized in Section 3.3.4.

6.3 Emitting Probes

A technique which is sometimes useful is to make a probe in the form of a small wire loop so that it can be heated to emission by the passage of a current. Whenever the probe is sufficiently positive, the emitted electrons will be drawn back to the probe, and the collected electron current will be essentially unaffected by the emission. On the other hand, when the probe is negative relative to V_s , the emitted electrons will be able to escape and contribute an apparent ion current to the probe.

The potential at which the hot-probe and cold-probe characteristics begin to disagree therefore is an indication of the space potential, as shown in Fig. 20.

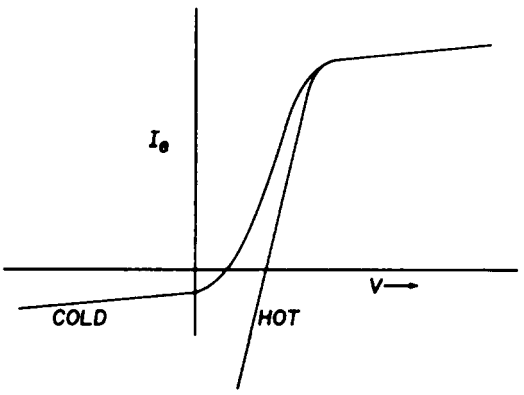

FIG. 20. Schematic of the difference between an ordinary probe characteristic and that of an emitting probe.

Since an emitting probe collects electrons when it is positive and emits them when it is negative, one might hope, by increasing the emission, to reach a point at which the probe will float at the space potential, giving a direct indication of V_s. Unfortunately, this is not generally possible because the emission cannot be increased indefinitely because of space-charge limitation. What will happen is that a double sheath will form next to the surface of a negative probe because of the excess of slow emitted electrons there. The potential distribution is shown schematically in Fig. 21; the theory has been worked out by Langmuir (*32*).

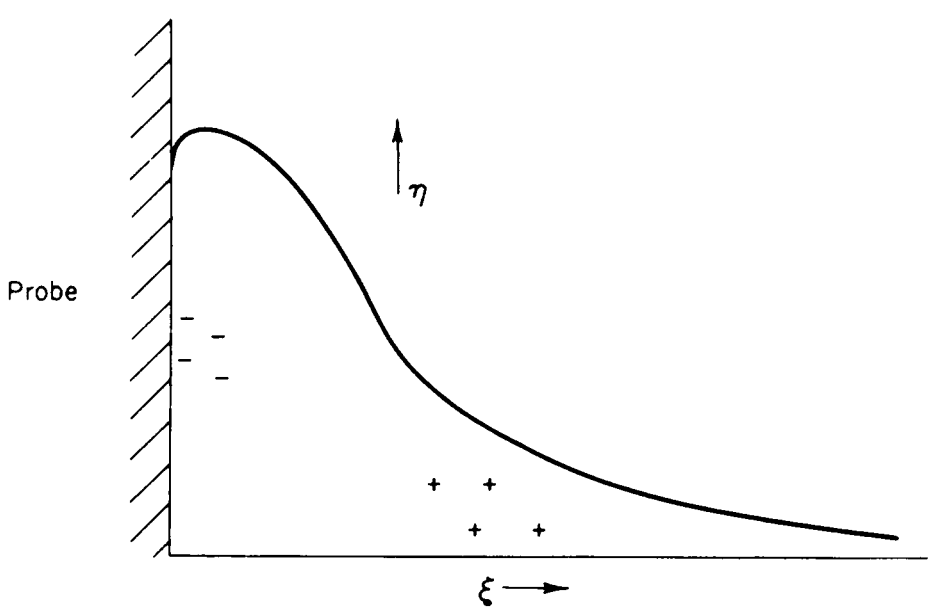

FIG. 21. Schematic of the potential distribution in a double sheath surrounding an emitting probe.

The potential hill as seen by the emitted electrons is of the order of kT_p, where T_p is the probe temperature, typically 0.2 eV. The potential hill seen by the plasma electrons is of order kT_e, if the probe is floating, so that for $T_e \gg T_p$ the value of V_f is not brought much closer to V_s by the emission. In other words, the maximum emitted current cannot be sufficient to compensate for the collected current because the plasma electrons have much higher velocities. The maximum emitted current is, however, much higher than in a vacuum because of the presence of positive ions to help cancel the space charge; the ion density is proportional to n_0, and therefore so is the emitted current. It is clear that the only case when V_f is equal to V_s is when $T_p = T_e$, so that the potential curve is symmetrical.

The same considerations apply when there is secondary emission of electrons due to bombardment by energetic ions. In this case the emitted electrons always have an effective temperature of about 1 to 3 eV. Since the secondary emission coefficient is angle dependent, the correction to I_i due to this effect is not easy to calculate.

7 *Time-Dependent Phenomena*

So far we have considered only measurements which are essentially steady-state. In many instances a plasma will be quite noisy and have fluctuations in V_s and n_0. The effect of these on the time-averaged measurements will be considered in Section 7.1. One of the most important applications of Langmuir probes is in the measurement of oscillations and fluctuations. Such measurements make full use of the spatial resolution of probes and are not subject to the errors in absolute calibration of probe currents. However, one must then worry about the speed of response of a probe. These considerations will be discussed in Sections 7.2 and 7.3.

7.1 Effect of Oscillations

The effect on the time-averaged probe characteristic of fluctuations in n_0, kT_e, and V_s in rf or unstable plasmas has been studied theoretically and experimentally by Garscadden and Emeleus (*33*), Sugawara and Hatta (*34*), Boschi and Magistrelli (*35*), and Crawford (*36*) with essentially the same results. Let $\tilde{j}_r(t)$, $k\tilde{T}_e(t)$, and $\tilde{V}_s(t)$ be the fluctuating component of the random electron current, the electron temperature, and the space

potential, respectively. Then in the transition region B of the probe characteristic in a Maxwellian plasma we have

$$j_e = (j_r + \tilde{j}_r) \exp\left[\frac{e(V_p - V_s - \tilde{V}_s)}{k(T_e + \tilde{T}_e)}\right]. \tag{226}$$

Since the $I_e - V$ curve is nonlinear, one would expect a fluctuation in V_s to affect the average value $\langle j_e \rangle$ of j_e. If kT_e does not vary, we have

$$\langle j_e \rangle = j_{e0} \langle (1 + \tilde{j}_r/j_r) e^{-e\tilde{V}_s/kT_e} \rangle, \tag{227}$$

where

$$j_{e0} = j_r e^{e(V_p - V_s)/kT_e}. \tag{228}$$

Since V_p appears only in j_{e0}, the slope of the I_e–V curve is unchanged by the fluctuating quantities; and the measurement of kT_e from the ln I_e–V curve is unaffected, as long as the probe remains on the exponential part of the characteristic. The ln I_e–V curve is merely shifted upward by a constant. For $\tilde{j}_r = 0$ and $\tilde{V}_s = \hat{V}_s \sin \omega t$, the shifted value is given by

$$\langle j_e \rangle = j_{e0} I_0(e\hat{V}_s/kT_e), \tag{229}$$

where I_0 is the Bessel function of imaginary argument. This result has been verified by all the above-mentioned authors by superimposing a sinusoidal signal on the probe voltage. If V_s is constant and only n_0 varies, Eq. (227) predicts that j_e is unchanged, since the average of $\tilde{j}_r$ is 0. This has been verified by Crawford (*36*) by modulating the discharge current. Sugawara and Hatta (*34*) have checked Eq. (227) experimentally for other shapes of signals.

If kT_e is not constant, its average value is not given exactly by the average slope of the ln I_e–V curve. This has been studied by Sugawara and Hatta (*34*). The error is small for V_p near V_s, but Boschi and Magistrelli (*35*) find that accurate measurements are impossible in this region. Crawford (*36*) gives a more general theory which includes cross-correlation effects due to simultaneous fluctuations in n_0, kT_e, and V_s with phase lags, and has checked experimentally the case when n_0 and V_s oscillate sinusoidally with a phase difference.

When the oscillations extend into the saturation parts (A and C) of the probe characteristic, the shape of the characteristic is altered. For potentials near V_s, the "knee" of the characteristic is rounded by the oscillations. This has been seen by Garscadden and Emeleus (*33*). For potentials near V_f, the I–V curve is bent into an S-shape by large-amplitude oscillations. This was predicted and observed by Boschi and Magistrelli (*35*).

The fact that the usual dc measurement of kT_e is not affected by large amplitude fluctuations in n_0 and V_s in a noisy discharge has been verified by Chen (*37*). The technique was to use a double probe, one of which measured V_f while the other measured I. The instantaneous I–V curve could then be displayed on an X–Y oscilloscope. The value of kT_e measured from this agreed with the usual method within the experimental error of 10%.

7.2 Response of a Pulsed Probe

By applying a sawtooth voltage pulse to a probe the entire characteristic can be traced in a microsecond or less. This is desirable under the following circumstances. First, in low-temperature plasmas the contact potential between the probe and the plasma is important, and it is necessary to obtain the probe characteristic before the contact potential is changed by the deposition of impurities on the probe surface. Second, in unsteady plasmas the time during which the plasma parameters are constant may be quite short. Third, in intense discharges a probe may melt when it draws a large electron current; by keeping it near V_f and pulsing it, one can use the heat capacity of the probe to keep it from melting during the voltage sweep. Finally, in the measurement of velocity distributions (Section 3.2.2) it is possible to obtain dI/dV or d^2I/dV^2 by pulsing the probe voltage and time-differentiating the probe current by RC networks. In addition, probes are often used to measure oscillations and fluctuations in a plasma. In all these applications one assumes that the probe sheath is in equilibrium with the plasma at all times. It is therefore important to know the frequency response of a probe and its sheath.

Although a complete, time-dependent theory of probes is not available, the physical nature of what happens when a probe is pulsed has been made clear by the experiments of Bills *et al.* (*38*) and Oskam *et al.* (*39*). One would expect that electrons would react almost instantaneously to an applied potential but that the ions would move much more slowly. Since their maximum velocity is of the order of $v_s = (kT_e/m_i)^{1/2}$ and they must travel a distance of the order of $h = (kT_e/4\pi n_0 e^2)^{1/2}$ to form a new sheath, the maximum frequency response would be expected to be of the order of the ion plasma frequency $\omega_{pi} = (4\pi n_0 e^2/m_i)^{1/2}$. The situation is, however, a little more complicated: there is a fundamental difference between positive and negative probes.

Suppose a probe, biased positive to draw saturation I_e, is pulsed further positive. The electron sheath must increase in thickness, and the sheath edge must move from $r = s_1$ to $r = s_2$, say. The ions originally

located between s_1 and s_2 are pushed away by the electric field. Before they have completed this motion, however, the value of I_e will be larger than in the final state, because the presence of ions inside $r = s_2$ serves to diminish the negative space charge. Thus a positive square wave will exhibit an overshoot in I_e. This has been observed by Bills *et al.* (*38*). Since this occurs only if V_p is positive, the onset of this overshoot as V_p is raised gives an indication of the space potential. The time it takes the ions to move out of the sheath and for the overshoot to die out is typically of the order of 1 μsec.

This overshoot does not exist in high-pressure discharges, as were used by Oskam *et al.* (*39*). There the electron current is limited by collisions in the plasma region and cannot rise abruptly. The final value of I_e is not reached until ions far from the probe can move to set up the density and potential gradient necessary to supply the electron current by diffusion. The time required depends on the ion mobility; at 1.2 Torr in He, it takes approximately 1 μsec.

Suppose now that a probe is biased negative to draw saturation I_i and is pulsed further negative. The ion sheath must grow and the electrons originally located between s_1 and s_2 must be pushed away; however, this occurs very rapidly. The ion density in the sheath must also be readjusted; in particular, the ion density between s_1 and s_2 must be decreased. This gives rise to a transient ion current to the probe. Kamke and Rose (*40*) have tried to measure this current; the time constant is of the order of 1 μsec. This current is, however, very small and is often completely negligible compared to the displacement current discussed below. If this overshoot in ion current is neglected, the frequency response of a negative probe is somewhat higher than that of a positive probe.

In the transition region the ion sheath hardly changes, and only the electron inertia limits the frequency response. Bills *et al.* (*38*) estimate that the response time is shorter than 10^{-8} sec, and the data of Takayama *et al.* (*41*) indicate that the probe response may be good all the way up to the electron plasma frequency. When there are collisions, however, large changes in the gradients in the quasi-neutral region must occur to accommodate the large change in electron current; Oskam *et al.* (*39*) find response times as long as 10 μsec in the transition region.

In addition to the effects mentioned above there is a displacement current due to the capacitance of the sheath. This current is the same order of magnitude for positive and negative probes and is negligible compared to the transient in I_e; however, it may be much larger than the transient in I_i. Thus in the experiment of Oskam (*39*) a large overshoot lasting about 0.4 μsec in the negative probe range is attributed to displacement current.

7.3 Use of Probes to Study Fluctuations

The use of electrostatic probes to detect waves or discrete oscillations in plasmas is commonplace. We wish to discuss here the use of probes to study continuous bands of noise which are often found in low-pressure discharges, particularly in magnetic fields. By treating the plasma as a turbulent fluid in which the local density and electric field fluctuate stochastically, much as the local velocity does in aerodynamic turbulence, one can, by measuring spectra and correlation coefficients, obtain information on the nature of the fluctuations and how they may be related to anomalous diffusion. The earliest measurements of this type were apparently made by Batten *et al.* (*42*) in a cold-cathode reflex discharge. Longitudinal correlations in a strong magnetic field have been measured by Chen and Cooper (*43*). The most extensive studies of this type, however, have been made by Bol (*44*) in a highly ionized plasma in a stellarator.

A typical spectrum of the oscillations of floating potential on a probe is shown in Fig. 22. Since the ion plasma frequency was about 150 Mc in this case, it is clear that the fluctuations are of sufficiently low frequency that the probe is in equilibrium with the plasma at all times. If kT_e is constant, $V_f - V_s$ is constant; and these oscillations reflect the oscillations in space potential. The fluctuations in local electric field can be measured by using two floating probes spaced much closer than the

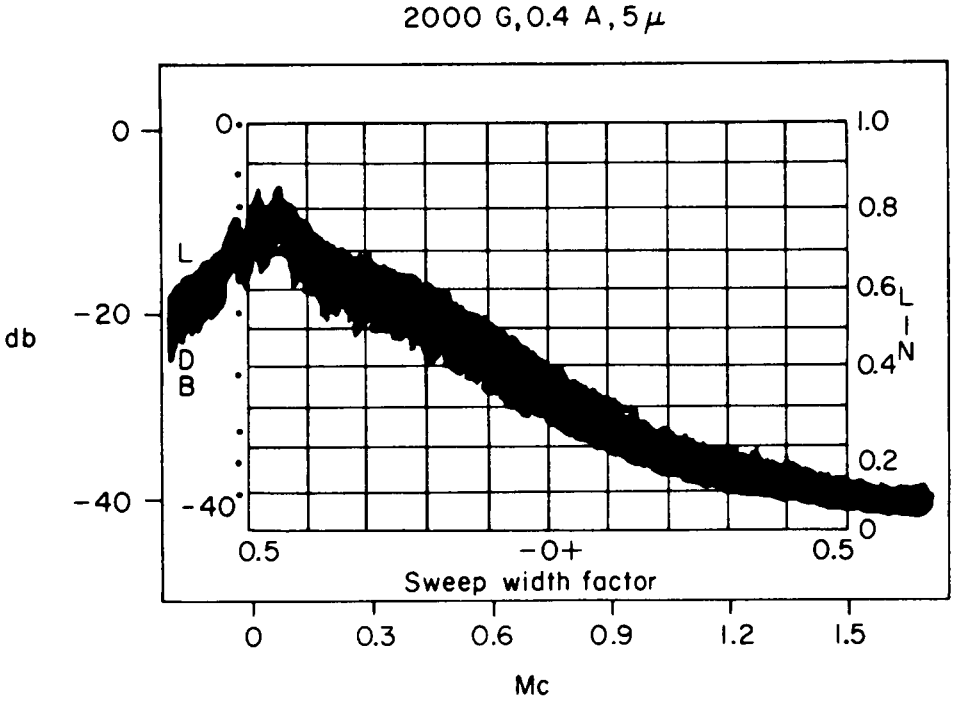

FIG. 22. A typical frequency spectrum of fluctuations in floating potential on a probe in a magnetically confined plasma. Note that the vertical scale is logarithmic. The data were taken in a hot-cathode reflex discharge in 5×10^{-3} Torr of He at 2000 G; the plasma density was of order 10^{12} cm^{-3}.

correlation distance and taking the difference in potentials by means of a transformer or a difference amplifier. The oscillations in local density can similarly be measured by using a negative probe collecting saturation ion current. If variations in kT_e and the slope of the I_i–V curve can be neglected, the fluctuations in I_i are proportional to those in n_0. The quantity I_i more convenient to work with than V_f because the signal is taken from a small resistor in series with the probe and hence is low-impedance.

Although in principle the information obtainable from correlation measurements is contained in the frequency spectrum, it is often more convenient to work with correlations. The cross-correlation coefficient between the density at two points is defined as

$$R = \frac{\langle n(x)\, n(x+d)\rangle}{\langle n^2(x)\rangle^{1/2}\langle n^2(x+d)\rangle^{1/2}}. \tag{230}$$

where $\langle\ \rangle$ indicates the time average. This can be obtained conveniently by taking the sum and difference of the I_i signals from two probes, squaring them, and taking the time average. If

$$P \equiv \frac{\langle (I_1 - I_2)^2\rangle}{\langle (I_1 + I_2)^2\rangle}, \qquad Q = \frac{\langle I_1^2\rangle}{\langle I_2^2\rangle}, \tag{231}$$

then R is given by

$$R = \frac{1}{2}\frac{1-P}{1+p}(Q^{1/2} + Q^{-1/2}). \tag{232}$$

The Q terms are very nearly unity if the probes have nearly equal areas and are located in a statistically uniform region of the plasma. The quantity P can be obtained from a differential amplifier and a squaring circuit. An example will be given in Section 8.3.

If the continuum of frequencies is composed of discrete waves with a definite dispersion relation but a continuum of wavelengths, the dispersion relation can be obtained by frequency analyzing the signals. At each frequency, a plot of R versus probe separation d will look like that in Fig. 23. A pure coherent wave of wavelength λ will give a curve of the form $R = \cos(2\pi d/\lambda)$; hence a measurement of the intercepts on the abscissa will yield the relation between ω and λ. A purely random fluctuation will give a Gaussian curve for $R(d)$. In general, the curve $R(d)$ will be a damped cosine whose envelope gives the length over which the wave is coherent. In this manner, Bol (*44*) was able to obtain the phase velocity of waves of each frequency propagating in the azimuthal direction in a stellarator. The direction of propagation could also be determined by inserting a time delay in one of the signals. By

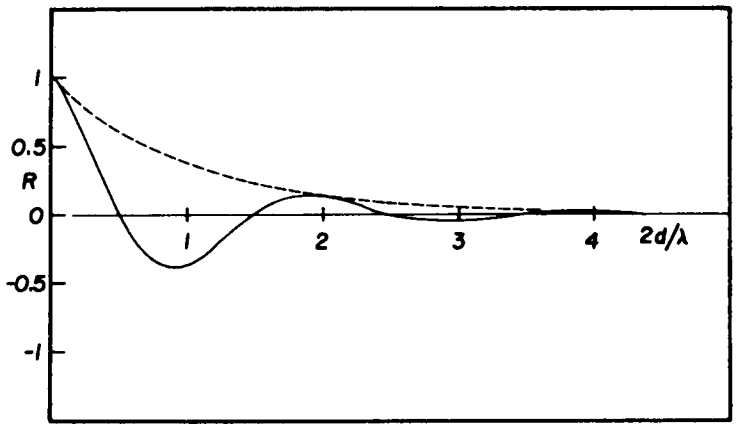

FIG. 23. Schematic of the cross-correlation coefficient R for fluctuations on two probes separated by a distance d. The solid curve shows the wavelength λ of the oscillations at the frequency of measurement. The dotted curve is the envelope of $R(d)$ and gives the correlation length.

aligning two probes accurately along the magnetic field by means of an electron beam, Chen and Cooper (*43*) determined that the velocity of propagation in the longitudinal direction in a reflex arc was much higher than the acoustic velocity.

Correlations between fluctuations in ∇V_s and in n_0 would be desirable to measure, but since this involves at least three probes, the effect on the plasma is appreciable. Correlations with temperature fluctuations would require more complicated techniques.

8 *Experimental Considerations*

8.1 EXPERIMENTAL COMPLICATIONS

We have seen that the behavior of probes in a collisionless plasma is fairly well predicted by theory. In the presence of collisions or magnetic fields the theory is not complete, but one can still make meaningful measurements if he stays in a regime where he knows how to correct for the effects of collisions or magnetic fields. All that remains is to insert an insulated wire into the plasma and take the probe characteristic. In most instances it is actually this simple; however, there are occasional pitfalls for the experimentalist. It is the purpose of this section to list the ones which are known.

1. *Surface layers.* The work function of the probe surface is affected by layers of impurities which are deposited there. If kT_e is below several electron volts, the variation of work function over the probe surface and its change in time will affect the probe characteristic. These layers may be adsorbed gases; metallic coatings, such as Hg or Cs; or even resistive

compounds. The effect of such contaminants has been shown by Wehner and Medicus (*45*), Howe (*46*), and Waymouth (*47*). It is good practice to "outgas" a probe the first time it is put under vacuum; this is conveniently done by drawing enough saturation electron current to heat the probe tip to incandescence. In some discharges the surface layers can reform quickly. It is then necessary to pulse the probe to obtain the characteristic before this happens. Between pulses, the probe is kept under electron or ion bombardment by a large positive or negative bias, whichever is more efficient in eliminating the contaminants.

2. *Secondary emission and arcing.* As mentioned in Section 6.3, a negative probe may collect a spuriously large apparent ion current if secondary electrons are liberated by the ions. At positive voltages the secondary electrons cannot escape from the probe and therefore are unimportant. The effect of secondary emission is difficult to correct for; and therefore it should be avoided by using materials with low emission yields and low probe voltages. In intense discharges, however, it is not always possible to avoid secondary emission. In fact, a "unipolar" arc can form, in which the probe is the cathode and the sheath edge the anode; the circuit is completed by currents flowing to a metallic discharge wall. Such arcs can destroy a probe. It is found that platinum is less subject to such arcs than is tungsten.

3. *Perturbation of the plasma.* In weakly ionized plasmas the presence of a probe perturbs a plasma by lowering the density in its neighborhood; this effect is part of the theory of probes in the presence of collisions. In well-confined, fully ionized plasmas, however, the probe can interfere in other ways. The most important is the liberation of impurity atoms from the probe shield or the probe tip. These impurities can cool the electron gas and reduce the conductivity by being excited in inelastic collisions and radiating away the energy. In thermally ionized Cs plasmas, magnetic confinement may be so good that a probe can become the major source of plasma loss.

4. *Effect of the probe shield.* Although it draws no net current, the insulating shield around a probe collects ions and can depress the plasma density in its neighborhood in the presence of collisions. This has been studied by Waymouth (*25*). To avoid this, one can make a density scan by moving a bare wire through the plasma and taking differential measurements.

5. *Change of probe area.* The current collected by a probe depends on its exposed area. This can change by sputtering or melting in intense discharges. Furthermore, a conducting layer may form on the insulator

either by deposition or by reduction of the oxide by hydrogen. If the probe tip is in electrical contact with this conducting layer, the effective collecting area is greatly increased. Fortunately, it is usually quite obvious when this occurs. To avoid this, it is good practice to center the probe tip in the insulating tube, so that the point of contact with the insulator is well away from the plasma.

6. *Oscillations.* The effect on the probe characteristic of fluctuations in the plasma has already been considered in Section 7.1.

7. *Reflection of electrons.* If the probe is not perfectly absorbing, the theory can be modified to take this into account, if the reflection coefficient is known. Fortunately, the determination of kT_e from transition region of the characteristic is unaffected by reflection, since in a Maxwellian gas the velocity distribution of electrons striking the probe is the same regardless of V_p, and therefore the reflection coefficient is constant.

8. *Photoemission.* In very tenuous plasmas, such as in the ionosphere, the ion currents are so small that photoemission must be taken into account. This occurs for densities of 10^6 cm^{-3} or below. Ichimiya *et al.* (*48*) have reduced the effect of photoemission by using a hollow probe with large holes in its surface. The holes apparently do not reduce the ion current, but the photocurrent is reduced in proportion to the exposed area.

9. *Macroscopic gradients.* In small discharges the length of the probe or the extent of the disturbed region of the plasma may be large compared to the length of macroscopic gradients of n_0 ot V_s in the discharge. In such a case the effect on the probe current must be considered.

10. *Negative ions.* In the presence of negative ions the collisionless theory can be modified straightforwardly to include their effect. This has been treated by Boyd and Thompson (*49*).

11. *Metastable atoms.* The liberation of electrons from the probe by metastables has been considered as a cause of discrepancies between theory and experiment by Schulz and Brown (*24*).

12. *Ion trapping.* The possibility of trapping ions in closed orbits around a negative probe has been pointed out by Bernstein and Rabinowitz (*17*). However, there has been no experimental evidence that this is important.

13. *External circuit.* The stray capacitance of the leads to a probe is of great importance if the probe is pulsed or if it is used to measure V_f

to high frequencies. A floating double-probe system will not follow fast changes in space potential unless the entire system has small leakage capacitance to ground. Around powerful, pulsed machines there are the usual problems of ground loops and rf pickup. At the Model C stellarator in Princeton, the power levels are so large that for safety all probe signals are telemetered to the control room without a direct electrical connection.

8.2 Probe Construction

Although the theory for spherical probes is better developed than for cylindrical probes, spherical probes are seldom used because of the difficulty of construction. Figure 24 shows three types of probes commonly used. These are designed for use in large magnetic fields. In the absence of such fields one would make the exposed tips of the wire probes (*A*) and (*B*) much longer so that they approximate infinitely long cylinders. In the simple probe (*A*) note that the tip is etched down in diameter so that if a conductive coating should form on the exposed surface of the insulator, the tip would not touch it.

Probe (*B*) is a shielded probe for use in detecting oscillations. The shield may be a tube of molybdenum or nickel; it is shown covered by

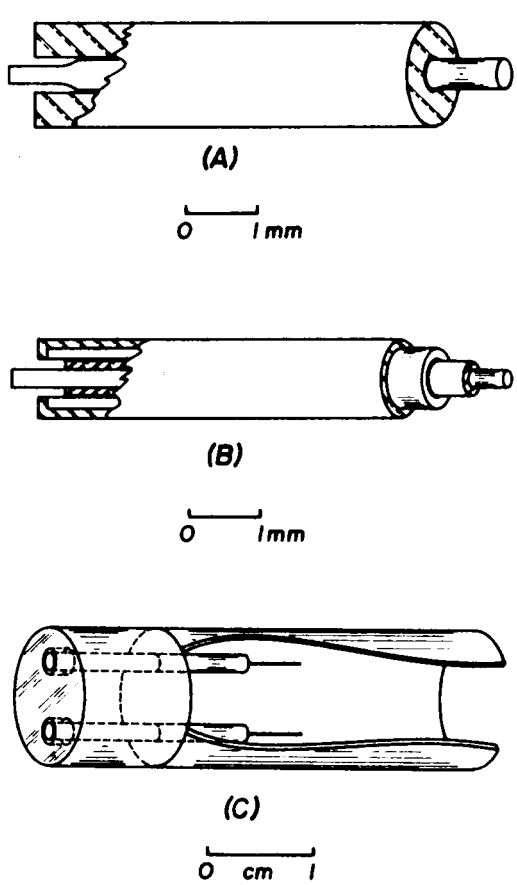

Fig. 24. Three types of probes commonly used in discharges in magnetic fields.

an insulator so that it may be grounded directly without affecting the discharge. This may not be necessary, since the shield need only be at ac ground and may be allowed to float dc-wise. The probability of contaminating the discharge would be reduced if the outer insulator were removed. In determining the length of the inner insulator, one is forced to choose between two evils. If the insulator is set back, as shown, arcs may form between the probe and the shield because of plasma which diffuses into the space between them. If the insulator extends beyond the shield, a short circuit may develop as a result of a conductive coating. To reduce the large capacitance of such a probe, one may want to drive the shield with a cathode follower fed by the floating probe signal. In practice a shielded probe is generally not necessary to eliminate capacitive pickup through the insulator. One merely has to load the floating probe with an impedance small compared to the capacitive impedance of the shield but large compared to the impedance of the plasma. This will be clarified in Section 8.3.

Probe (*C*) is a double plane probe of the type used at Harwell, England. The platinum rods are sealed to the Pyrex insulator, and then the end of the entire assembly is ground flat. As explained in Section 2.3, the current from a plane probe is difficult to interpret in terms of the plasma parameters; however, plane probes are useful to give a rough indication of the behavior of an unstable discharge. Plane probes are often simply isolated sections of the tube wall or an aperture limiter.

The material used for the probe tip is most often tungsten or molybdenum because of their refractive properties. Molybdenum can be machined, and tungsten can be etched by heating to redness and then drawing over a bar of sodium nitrite. Platinum is used when necessary to avoid unipolar arcs. In ordinary discharges the insulator is usually glass or quartz, but in intense discharges a more refractory material is required. The best material is probably high-density, high-purity alumina. Beryllium oxide has a higher thermal conductivity and hence resistance to thermal shock, but its superiority has not been established. These materials are available in tube form but are not machinable. If machining is required, one can use boron nitride.

The use of probes in high-density, high-temperature plasmas is often limited simply by the ability of a probe to withstand the energy dissipation. The problems in intense discharges have been discussed by Jones and Saunders (*50*) and Chen (*51*). The heating of the probe can be lessened by keeping it at floating potential, by pulsing the discharge for short times, or by physically moving the probe through the plasma at a high velocity. A system for doing the latter has been described by Gardner *et al.* (*52*). In toroidal plasmas it is found that "runaway"

electrons have a much larger effect of the life of a probe than the ions, and often probes cannot be inserted into the plasma column until such "runaways" have been eliminated. A complete system for mounting and remote-controlling probes in an ultra-high-vacuum system has been described by Chapuk *et al.* (*53*).

8.3 Typical Circuits

Figure 25 shows the basic circuit for probe measurements. For probe current measurements, the resistor R is small, and the current is given

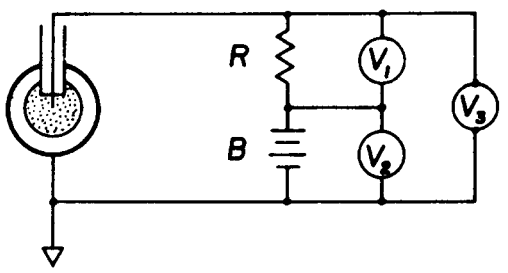

Fig. 25. A simple probe circuit.

by the meter V_1. The resistance R is represented by the slope of the load line L_1 in Fig. 26. As the probe bias is changed, the intercept of this line with the V-axis is shifted, and the probe characteristic A is traced by measuring the current at the intersection of L_1 with A. If R is small enough that L_1 is almost vertical compared to the maximum slope of A, the probe voltage can be measured by either meter V_2 or meter V_3. For floating potential measurements, R is large, the voltage source B is omitted, and V_f is given by meter V_3. The load line is shown by L_2 and should be sufficiently horizontal that the intersection with A occurs near the floating potential. Note that if V_f is much

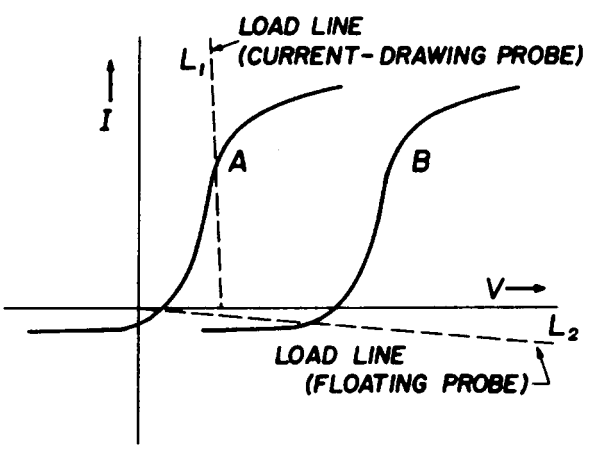

Fig. 26. Diagram of load lines representing the external circuit and their relation to the probe characteristic.

different from ground, as for curve B, the resistor R must be made larger.

Figure 27 shows a typical circuit for taking the dc probe characteristic

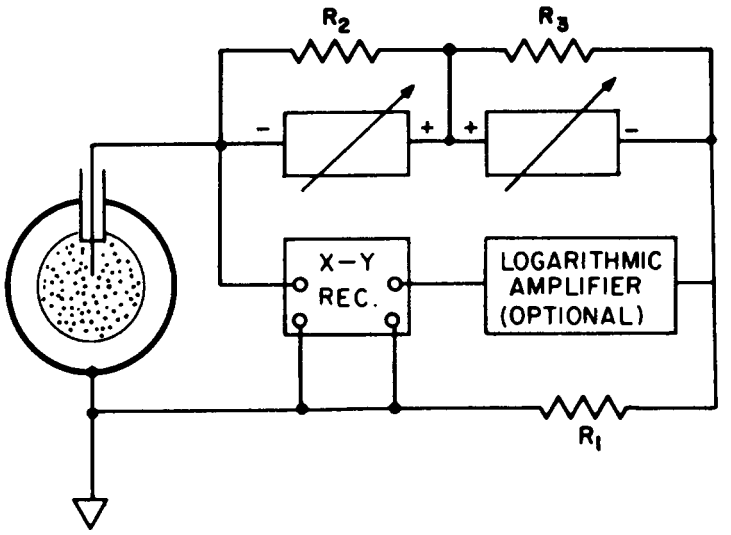

FIG. 27. Block diagram of a circuit used for obtaining dc probe characteristics.

on an x–y recorder or an x–y oscilloscope. Two opposing voltage supplies are used to allow a continuous sweep through 0 potential. If these supplies are electronic, bleed resistors R_2 and R_3 may be necessary to allow current to pass through them in the reverse direction. For dc measurements the current-detecting resistor R is located on the ground side of the supplies. For high-frequency measurements it must be located on the probe side to avoid the effects of stray capacitance in the supplies. The current detector must then be floating, or a differential amplifier with high rejection ratio must be used. The availability of clip-on current detectors greatly simplifies this measurement.

Figure 28 shows schematically a circuit for measuring the amplitude

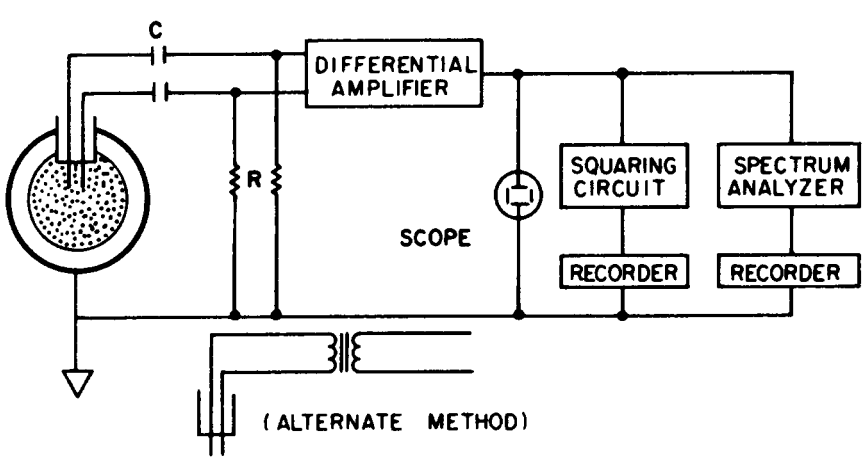

FIG. 28. Block diagram of a circuit for measuring the fluctuations in a local electric field by means of two floating probes.

and spectrum of oscillations in local electric field. Two floating probes are used. The blocking capacitors C are used to allow a smaller value of R to be used, as was discussed in connection with curves A, B, and L_2 of Fig. 26. The resistance R is chosen so that the signal from the probe is not affected but the signal due to capacitive pickup through the probe shield is attenuated.

Figure 29 is a block diagram for obtaining the probe characteristic quickly by applying a sawtooth pulse to the probe. A dummy probe is

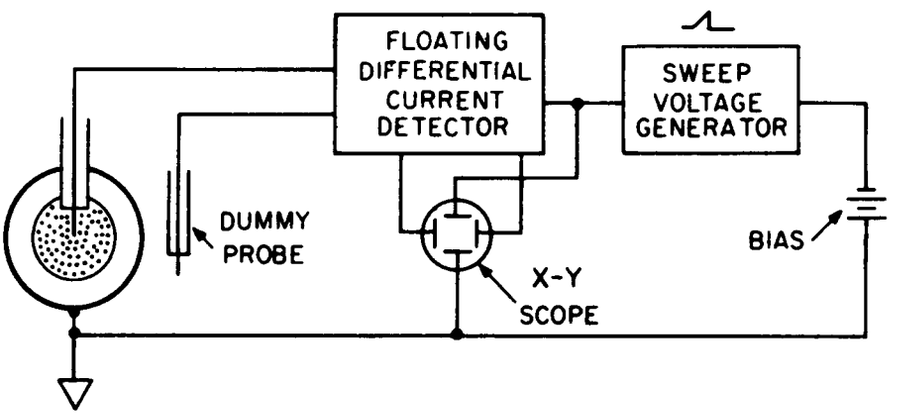

FIG. 29. Block diagram of a circuit for obtaining the probe characteristic in a few microseconds.

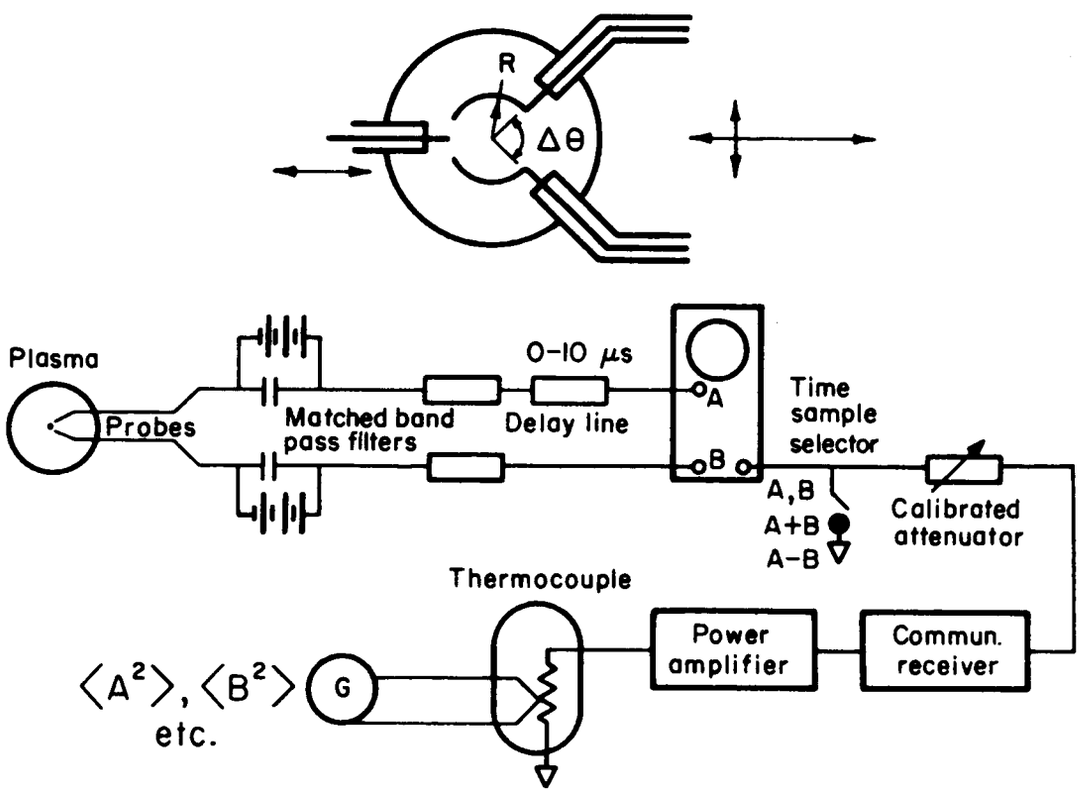

FIG. 30. Block diagram of a circuit used for measuring the cross-correlation coefficient for fluctuating signals on two probes. [K. Bol, *Phys. Fluids* **7**, 1855 (1964).]

used to buck out the stray capacitance. The current detector may be, for instance, two clip-on current probes attached to a differential amplifier.

Figure 30 shows the circuit used by Bol (*44*) to measure the correlation between the voltage or current signals from two movable probes. The sum and difference signals are obtained merely by inverting the phase of one signal at the input of the oscilloscope preamplifier. These signals are squared by a thermocouple. Linearity is preserved by keeping the signal amplitude constant at the thermocouple by means of an attenuator. Note that the frequency analysis is performed by a communications receiver after the signals are added; this obviates the need for two receivers.

REFERENCES

1. I. Langmuir, *in* "Collected Works of Irving Langmuir" (G. Suits, ed.), Vol. 4, Macmillan (Pergamon), New York, 1961; originally published in *Gen. Elec. Rev.* **27**, 449 ff. (1924), and *Phys. Rev.* **28**, 727 (1926).
2. I. Langmuir, *in* "Collected Works of Irving Langmuir" (G. Suits, ed.), Vol. 5. Macmillan (Pergamon), New York, 1961; originally published in *Phys. Rev.* **33**, 954 (1929), and **34**, 876 (1929).
3. D. Bohm, *in* "The Characteristics of Electrical Discharges in Magnetic Fields" (A. Guthrie and R. K. Wakerling, eds.). McGraw-Hill, New York, 1949.
4. J. E. Allen and P. C. Thonemann, *Proc. Phys. Soc.* (*London*) **B67**, 768 (1954).
5. G. Ecker and J. J. McClure, *Z. Naturforsch.* **17a**, 705 (1962).
6. E. R. Harrison and W. B. Thompson, *Proc. Phys. Soc.* (*London*) **74**, Pt. 2, 145 (1959).
7. P. L. Auer, *Nuovo Cimento* **22**, 548 (1961).
8. S. A. Self, *Phys. Fluids* **6**, 1762 (1963).
9. A. Caruso and A. Cavaliere, *Nuovo Cimento* **26**, 1389 (1962).
10. F. F. Chen, *Nuovo Cimento* **26**, 698 (1962).
11. J. E. Allen and F. Magistrelli, *Nuovo Cimento* **18**, 1138 (1960).
12. I. Langmuir, *in* "Collected Works of Irving Langmuir" (G. Suits, ed.), Vol. 3. Macmillan (Pergamon), New York, 1961; originally published in *Phys. Rev.* **22**, 347 (1923), and **23**, 49 (1924).
13. A. H. Heatley, *Phys. Rev.* **52**, 235 (1937).
14. G. Medicus, *J. Appl. Phys.* **33**, 3094 (1962); **32**, 2512 (1961).
15. T. Dote, K. Takayama, and T. Ichimiya, *J. Phys. Soc. Japan* **17**, 174 (1962).
16. J. E. Allen, R. L. F. Boyd, and P. Reynolds, *Proc. Phys. Soc.* (*London*) **B70**, 297 (1957).
17. I. B. Bernstein and I. Rabinowitz, *Phys. Fluids* **2**, 112 (1959).
18. F. F. Chen, *J. Nucl. Energy: Pt. C* **7**, 47 (1965).
19. S. H. Lam, *Phys. Fluids* **8**, 73 (1965).
20. C. H. Su and S. H. Lam, *Phys. Fluids* **6**, 1479 (1963).
21. I. Cohen, *Phys. Fluids* **6**, 1492 (1963).
22. B. Davydov and L. Zmanovskaja, *Tech. Phys. USSR* **3**, 715 (1936).
23. R. L. F. Boyd, *Proc. Phys. Soc.* (*London*) **B64**, 795 (1951).
24. G. J. Schulz and S. C. Brown, *Phys. Rev.* **98**, 1642 (1955).

25. J. F. Waymouth, *Phys. Fluids* **7**, 1843 (1964).
26. G. Ecker, K. S. Masterson, and J. J. McClure, *Univ. Calif. Radiation Lab. Rept.* No. UCRL-10128, TID-4500 (17th ed.) (1962).
27. B. Bertotti, *Phys. Fluids* **4**, 1047 (1961); **5**, 1010 (1962).
28. G. Spivak and E. Reichrudel, *Physik Z. Sowjetunion* **9**, 655 (1936); also *Izv. Akad. Nauk SSSR* p. 479 (1938); and *Zh. Eksperim. i Teor. Fiz.* **8**, 319 (1938).
29. R. J. Bickerton, Thesis, Oxford University (1954).
30. R. J. Bickerton and A. von Engel, *Proc. Phys. Soc. (London)* **B69**, 468 (1955).
31. E. O. Johnson and L. Malter, *Phys. Rev.* **80**, 58 (1950).
32. I. Langmuir, *Phys. Rev.* **33**, 954 (1929).
33. A. Garscadden and K. G. Emeleus, *Proc. Phys. Soc. (London)* **79**, 535 (1962).
34. M. Sugawara and Y. Hatta, *Inst. Plasma Phys. (Nagoya Univ., Japan) Res. Rept.* No. IPPJ-4 (1963).
35. A. Boschi and F. Magistrelli, *Nuovo Cimento* **29**, 487 (1963).
36. F. W. Crawford, *J. Appl. Phys.* **34**, 1897 (1963).
37. F. F. Chen, *Rev. Sci. Instr.* **35**, 1208 (1964).
38. D. G. Bills, R. B. Holt, and B. T. McClure, *J. Appl. Phys.* **33**, 29 (1962).
39. H. J. Oskam, R. W. Carlson, and T. Okuda, *Aeronaut. Res. Labs. Rept.* No. ARL 62-417 (1962).
40. D. Kamke and H.-J. Rose, *Z. Physik* **145**, 83 (1956).
41. H. Takayama, H. Ikegami, and S. Miyasaki, *Phys. Rev. Letters* **5**, 238 (1960).
42. H. W. Batten, H. L. Smith, and H. C. Early, *J. Franklin Inst.* **262**, 17 (1956).
43. F. F. Chen and A. W. Cooper, *Phys. Rev. Letters* **9**, 333 (1962).
44. K. Bol, *Phys. Fluids* **7**, 1855 (1964).
45. G. Wehner and G. Medicus, *J. Appl. Phys.* **23**, 1035 (1952).
46. R. M. Howe, *J. Appl. Phys.* **24**, 881 (1953).
47. J. F. Waymouth, *J. Appl. Phys.* **30**, 1404 (1959).
48. T. Ichimiya, K. Takayama, and Y. Aono, *Proc. 1st Intern. Space Sci. Symp., Nice, 1960* p. 397 (North-Holland, Amsterdam, 1960).
49. R. L. F. Boyd and J. B. Thompson, *Proc. Roy. Soc.* **A252**, 102 (1959).
50. H. W. Jones and P. A. H. Saunders, *U. K. At. Energy Authority Rept.* No. AERE-R3611 (1961).
51. F. F. Chen, *IRE Trans. Nucl. Sci.* **8**, No. 4, 150 (1961).
52. A. L. Gardner, W. L. Barr, R. L. Kelly, and N. L. Oleson, *Phys. Fluids* **5**, 794 (1962).
53. J. M. Chapuk, V. L. Corso, V. S. Foote, W. L. Harries, R. M. Sinclair, J. L. Upham, and S. Yoshikawa, *Rev. Sci. Instr.* **34**, 1377 (1963).